

See discussions, stats, and author profiles for this publication at: <https://www.researchgate.net/publication/37452750>

# Nucleus-Independent Chemical Shifts (NICS) as an Aromaticity Criterion

ARTICLE in CHEMICAL REVIEWS · OCTOBER 2005

Impact Factor: 46.57 · DOI: 10.1021/cr030088+ · Source: OAI

CITATIONS

1,141

READS

377

5 AUTHORS, INCLUDING:



Zhongfang Chen

University of Puerto Rico at Rio Piedras

220 PUBLICATIONS 7,763 CITATIONS

SEE PROFILE



Chait Wannere

Merck

44 PUBLICATIONS 2,924 CITATIONS

SEE PROFILE



Clémence Corminboeuf

École Polytechnique Fédérale de Lausanne

120 PUBLICATIONS 4,604 CITATIONS

SEE PROFILE



Ralph Puchta

Friedrich-Alexander-University of Erlangen-N...

133 PUBLICATIONS 3,989 CITATIONS

SEE PROFILE

# Nucleus-Independent Chemical Shifts (NICS) as an Aromaticity Criterion

Zhongfang Chen,<sup>\*,†</sup> Chaitanya S. Wannere,<sup>†</sup> Clémence Corminboeuf,<sup>†</sup> Ralph Puchta,<sup>‡</sup> and Paul von Ragué Schleyer<sup>\*,†</sup>

Computational Chemistry Annex, The University of Georgia, Athens, Georgia 30602-2525, and Computer Chemie Centrum, Universität Erlangen-Nürnberg, Nägelbachstr. 25, D-91052 Erlangen, Germany

Received April 9, 2005

## Contents

1. Introduction	3842
1.1. Structural Criteria	3844
1.2. Energetic Criteria	3845
1.3. Reactivity Criterion	3846
1.4. <sup>1</sup> H NMR Chemical Shifts	3846
2. Original and Refined NICS-Based Techniques	3846
2.1. Pre-NICS Period	3846
2.1.1. Magnetic Susceptibility Exaltation ( $\Lambda$ )	3846
2.1.2. Li <sup>+</sup> NMR Chemical Shift	3848
2.2. Original NICS Technique	3849
2.3. Dissected NICS Techniques	3851
2.3.1. LMO–NICS Method	3851
2.3.2. CMO–NICS Method	3852
2.4. Comparison of NICS-Based Methods	3854
3. Selected Applications	3855
3.1. Aromaticity in Annulenes	3855
3.1.1. Aromatic Annulenes	3855
3.1.2. Antiaromatic Annulenes	3857
3.2. Aromaticity in Polycyclic Aromatic Hydrocarbons (PAHs)	3859
3.3. Möbius Aromaticity	3860
3.4. Aromaticity in Hydrocarbon Pericyclic Reaction Transition States	3861
3.4.1. Sigmatropic Shifts	3862
3.4.2. Cope and Claisen Rearrangements	3862
3.4.3. Electrocyclic Reactions	3864
3.4.4. Group Transfers	3864
3.4.5. Ene Reactions	3864
3.4.6. Cycloaddition Reactions	3865
3.4.7. Pericyclic Reactions Involving Möbius Transition States	3865
3.5. $\sigma$ -Aromaticity and $\sigma$ -Antiaromaticity	3865
3.6. Aromaticity in Metal Clusters	3867
4. The Relationship among Geometric, Energetic and Magnetic Aromaticity Criteria	3868
5. Concluding Remarks	3870
6. Acknowledgment	3871
7. Appendix	3871
8. References	3883

## 1. Introduction

Few concepts are as frequently used as aromaticity in the current chemical literature.<sup>1</sup> This may be quantified by ca. 300 000 papers dealing with the aromatic properties of chemical systems published in the scientific literature since 1981. Chemists in the early 19th century first just used the term “aromatic” to describe organic substances with a pleasant smell but then to designate a class of chemically related compounds, distinguished from those belonging to the aliphatic class. The term “aromaticity” became indissolubly associated with benzene (despite its unattractive odor) after its first isolation and characterization by Michael Faraday in 1825.<sup>2</sup> During the subsequent centuries, very many chemists attempted to explain the stability and the exceptional chemical behavior of this highly unsaturated molecule in terms of its structure and the nature of its chemical bonding. Very slowly at first, the range of compounds considered to be “aromatic”, once restricted to benzene and its close relatives, was enlarged. The extension to naphthalene, anthracene, and phenanthrene seems obvious; five-membered ring heterocycles (e.g., thiophene and pyrrole) were included before the end of the 19th century. The six special “affinities” associated with benzene in the 19th century were identified as “aromatic electrons” in the 1920s. The understanding furnished by the remarkable theoretical developments of the following decade resulted in ever broadening applications of the aromaticity concept, for example, (a) to annulenes, their ions, and their relatives such as tropolone, (b) to azulene and other nonbenzenoid aromatics, (c) to inorganic analogues of the aromatic planar hydrocarbons, involving both nonmetallic as well as metallic elements, such as gallium, and (d) to the recognition that the considerable nonplanar distortion in bridged annulene and, more recently, in large carbon fullerene clusters could be tolerated. Extension to (e) the three-dimensional boron and carborane cage molecules based upon triangular face polyhedra, as well as to small elemental clusters, broke the planar restriction completely. Likewise, the recognition that molecules can be stabilized by (f)  $\sigma$ -electron delocalization as well as by (g) delocalization of transition metal d-electrons ended the  $\pi$  electron restriction. Table 1 summarizes a few of the post-Hückel developments of conceptual importance.

\* E-mail: schleyer@chem.uga.edu (P.v.R.S.) and chen@chem.uga.edu (Z.C.).

<sup>†</sup> The University of Georgia.

<sup>‡</sup> Universität Erlangen-Nürnberg.



Zhongfang Chen was born in Liaoyang, P. R. China, in 1971. He earned his B.Sc. (organic chemistry in 1994), M.Sc. (physical chemistry, with Xuezhuan Zhao, in 1997), and Ph.D. (physical chemistry, with Xuezhuan Zhao and Auchin Tang, in 2000) at Nankai University, Tianjin, P. R. China. In late 1999, he began to work in Germany with Andreas Hirsch (Universität Erlangen-Nürnberg) and Walter Thiel (Max-Planck-Institut für Kohlenforschung in Mülheim/Ruhr) as a postdoc, under the support of Alexander von Humboldt foundation and Max-Planck society. He joined Paul v. R. Schleyer's group in late 2002 but physically remained in Erlangen until his move to the University of Georgia (Athens, GA) in October of 2003. His early research was on the synthesis of fullerenes and their derivatives. Tempted by the charm of modern computational chemistry, in 1997, he switched to apply these powerful tools to characterize the experimentally synthesized structures, to design new materials with novel chemical bonding and potential applications, and to investigate rules and trends in chemistry. His main research areas are fullerenes, nanotubes, aromaticity of spherical molecules and clusters, and molecules with novel chemical bonding. He enjoys his extensive collaborations with peer experimentalists and theoreticians. So far, he has given over 30 lectures and has around 70 publications.



Chaitanya S. Wannere completed his B.Sc. in Chemistry in 1994 from the Kelkar Education Trust Vinayak Ganesh Vaze College of Arts, Science, and Commerce (Mulund) affiliated with the University of Bombay. He graduated with M.Sc. in Organic Chemistry from the Indian Institute of Technology-Bombay Powai, India, in 1996. His project, under the supervision of Prof. S. S. Talwar, involved synthesis of quinoline polydiacetylenes. For one year, he continued working on the synthesis of natural product heterocycles under the direction of Prof. K. D. Deodhar. In 1998, he joined the Ph.D. program at the University of Georgia under the direction of Prof. Paul v. R. Schleyer. A major topic of his dissertation was studying the bond alternation in annulenes and validating NICS with various other aromaticity criteria. After successfully completing his Ph.D. in 2003, he has continued his postdoctoral research with Prof. Schleyer. His recent work includes analyzing stabilities of zwitterionic "neutral" and "anion" carbocations, studying aromaticity in transition metal clusters, investigating enzyme-catalyzed reaction mechanisms, and computationally designing compounds that inhibit mannosidase activity of ER1 enzyme.

Despite its continuing very frequent use in the scientific literature, aromaticity, like many other



Clémence Corminboeuf studied Chemistry at the University of Geneva. After graduating in 2000, she carried out her Masters research in theoretical chemistry at the National Research Council in Ottawa, Canada, with Prof. D. R. Salahub. She completed her Ph.D. in quantum chemistry in 2004 at the University of Geneva, working with Professor J. Weber and Dr. T. Heine of the TU-Dresden. The majority of her research has been devoted to investigations of electronic delocalization in annulenes and inorganic clusters. Since 2001, she has collaborated with Prof. P. v. R. Schleyer at the University of Georgia, where she occupied a postdoctoral position in 2004. She is presently at New York University under a Swiss NSF research grant.

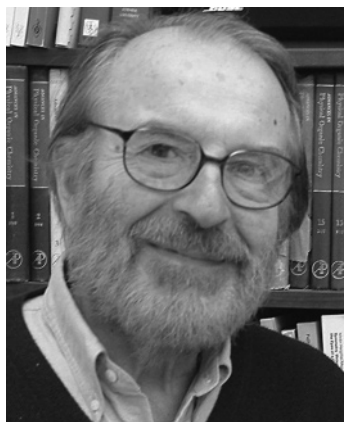


Ralph Puchta was born in Munich, Germany, in 1971. He studied chemistry at the Friedrich-Alexander University Erlangen-Nürnberg and in 2003 obtained his Ph.D. in organic chemistry on a quantum chemical and experimental study in the field of supramolecular chemistry with Tim Clark and Rolf W. Saalfrank. Presently, he is a postdoctoral fellow with Rudi van Eldik at the Institute for Inorganic Chemistry in Erlangen, working computationally on mechanistic problems in metal-organic and coordination chemistry.

useful and popular chemical concepts (charges, chemical bonds, hyperconjugation, electronegativity, etc.) is nonreductive and lacks an unambiguous basis. It has no precise quantitative definition and is not directly measurable experimentally. In other words, aromaticity is a virtual quantity, rather than a physical observable.

We have to confess Beauty (or Aromaticity) is in the eye of the beholder. Both are easy to recognize, but difficult to define quantitatively (Chart 1).

Actually, the concept of aromaticity continues to evolve over time. New aspects await discovery. Nevertheless, "it would be inconceivable to discontinue the use of the concept of aromaticity because of difficulties in its definition and/or measurement"<sup>19</sup>



Paul von Ragué Schleyer was born in Cleveland, Ohio, in 1930. After education at Princeton and at Harvard (Ph.D. in physical organic chemistry with P. D. Bartlett), he returned to Princeton as Instructor in 1954 and was named Eugene Higgins Professor of Chemistry in 1969. Needing more computer time, he accepted in 1976 the Chair once held by Emil Fischer and became Co-Director of the Organic Institute of the University of Erlangen-Nuremberg, Germany. He founded its Computer Chemistry Center in 1993. Schleyer has been Professor Emeritus at Erlangen since 1998, but continues his career as Graham Perdue Professor of Chemistry at the University of Georgia, Athens. He has received honorary doctorates from the Universities of Lyon, France, Munich, Germany, and Kiev, Ukraine, as well as awards in seven countries and in different areas: physical organic, computational, boron, lithium, and most recently theoretical chemistry. He is past President of the World Association of Theoretically-Oriented Chemists (WATOC), a Fellow of the Bavarian Academy and the International Academy of Quantum Chemical Science, Coeditor Emeritus of the *Journal of Computational Chemistry*, and the Editor-in-Chief of the *Encyclopedia of Computational Chemistry*. His 12 books deal with carbonium ions, ab initio molecular orbital theory, lithium chemistry, and ab initio structures and involve collaborations with Nobel Laureates H. C. Brown, G. A. Olah, and J. A. Pople. A 1981–1997 survey identified him as being the third most cited chemist. He has published over 1100 papers.


**Table 1. A Few Selected Post-Hückel Extensions of the Aromaticity Concept**

1938	Evans, Warhurst <sup>3</sup>	transition state stabilization by aromaticity
1945	Calvin, Wilson <sup>4</sup>	metalloaromaticity
1959	Winstein <sup>5</sup>	generalization of homoaromaticity
1964	Heilbronner <sup>6</sup>	Möbius aromaticity
1965	Breslow <sup>7</sup>	recognition of antiaromaticity
1970	Osawa <sup>8</sup>	“superaromaticity”: original concept of fullerene C <sub>60</sub>
1972	Baird <sup>9</sup>	triplet aromaticity
1978	Aihara <sup>10</sup>	three-dimensional aromaticity
1979	Dewar <sup>11</sup>	$\sigma$ -aromaticity
1979	Schleyer <sup>12</sup>	double and in-plane aromaticity
1982	Jemmis, Schleyer <sup>13</sup>	$4n + 2$ interstitial electron rule
1985	Shaik and Hiberty <sup>14</sup>	bond length-alternating effect of $\pi$ -electrons in benzene
1985	Kroto, Heath, O'Brien, Curl, Smalley <sup>15</sup>	discovery of fullerenes
1991	Iijima <sup>16</sup>	discovery of nanotube
1998	Schleyer <sup>17a</sup>	trannulenes
2005	Schleyer <sup>18</sup> and Tsipis <sup>18b,c</sup>	$d$ -orbital aromaticity

(Chart 2). The following qualitative definition covers various aspects of the concept and is compatible with

**Chart 1**

Aromaticity



Easily recognized (but not always)  
Many kinds  
Hard to compare  
Difficult to quantify  
Various opinions, no general agreement  
Interpreted differently

**Chart 2**

....classification and theory are not ends in themselves. If they generate new experimental work, new compounds, new methods—they are good; if they are sterile—they are bad.  
E.D. Bergmann 1970

the rapid further developments of this field of research:

*Aromaticity is a manifestation of electron delocalization in closed circuits, either in two or in three dimensions. This results in energy lowering, often quite substantial, and a variety of unusual chemical and physical properties. These include a tendency toward bond length equalization, unusual reactivity, and characteristic spectroscopic features. Since aromaticity is related to induced ring currents, magnetic properties are particularly important for its detection and evaluation.*

The main criteria characterizing aromaticity comprise four main categories. The following are illustrative, but each has its drawbacks:

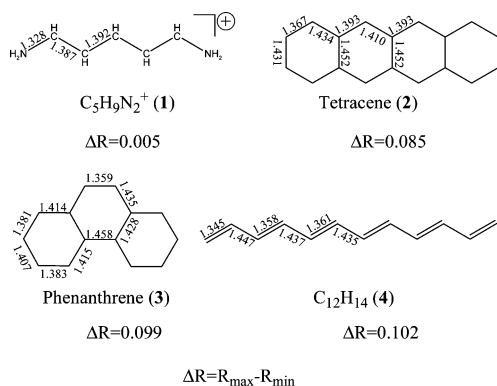
Structure—tendency toward bond length equalization and planarity (if applicable).  
Energy—enhanced stability.  
Reactivity—lowered reactivity, electrophilic aromatic substitution (if applicable).  
Magnetic properties—proton chemical shift, magnetic susceptibility exaltation, NICS, ring current plots.

### 1.1. Structural Criteria

Bond length equalization cannot be used as the only criterion for aromaticity because some bond-equalized systems are not aromatic. For instance, borazine, isoelectronic with benzene, has six  $\pi$  electrons and equalized bond lengths, but its  $\pi$  electrons are largely localized on the nitrogen atoms. Consequently, borazine hardly exhibits a  $\pi$  ring current and is only weakly aromatic. Moreover, bond length equalization due to  $\pi$  electron delocalization is found not only in cyclic systems but also in highly conjugated acyclic compounds. For example, the C<sub>5</sub>H<sub>9</sub>N<sub>2</sub><sup>+</sup> polymethinium cation (**1**) possesses nearly equalized C–C bond lengths but is not aromatic; Conversely, CC bond length variations in polybenzenoid hydrocarbons can be as large as those in linear conjugated polyenes. For example, in tetracene (**2**) and phenan-



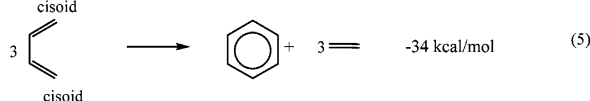
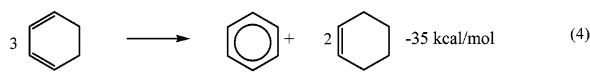
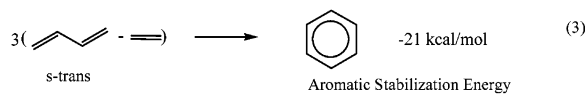
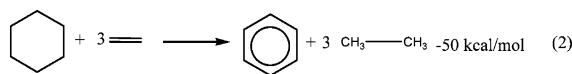
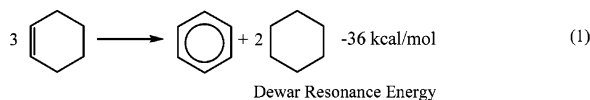
threne (**3**), the maximum differences of bond lengths of 0.085 Å (tetracene) and 0.099 Å (phenanthrene) are scarcely smaller than the 0.102 Å range in all-*trans*-dodecahexaene (**4**). These examples illustrate well that bond length variations in the absence of other considerations cannot be used to characterize aromaticity unambiguously.



## 1.2. Energetic Criteria

Enhanced resonance energies (REs) and the aromatic stabilization energies (ASEs) have long been recognized to be the cornerstone of aromaticity. However, ASEs and REs even of unstrained and uncomplicated systems are difficult to evaluate unambiguously. Indeed, published energy estimates vary significantly, depending strongly on the equations used (various isodesmic, homodesmotic, and hyperhomodesmotic reactions) and on the choice of reference molecules. Note that the signs of the REs and ASEs depend on the manner in which the defining equations are written. Aromatic systems are more stable than their reference models.

It is far from trivial to balance strain, hyperconjugative effects, and the differences in the type of bonds and atom hybridizations using energy evaluation schemes. For example, the REs given by eqs 1 and 2 are  $-36$  and  $-50$  kcal/mol, respectively.



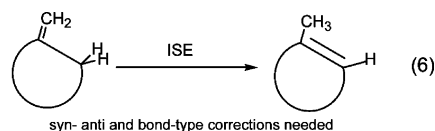
The rather large discrepancy is due to the neglect of other effects influencing the energies of the systems involved in the equation. Thus, the three cyclo-

hexenes in eq 1 are each stabilized by two hyperconjugative interactions; this lowers the exothermicity considerably.

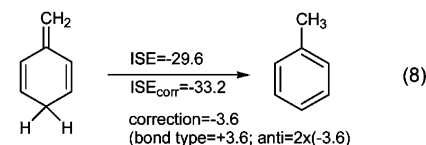
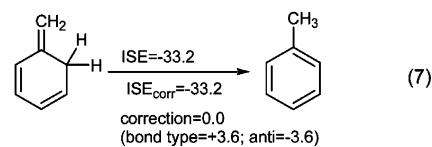
Furthermore, one must differentiate between reactions that model resonance (total) energies (RE, eqs 1 and 2) and aromatic stabilization energies (ASE), which measure the extra stabilization (over topologically acyclic conjugated polyene models) due to cyclic delocalization. The ASEs given by eqs 3–5 also vary significantly; the anti-*syn* butadiene energy difference (3.6 kcal/mol) diminishes the exothermicity given by Dewar's eq 3. Benzene has only *syn* diene components, and its ASE is modeled more appropriately by eqs 4 and 5.

The recent critical examination of ASEs of 105 five-membered  $\pi$ -electron systems illustrates that the resonance energies derived from even the best-chosen schemes have flaws and do not correctly cancel other contributions to the energy. In particular, ASEs derived from homodesmotic schemes based on acyclic reference compounds do not give satisfactory results. Cyclic reference compounds balance ring strain and other errors more effectively and are better suited for ASE and other aromaticity evaluations.<sup>20</sup> Nevertheless, imperfections remain, including inadequately compensated strain, changes of hybridization, heteroatom interactions involving lone pairs, topological charge stabilization, homoconjugation of heterosubstituted cyclopentadienes, and overestimation of the conjugative interactions of the model compounds.

To overcome complications due to such perturbing influences, the isomerization stabilization energy (ISE)<sup>21</sup> was suggested to afford better ASE evaluations. ISE is based on the (corrected) differences between total energies computed for only two species: a methyl derivative of the aromatic system and its nonaromatic exocyclic methylene isomer (eq 6).



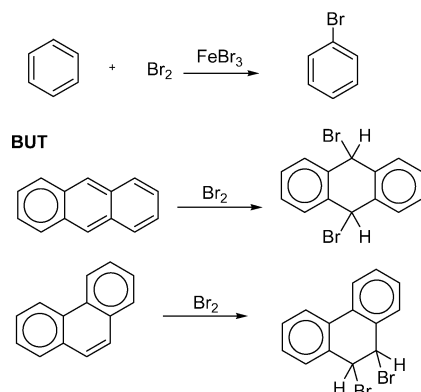
### Application to benzene



The computed ISE of benzene is  $-33.2$  kcal/mol. Note that the 3.6 kcal/mol difference between the ISEs based on eqs 7 and 8 is eliminated when the syn-anti correction is applied. Generally, the ISE is essentially independent of the isomers chosen if the corrections are properly made.

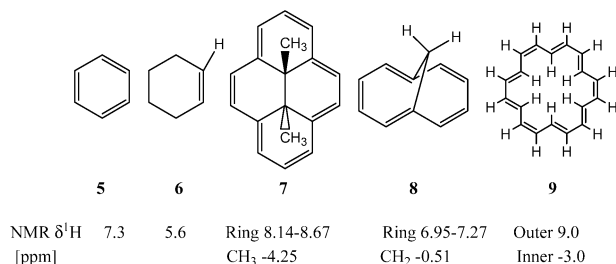
### 1.3. Reactivity Criterion

Reactivity is dominated by the transition state rather than the initial state energy. Since aromaticity is a property of the initial state, criteria based on chemical reactivity are not straightforward to quantify. The traditional reactivity characteristic of aromatic compounds—electrophilic aromatic substitution, rather than addition—has many exceptions. Phenanthrene and anthracene add bromine like olefins! Substitution is not a general criterion. Some systems, notably the fullerenes (e.g.,  $C_{60}$  or  $C_{70}$ ) are completely devoid of hydrogens and can only undergo addition.<sup>22,23</sup>

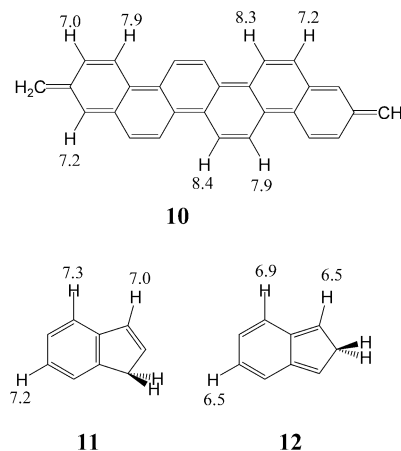


### 1.4. $^1H$ NMR Chemical Shifts

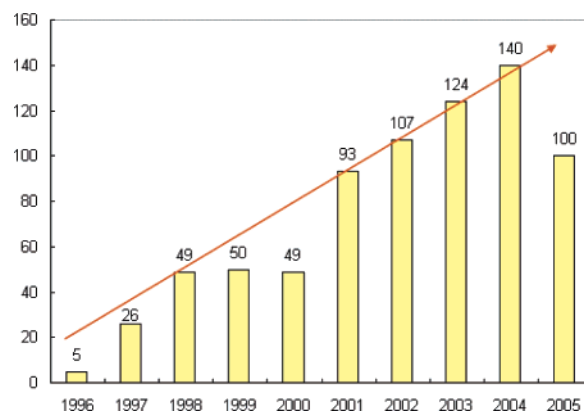
Experimentally,  $^1H$  chemical shifts are perhaps the most often used criteria for characterizing aromatic and antiaromatic compounds. The ca. 2 ppm greater deshielding of the benzene (**5**) protons (7.26) relative to the vinyl protons of cyclohexene (**6**) (5.6 ppm) is, in part, a manifestation of the molecular ring current induced by an external magnetic field. The effects of the induced current inside the ring are even much stronger than those on the outside (see **7–9**). Indeed, the inner protons are shifted more upfield (shielded) than outer protons are shifted downfield (deshielded). The aromatic [18]annulene (**9**) is a good example; the experimental  $^1H$  NMR chemical shifts are 9.28 ppm (outer protons) and  $-3.0$  ppm (inner protons). In sharp contrast, the antiaromatic  $20\pi$  electron annulene [18]annulene dianion (obtained by alkali metal reduction) exhibits completely reversed  $\delta$   $^1H$  positions:  $-1.13$  ppm (outer) vs 28.1 and 29.5 ppm (inner).<sup>24</sup> The difference between aromaticity and antiaromaticity is indeed dramatic.



However, proton chemical shifts of arene hydrogens do not depend solely on ring current effects. Polyolefins (e.g., **10–12**) can have arene-like  $\delta$   $^1H$ 's.<sup>25</sup>



The imprecise nature of the aromaticity concept has stimulated the search for a quantitative definition and the development of numerous aromaticity criteria and indices. Table 2 summarizes the progress. (We apologize for omissions, as well as for the personal bias in the selection.) Among the indexes, a magnetic criterion, nucleus-independent chemical shifts (NICS),<sup>26</sup> has become the most widely used aromaticity probe due to its simplicity and efficiency. NICS has been employed increasingly since its introduction in 1996, judging from the citations to the original paper (Figure 1), which have reached 743 (as of September 18, 2005). With use of this easily computable quantity, various long-standing chemical questions have been solved and novel aromatic systems have been designed. NICS evaluation methods have been enhanced and refined. These developments are presented here, along with an overview of NICS methods and illustrative applications. The Appendix summarizes NICS data for a large number of molecules.



**Figure 1.** The number of citations of the original NICS paper<sup>26</sup> (statistics based on September 18, 2005).

## 2. Original and Refined NICS-Based Techniques

### 2.1. Pre-NICS Period

#### 2.1.1. Magnetic Susceptibility Exaltation ( $\Lambda$ )

Magnetic criteria constitute the most frequently used aromaticity indices (see Table 2). Significantly exalted magnetic susceptibilities ( $\Lambda$ )<sup>44</sup> resulting from the presence of cyclic delocalization of electrons (induced ring currents) were the first magnetic

**Table 2. Some Important Aromaticity Criteria and Key Developments**

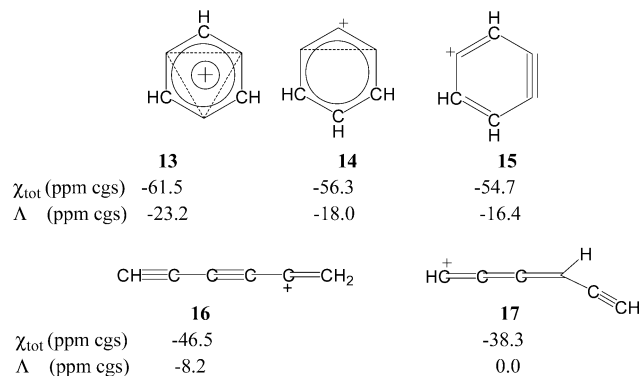
	main contributor(s)	contribution	type <sup>a</sup>
before 1825		distinctive “aromatic” smell	
1825	Faraday <sup>2</sup>	isolation of benzene, high carbon–hydrogen ratios, stable despite considerable unsaturation	
1861	Loschmidt <sup>27</sup>	a circle used indefinitely to represent the six benzene carbon atoms	
1865	Kekulé <sup>28</sup>	cyclohexatriene benzene formula; structural basis of aromaticity	
1866	Erlenmeyer <sup>29</sup>	reactivity basis for aromaticity: substitution is more favorable than addition	R
1910	Pascal <sup>30</sup>	increment system for diamagnetic susceptibility–aromatic exaltation	M
1922	Crocker <sup>31</sup>	aromaticity sextet	
1925	Armit/Robinson <sup>32</sup>	aromatic sextet; inscribed circle notation	
1931	Hückel <sup>33</sup>	theory of cyclic ( $4n + 2$ ) $\pi$ electron systems	
1933	Pauling <sup>34</sup>	valence bond method and resonance	E
1936	Kistiakowski <sup>35</sup>	experimental resonance energy of benzene	E
1936	Pauling and others <sup>36</sup>	ring current theory	M
1937	London <sup>37</sup>	quantum mechanical treatment of the ring current, London diamagnetism	M
1937	London <sup>16,38</sup>	GIAO method	
1953	Meyer and others <sup>39</sup>	the difference in the proton magnetic shielding between benzene and noncyclic olefins observed	
1956	Pople <sup>40</sup>	Induced ring current effects on NMR chemical shifts: deshielding of benzene protons	M
1969	Dewar <sup>41</sup>	Dewar resonance energy	E
1967	Garratt <sup>42</sup>	define molecules with an induced diamagnetic ring current as diatropic	M
1967	Julg and François <sup>43</sup>	Julg structural index	S
1968	Dauben <sup>44</sup>	diamagnetic susceptibility exaltation as a criterion of aromaticity	M
1970	Flygare <sup>45</sup>	microwave spectroscopy, aromatic systems shown enhanced magnetic anisotropies	M
1971	Hess and Schaad <sup>46</sup>	Hess-Schaad resonance energy	E
1972	Clar <sup>47</sup>	Clar “aromatic sextet”	
1972	Krygowski <sup>48</sup>	harmonic oscillator model of aromaticity (HOMA) as structural index of aromaticity	S
1974	Fringuelli <sup>49</sup>	Fringuelli structural index	S
1975	Gutman, Milun, Trinajstić, Aihara <sup>50</sup>	topological resonance energy	E
1980	Kutzelnigg <sup>51</sup>	IGLO calculation of magnetic properties: chemical shifts, magnetic susceptibilities and magnetic susceptibility anisotropies	M
1981	Lazzeretti and Zanasi <sup>52</sup>	ab initio current density plots	M
1983	Jug <sup>53</sup>	Jug structural index	S
1985	Pozharskii <sup>54</sup>	Pozharskii structural index	S
1985	Bird <sup>55</sup>	Bird structural index	S
1987	Mizoguchi <sup>56</sup>	magnetic susceptibilities of Hückel and Möbius annulenes show an opposite tendency	M
1988	Zhou Parr, Garst <sup>57</sup>	hardness (low reactivity) as aromaticity index	R
1990–1995	Schleyer <sup>58</sup>	extensively using $\text{Li}^+$ NMR to study aromaticity	M
1994–1996	Schleyer and Jiao <sup>59,60</sup>	extensively using magnetic exaltation criterion to study aromaticity	M
1994	Saunders et al. <sup>22,61</sup>	experimental endohedral $^3\text{He}$ NMR to measure aromaticity in fullerenes and their derivatives	M
1994	Bühl and Hirsch <sup>22,62</sup>	computed endohedral $^3\text{He}$ NMR to measure aromaticity in fullerenes and their derivatives	M
1995	Krygowski <sup>63</sup>	bond alternation coefficient (BAC) structural index	S
1996	Schleyer <sup>26</sup>	nucleus-independent chemical shifts (NICS)	M
1996	Fowler and Steiner <sup>64</sup>	extensive application of current density plots to study aromaticity	M
1997	Schleyer <sup>65</sup>	dissected NICS, localized molecular orbital (LMO) IGLO	M
1997	Bohmann, Weinhold, Farrar <sup>67</sup>	NBO-GIAO dissected canonical molecular orbital (CMO) and LMO NICS	M
1998	Bean, Sadlej-Sosnowska <sup>68</sup>	application of natural bond orbital analysis to delocalization and aromaticity	
1998	Balawender, Komorowski, De Proft, Geerlings <sup>69</sup>	derivatives of molecular valence as a measure of aromaticity	
1998	Chesnut <sup>70</sup>	differences in ring proton shieldings between the fully unsaturated species and its monoene counterpart recommended as aromaticity measure	
1999	Mo <sup>71</sup>	block-localized wave function (BLW) method based on modern ab initio valence bond theory to approach the absolute resonance energy	E
1999	Sundholm <sup>72</sup>	aromatic ring-current shielding (ARCS)	M
2000	Giambiagi <sup>73</sup>	multicenter bond indices as a measure of aromaticity	

Table 2 (Continued)

	main contributor(s)	contribution	type <sup>a</sup>
2000	Chesnut, <sup>74a</sup> Silvi <sup>74b,c</sup>	using the electron localization function (ELF) to measure aromaticity	
2000	Patchkovskii and Thiel <sup>75</sup>	computing NICS using MNDO method	M
2001	Herges <sup>76</sup>	ACID (anisotropy of the current induced density)	M
2001	Fowler and Steiner <sup>77</sup>	ipsocentric partition of total ( $\sigma + \pi$ ) current density into orbital contributions	M
2002	Schleyer <sup>21</sup>	isomerization stabilization energy (ISE),	E
2002	Sakai <sup>78</sup>	CiLC (CI/LMO/CASSCF) analysis; Index of deviation from the aromaticity (IDA)	
2003	Solá <sup>79</sup>	para-delocalization index (PDI) as an electronic aromaticity criterion	
2003	Matta, Hernández-Trujillo <sup>80</sup>	aromaticity index based on the delocalization of the Fermi hole density	
2003	Corminboeuf, Heine, Weber, Seifert, Reviakine, Schleyer <sup>81</sup>	GIAO-CMO NICS NICS <sub>zz</sub> and NICS <sub>πzz</sub> tensors as aromaticity index	M
2004	Merino, Heine, Seifert <sup>82</sup>	induced magnetic field as aromaticity index	M
2004	Santos, Tiznado, Contreras, Fuentealba <sup>83</sup>	topological analysis of the $\sigma$ - and $\pi$ -contribution to electron localization function (ELF) to quantify aromaticity	
2005	Solá <sup>84</sup>	aromatic fluctuation index (FLU) (describing the fluctuation of electronic charge between adjacent atoms in a given ring)	
2005	Sundholm <sup>85</sup>	integrated induced currents as aromaticity index	M

<sup>a</sup> Structural (S), energetic (E), magnetic (M), reactivity (R).

criteria to be employed to characterize aromaticity. The magnetic susceptibility is a global property of the molecule, unlike NMR chemical shifts and NICS, which are local in nature and much less dependent on the ring size. Generally, magnetic susceptibility exaltation,  $\Lambda$ , is defined as the difference between the measured bulk magnetic susceptibility value and the susceptibility evaluated on the basis of an increment system ( $\Lambda = \chi_M - \chi_M'$ ). In more recent work, Cremer et al.<sup>86</sup> used computed magnetic susceptibility exaltations to characterize the homo- and bis-homoaromaticity in the homo- and bishomotropylium cations, as well as in the barbaralyl cation. Prior to employing NICS, the Schleyer group used magnetic susceptibility exaltation extensively to study aromaticity, both for ground-state molecules<sup>59</sup> and for pericyclic transition states.<sup>60</sup> An illustrative example is the quantification of the double aromaticity of the 3,5-dehydrophenyl cation (**13**).<sup>59a</sup> The magnetic sus-



ceptibility exaltation of **13** is large,  $\Lambda = -23.2$  (based on the more appropriate acyclic reference isomer, **17**, which also has three CH groups), and is  $-5.2$  and  $-6.8$  larger in magnitude than the six  $\pi$  monoaromatic cyclic isomers **14** and **15**, respectively.

In the 1996 review article entitled “What is aromaticity”, Schleyer and Jiao<sup>1b</sup> asserted that “While

chemical reactivity, geometrical and energetic properties, and  $^1\text{H}$  NMR chemical shifts as well as magnetic susceptibility anisotropies are useful for characterizing aromaticity, magnetic susceptibility exaltation is the only uniquely applicable criterion”. In this context, they suggested a new definition of aromaticity based on the magnetic susceptibility exaltation, “compounds which exhibit significant exalted diamagnetic susceptibility are aromatic. Those compounds with exalted paramagnetic susceptibility may be antiaromatic”. However, Schleyer and Jiao warned, “magnetic susceptibility exaltation depends on the ring area, this must be appreciated in comparing systems of different rings”.

### 2.1.2. $\text{Li}^+$ NMR Chemical Shift

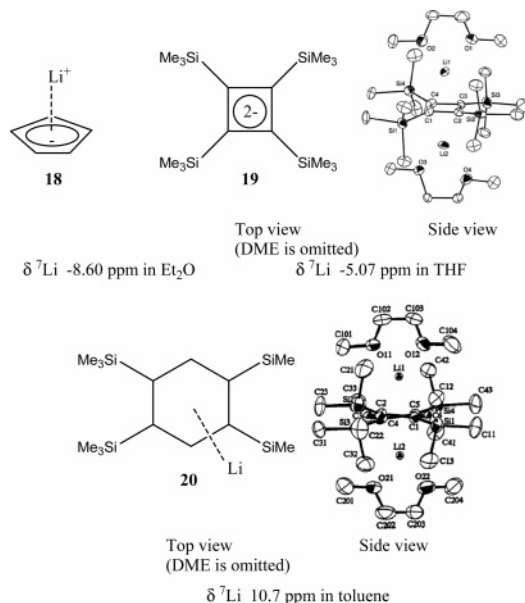
Calculations of NMR chemical shifts at various levels of theory have become a standard tool in chemistry.<sup>87</sup> Because of the sensitivity to the electronic structure in their environment, magnetically active nuclei can be used to probe the nearby shielding influences. This is one of the reasons why NMR spectroscopy rivals X-ray diffraction as best analytical method for characterizing molecular structure.<sup>88</sup>

$^1\text{H}$  NMR chemical shifts are used frequently to demonstrate aromaticity. While the rings of most aromatic systems are too small to accommodate inner protons, the chemical shifts of hydrogens in bridging positions serve as aromaticity and antiaromaticity probes instead.<sup>89</sup>

Akin to  $^1\text{H}$  NMR chemical shifts,  $\delta$   $^7\text{Li}$  were employed to probe electron delocalization before the development of NICS.<sup>26</sup> Lithium cations typically complex preferentially at the ideal positions, the  $\pi$  faces of aromatic systems. Because lithium bonding is primarily electrostatic, experimental  $^7\text{Li}$  chemical shifts (based on lithium salts as the NMR reference) generally are near zero and show little variation among different compounds. However,  $\text{Li}^+$  complexes



of aromatic (or anti-aromatic) compounds exhibit significant shielding (or deshielding) of the  $^7\text{Li}$  NMR signals due to the induced ring current effects. The experimental  $^7\text{Li}$  NMR signal of lithium cyclopentadienide ( $\text{LiCp}$ ) (**18**) is unusually shifted upfield ( $-8.60$



ppm in  $\text{Et}_2\text{O}$ ,<sup>58a</sup>  $-8.68$ ,  $-8.37$ ,  $-8.67$ , and  $-8.35$  ppm in dioxane, THF, dimethoxyethane, and diglyme, respectively<sup>90</sup>, due to the highly diatropic six  $\pi$  electron ring current in  $\text{Cp}^-$ . The highly shielded  $^6\text{Li}$  NMR chemical shift ( $-5.07$  ppm), measured for cyclobutadiene dianion dithium salt (**19**), supports its six  $\pi$  electron aromaticity.<sup>91</sup> In contrast,  $^7\text{Li}$  resonates at  $\delta = 10.7$  ppm in the bis[(dimethoxyethane)lithium-(I)] 1,2,4,5-tetrakis(trimethylsilyl) benzenide (**20**), the six-center eight  $\pi$  electron antiaromatic benzene dianion.<sup>92</sup> This appreciable lithium downfield chemical shift is a direct consequence of the strong paratropic ring current induced in the eight  $\pi$  antiaromatic system. Experimental  $^7\text{Li}$  NMR chemical shifts can be reproduced well by modern computations. For instance, the upfield chemical shift of lithium in  $\text{CpLi}$  was correctly reflected by the individual gauge for localized orbital (IGLO) technique ( $-6.9$  ppm), and the computed Li chemical shifts in  $\text{Li}_2\text{C}_4\text{R}_4$  are around  $-3$  ppm,<sup>93</sup> indicating a strong diatropic ring current resulting from the six  $\pi$  electron systems. The clear advantage of using  $\delta\ \text{Li}$  as a theoretical probe lies in the possibility of comparison with experimental  $\delta\ \text{Li}$  NMR data of  $\text{Li}^+$  complexes. A drawback is that the  $\text{Li}^+$  to arene  $\pi$  face separations are ca.  $2\ \text{\AA}$  or more, so the ring current effects are relatively small. Moreover, the number of  $\text{Li}^+$  complexes and therefore the utility of  $\text{Li}^+$  as an aromaticity probe are rather limited.

## 2.2. Original NICS Technique

The development of NICS at Erlangen emanated from the studies of ring current effects on  $\text{Li}^+$  chemical shifts described above as well as from the known  $\delta\ ^1\text{H}$  behavior of hydrogens in bridging positions above aromatic rings as well as inside larger annulenes. However, such H and Li probe nuclei also

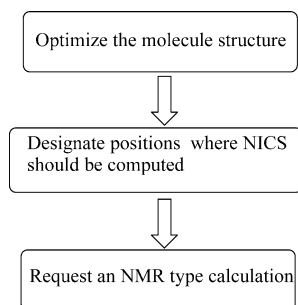
can perturb the wave functions of the system under consideration. To avoid such interferences, why not compute the absolute chemical shielding of a virtual nucleus to probe aromaticity? Such simple reasoning led to the nucleus-independent chemical shifts (NICS) introduced by Schleyer, Maerker, Dransfeld, Jiao, and Hommes in 1996.<sup>26</sup>

As often happens in science, one becomes aware subsequently that others had similar ideas earlier, and one regrets that their publications were overlooked. In the landmark  $\text{C}_{60}$  paper in *Nature*, Kroto, Curl, Smalley, et al.<sup>15</sup> noted, "The inner and outer surfaces are covered by a sea of  $\pi$  electrons" and "... the chemical shift in the NMR of a central [endohedral] atom should be remarkable due to the ring currents". This suggestion (but not the anticipated result) was realized much later by measurements and computations on included  $^3\text{He}$  atoms.<sup>22,61</sup> Elser and Haddon<sup>94</sup> assumed "a magnetically isotropic molecule, with  $\pi$  electrons on the surface of a sphere" and employed London computations to estimate "the ring-current contribution to the chemical shift of a central atom" (what is now known as NICS). A negligible effect ( $+0.5$  ppm) was predicted for  $\text{C}_{60}$  itself but a much larger one (ca  $-32$  ppm) for  $\text{C}_{60}^{6-}$ . Such computations were extended to larger fullerenes.<sup>95</sup> Ab initio magnetic property computations were applied to endohedral  $\text{Li}^+$  and He atoms at the centers of  $\text{C}_{60}$ ,  $\text{C}_{60}^{6-}$ , and  $\text{C}_{70}$  in 1994<sup>58c,96</sup> and in 1995 to the  $\text{He@C}_n$  ( $n = 32-180$ ) set.<sup>97</sup>

To match the familiar NMR convention, NICS indices correspond to the negative of the magnetic shielding computed at chosen points in the vicinity of molecules (one simply changes the sign). NICS is typically computed at ring centers (nonweighted mean of the heavy atoms), at points above, and even as grids in and around the molecule. Significantly negative (i.e., magnetically shielded) NICS values in interior positions of rings or cages indicate the presence of induced diatropic ring currents or "aromaticity", whereas positive values (i.e., deshielded) at each point denote paratropic ring currents and "antiaromaticity".

Being based directly on cyclic electron delocalization, the essence of aromaticity, NICS has several advantages over many other aromaticity criteria: (i) NICS does not require reference standards, increment schemes, or calibrating (homodesmotic) equations for evaluation. (ii) Unlike  $\Delta$ , which depends on the square of the ring area, NICS only shows a modest dependence on the ring size (see values for  $[n]$ annulenes). It does depend on the number of  $\pi$  electrons. The  $10\ \pi$  electron systems give significantly higher values than those with six  $\pi$  electrons, for example, the cyclooctatetraene dication and dianion. (iii) Importantly, in several sets of related molecules, NICS correlates well with other aromaticity indexes based on energetic, geometric, and other magnetic criteria<sup>98</sup> (see section 4 for details). (iv) NICS can be computed easily using standard quantum chemical programs such as Gaussian 98, Gaussian 03, ADF, and deMon. In all these program packages, NICS values can be computed according to the procedure in Chart 3.

## Chart 3



Given below is an example in Gaussian input format to compute NICS values at various points at and above the center of the benzene ring. Note that the

```

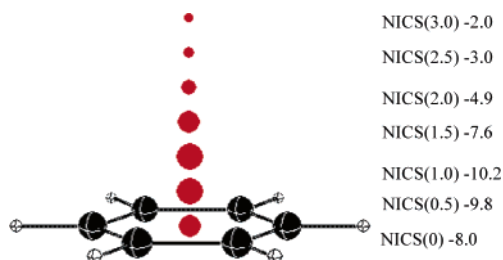
$RunGauss
# RB3LYP/6-311+G** NMR

C6H6 OPT RBECKE3LYP 6-311+G(D,P)

0 1
C 0.697315 0.000000 1.207786
C 1.394632 0.000000 0.000000
C 0.697315 0.000000 -1.207786
C -0.697316 0.000000 -1.207786
C -1.394631 0.000000 0.000000
C -0.697316 0.000000 1.207786
H 1.239533 0.000000 2.146935
H 2.479067 0.000000 0.000000
H 1.239534 0.000000 -2.146935
H -1.239533 0.000000 -2.146935
H -2.479067 0.000000 0.000000
H -1.239534 0.000000 2.146935
Bq 0.000000 0.000000 0.000000
Bq 0.000000 0.500000 0.000000
Bq 0.000000 1.000000 0.000000
Bq 0.000000 1.500000 0.000000
Bq 0.000000 2.000000 0.000000
Bq 0.000000 2.500000 0.000000
Bq 0.000000 3.000000 0.000000
  
```

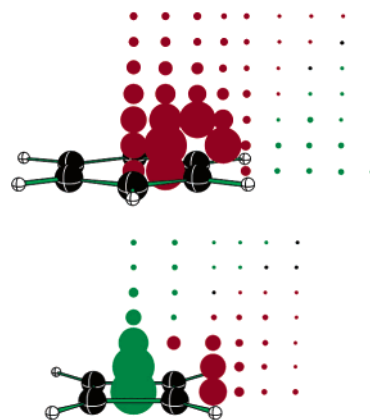
Bq ghost atoms (Banquo, that is, ghost atoms, taken from Macbeth) are used to designate the positions for the NICS evaluations.

Figure 2 displays the computed NICS values requested in the above input.

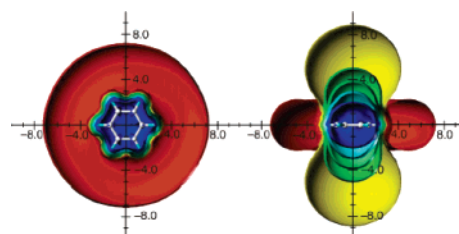


**Figure 2.** The NICS values computed at and above the ring center of benzene (at the GIAO-B3LYP/6-311+G\*\*//B3LYP/6-311+G\* level). The red dots denote diatropic character, and the dot size is in line with the NICS magnitude.

The grid distribution of NICS values around molecules has been widely employed<sup>65b</sup> to provide better insights of the overall molecular magnetic properties, as illustrated for  $C_4H_4$  and  $C_6H_6$  in Figure 3.



**Figure 3.** The NICS grid plot of benzene and cyclobutadiene at the GIAO-B3LYP/6-311+G\*\*//B3LYP/6-311+G\* level of theory. The red and green dots denote diatropic (aromatic) and paratropic (antiaromatic) ring currents, respectively.



**Figure 4.** Calculated ring current effect of benzene (shielding surfaces at 0.1 ppm in yellow, at 0.5 ppm in green, at 1 ppm in green-blue, at 2 ppm in cyan, and 5 ppm in blue; deshielding surface at 0.1 ppm in red): views from perpendicular to the molecule and in the plane of the molecule.

The magnetic shielding function provides exactly the same information on the electron delocalization and molecular aromaticity as NICS.<sup>99</sup> In this context, Klod and Kleinpeter<sup>99</sup> deduced anisotropic effects by evaluating the grid distribution of NICS in annulenes. By plotting the “iso-chemical-shielding surfaces” (ICSS), which actually are isosurfaces of NICS values, one can obtain and visualize quantitative information about the spatial extension and the sign and scope of the corresponding ring current/anisotropic effects of double or triple bonds or of aromatic rings. For benzene (Figure 4), a deshielding of 0.1 ppm at 7 Å from the center in the molecular plane and a shielding of -0.1 ppm at 9 Å perpendicular to the benzene ring were computed.

Concerns have been raised by experimentalists and theoreticians regarding the use of a nonmeasurable (“virtual”) index (NICS) to evaluate another intangible quantity, aromaticity.<sup>36e,100</sup> Actually, NICS can be approached experimentally in some, though rare, cases. The introduction of probe atoms at positions reasonably distant from the molecule can provide a good estimation of the shielding function. For example, NICS and NMR shifts of chemically inert  $^3\text{He}$  at fullerene centers (see above) agree very well.<sup>22</sup> Thus, both serve as effective tools for characterizing electron delocalization in fullerenes (see also the review on spherical aromaticity in this issue<sup>101</sup>). At very low temperatures, it should also be possible to measure  $^3\text{He}$  NMR chemical shifts of helium nuclei physisorbed above the  $\pi$  system of an aromatic ring.

Other possibilities to evaluate NICS experimentally include  $^1\text{H}$  NMR chemical shifts of protons of remote parts of molecules (e.g., as in paracyclophanes<sup>102</sup>) or of methane located in the middle of shielding cones, that is, on the top of aromatic rings. (e.g., **7**).<sup>103,104</sup>

Aside from its lack of direct experimental validations, the NICS is now well accepted by the chemical community. However, although the magnetic index has been proven to be an efficient way to quantify aromaticity, it does not depend purely on the  $\pi$  system but also on other magnetic shielding contributions due to local circulations of electrons in bonds, lone pairs, and core electrons. Indeed, chemical shifts of organic molecules are also affected by the  $\sigma$  framework of the CC and CH bonds. For this reason, the NICS is nonzero for nonaromatic, saturated, and unsaturated hydrocarbon rings.<sup>105</sup> NICS constitutes therefore an appropriate index of cyclic electron delocalization only when the radii of the systems are relatively large. In this case, the  $\sigma$ -orbital contributions to NICS will be very little. For planar or nearly planar molecules, these complicating influences are reduced 1 Å above ring centers, where the  $\pi$  orbitals have their maximum density. Also, NICS(1) (i.e., at points 1 Å above the ring center) was recommended as being a better measure of the  $\pi$  electron delocalization as compared to NICS(0) (i.e., at the ring center).<sup>65</sup>

In direct relation with NICS(1), Juselius and Sundholm introduced the aromatic ring-current shielding (ARCS) in 1999.<sup>72</sup> The ARCS approach indeed uses the long-range contribution of the shielding function (NICS points 3–20 Å from the ring) to provide information about the strength and the radius of the induced ring. This technique, which has already been applied to various organic and inorganic rings, is discussed further in “The Magnetic Shielding Function of Molecules and  $\pi$ -Electron Delocalization”<sup>106</sup> in this issue.

However, refinements of the original NICS technique offer better insights into the nature of the magnetic response to induced ring currents. The next development was based on the NICS dissection into orbital contributions.

### 2.3. Dissected NICS Techniques

To introduce the dissected NICS techniques, details of the chemical shielding definition are essential. NICS indices correspond to the negative value of the magnetic shielding computed at chosen points in a molecule. In an uncoupled density functional treatment, i.e., where the perturbation of the magnetic field  $\mathbf{B}$  to the wave function is not calculated in a self-consistent way, the chemical shielding tensors (and the NICS tensors) can be described by a sum of partial chemical shifts arising from occupied molecular orbitals (MOs)  $\Psi_{k0}$ .<sup>107</sup>

$$\sigma = \frac{1}{2c^2} \sum_k^{\text{occ}} \langle \Psi_{k0} | \frac{\mathbf{r} \mathbf{r}_N \mathbf{I} - \mathbf{r}_N \otimes \mathbf{r}}{|\mathbf{r} - \mathbf{R}_N|^3} | \Psi_{k0} \rangle - \frac{2}{c} \sum_k^{\text{occ}} \langle \Psi_{k0} | \frac{(\mathbf{L}_N)}{|\mathbf{r} - \mathbf{R}_N|^3} | \Psi_{k1} \rangle \quad (9)$$

diamagnetic term paramagnetic term

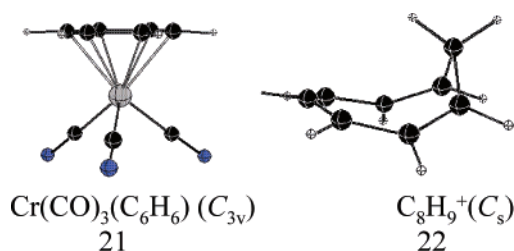
$$\text{where } \mathbf{L}_N = \mathbf{r}_N \times \nabla \quad \text{and } \mathbf{r}_N = \mathbf{r} - \mathbf{R}_N$$

In this equation,  $\mathbf{r}$  refers to the electronic position,  $\mathbf{R}_N$  to the vector position where the NICS is calculated, and  $\mathbf{L}_N$  to the angular momentum operator.

This corresponds to the common gauge formulation of the NMR shielding tensor, where each of two components (diamagnetic and paramagnetic) depends on the selected gauge origin. In practical computations, eq 9 is modified to deal with the gauge-origin problem.<sup>108</sup> However, the formalism of all the commonly used techniques such as IGLO<sup>51,109</sup> and gauge-independent atomic orbital (GIAO)<sup>37,110</sup> can be applied to subsets of MOs in the same manner as in eq 9 and the shielding tensor can thus be calculated in a sum of MO contributions.<sup>81</sup> Based on these considerations, two alternative ways for the calculation of dissected NICS have been proposed.

#### 2.3.1. LMO–NICS Method

In the original 1997 method,<sup>65a</sup> based on the IGLO formalism, the  $\sigma$  and  $\pi$  subspaces are separated using the Pipek–Mezey localization procedure.<sup>111</sup> In this approach, the aromatic ring current can be related to the shielding contributions arising from C–C  $\pi$  electrons. The canonical MOs are transformed into localized MOs; these LMOs (rather than canonical MOs) are then summed up.<sup>109</sup> The localized molecular orbitals (LMOs), with a center placed where a Kekulé-cyclohexatriene double bond would be located, are chosen as the localized  $\pi$  orbitals; these are selected for the calculation of the NICS $_{\pi}$  value of the ring. A disadvantage of this version of dissected LMO–NICS is the restriction to a  $\sigma$ – $\pi$  separation procedure, followed by an IGLO calculation, which limits the usage to only a few computer programs. Most of the available program packages in quantum chemistry include the GIAO method for NMR calculations and are not applicable for these LMO–NICS $_{\pi}$  calculations. Beside this practical disadvantage, there is a fundamental problem when addressing nonplanar molecules. Pipek and Mezey showed that strict  $\sigma$ – $\pi$  separation is only suitable for planar molecules.<sup>111</sup> In practice,  $\sigma$ – $\pi$  separation still might be achieved, especially if a planar ring has nonplanar substituents (example cyclohexene) but the degree of contamination of the  $\pi$  type LMOs should be checked by looking at the LMOs coefficient. Also, for molecules containing a complexed ring, such as  $(\text{C}_6\text{H}_6)\text{Cr}(\text{CO})_3$  (**21**) or  $\text{C}_4\text{H}_4\text{Fe}(\text{CO})_3$ , the multicentered bond in the mol-



ecules mixes strongly with the ring  $\pi$  orbitals. Thus, a clear separation of a  $\pi$  subset cannot be achieved. To avoid these difficulties, a refined version of this technique has been suggested by Corminboeuf, Heine, and Weber.<sup>81a</sup> This so-called NICS $_{\text{CT}}$  technique has been alternatively proposed to calculate dissected



**Table 3.** NICS(tot), NICS( $\pi$ ), and NICS( $\sigma$ ) at the Ring Centers<sup>a</sup>

molecules	<i>R</i>	NICS( $\pi$ )	NICS( $\sigma$ )	NICS(tot)
C <sub>6</sub> H <sub>6</sub> ( <i>D</i> <sub>6h</sub> )	1.396	−20.7	13.8	−8.9
Si <sub>6</sub> H <sub>6</sub> ( <i>D</i> <sub>6h</sub> )	2.217	−15.0	0.6	−13.1
Si <sub>6</sub> H <sub>6</sub> ( <i>D</i> <sub>3d</sub> )	2.240			−11.2
Ge <sub>6</sub> H <sub>6</sub> ( <i>D</i> <sub>6h</sub> )	2.305	−15.0	−1.5	−14.6
Ge <sub>6</sub> H <sub>6</sub> ( <i>D</i> <sub>3d</sub> )	2.384			−10.0
B <sub>3</sub> N <sub>3</sub> H <sub>6</sub> ( <i>D</i> <sub>3h</sub> )	1.431	−12.0	11.4	−2.1

<sup>a</sup> The remaining contributions, due to core orbitals, X–H bonds, and in-plane lone pairs, are small.

NICS of selected canonical molecular orbitals. In this procedure, molecular orbitals that have (at least partial)  $\pi$  contributions are selected manually. For the technical implementation within the IGLO method, as also defined in the original version of dissected NICS, the selected  $\pi$  MOs are split into one subgroup of LMOs, which are localized independently. For that purpose, the technique of Pipek and Mezey was again used, but, in principle, any of the localization procedures, such as those of Foster and Boys<sup>112</sup> or Bohmann et al.,<sup>67</sup> could also be applied. The dissected NICS<sub>cr</sub> of this subgroup is then calculated following the standard IGLO technique.

Using the modified version of dissected NICS, one can select all orbitals showing  $\pi$  character of a given ring without including contributions from the  $\sigma$  framework for the calculation of its dissected NICS<sub>cr</sub>. Of course, canonical MOs of clean  $\pi$  character can be easily distinguished for planar molecules by checking the MO coefficients. For nonplanar molecules, however, the selection becomes more arbitrary. Illustrative examples have already shown that the  $\sigma$  framework and  $\pi$  orbitals indeed never mix. However, for transition metal-containing compounds such as [(C<sub>n</sub>H<sub>n</sub>)M(CO)<sub>3</sub>]<sup>m+</sup>, d shells of the transition metal complex mix strongly with the  $\pi$  orbitals of the ring.

Finally, it is worth noting that strongest localization can be achieved if LMOs are created using all the valence MOs. Using separated subgroups can, therefore, lead to weaker localization and hence less accurate shielding tensors. Hence, a good test is to compare the total NICS value obtained by this modified method to that obtained with the unmodified IGLO calculation.<sup>65a</sup>

The NICS aromaticity criteria are often difficult to apply to inorganic benzene analogues.<sup>65a</sup> Indeed, the conventional total NICS value does not efficiently evaluate the aromatic character of these inorganic rings due to the large influences of  $\sigma$ -bonds.<sup>65a</sup> For example, the total NICS(0) values of *D*<sub>6h</sub> Si<sub>6</sub>H<sub>6</sub> and Ge<sub>6</sub>H<sub>6</sub> (−13.1 and −14.6 ppm, respectively, at the SOS-FPT-IGLO/III/B3LYP/6-311+G\*\* level) are larger than the benzene value (−8.9 ppm).<sup>65a</sup> Also, these systems were the first studied using the original IGLO-based dissected NICS technique. However, both NICS( $\pi$ ) and NICS( $\sigma$ ) decrease with increasing ring size (longer ring bond lengths), for example, benzene > Si<sub>6</sub>H<sub>6</sub> ≈ Ge<sub>6</sub>H<sub>6</sub> (Table 3). The NICS( $\pi$ ) aromaticity index indicates benzene to be more aromatic than silabenzene and germa-benzene. The NICS( $\pi$ ) values agree well with the other mag-

netic aromaticity criteria (exalted magnetic susceptibilities and magnetic susceptibility anisotropies) for this set of molecules. The degree of aromaticity of borazine, compared to benzene, is another controversial example.<sup>113</sup> The small total NICS(0) value (−2.1 ppm) of the often called “inorganic benzene” supports a localized electronic structure. However, the NICS( $\pi$ ) (−12.0 ppm) is half of that of benzene (−20.7 ppm), in agreement with the aromatic stabilization energy (ASE) of borazine, which is approximately half of that of benzene.<sup>114</sup>

### 2.3.2. CMO–NICS Method

The second alternative way for calculating the dissected NICS strictly focuses on the use of canonical MOs. This dissected NICS variation has been called MO–NICS by Heine et al.,<sup>81b</sup> but to avoid ambiguity, CMO–NICS is preferable. Individual canonical molecular orbital (CMO) contributions to the magnetic shielding of atoms, as well as to the NICS of aromatic compounds, can be computed by the widely used GIAO method. Detailed analyses of magnetic shielding CMO–NICS contributions provide interpretive insights that nicely complement and extend the results provided by the localized MO (“dissected NICS”, LMO–NICS) methods. CMO–NICS is based on the uncoupled form of current-density functional theory and is restricted to “pure” DFT calculation (i.e., hybrid functionals cannot be used). The shielding tensor can then be written as a sum of canonical orbital contributions, each of which can be very important for the chemical interpretation.

$$\sigma_{\text{tot}} = \sum_{i=1}^{\text{occ}} \sigma_{\text{CMO}_i} \quad (10)$$

Therefore, CMO–NICS corresponds to the NICS dissection into canonical molecular orbital contributions as expressed in eqs 9 or 10. Note that in the case of the widely used B3LYP hybrid functional, which includes a fraction of orbital exchange, the Kohn–Sham operator is nonmultiplicative. In this case, the calculation of shielding constants requires the solution of a set of coupled perturbed equations preventing the decomposition of NICS into canonical orbital contributions. Another CMO–NICS implementation scheme using natural bond orders (NBOs) has been suggested by Bohmann et al.<sup>67</sup> and has been implemented in the NBO program.<sup>115</sup> In this implementation, the so-called natural chemical shielding contributions are further transformed into shielding contributions from canonical orbitals (NBO–CMO–NICS). In both CMO–NICS analyses, the nonphysical gauge dependence of the shielding tensor is avoided using the GIAO method. Indeed, the GIAO technique provides the most convenient as well as popular way to arrive at the orbital contributions to the shielding tensor.

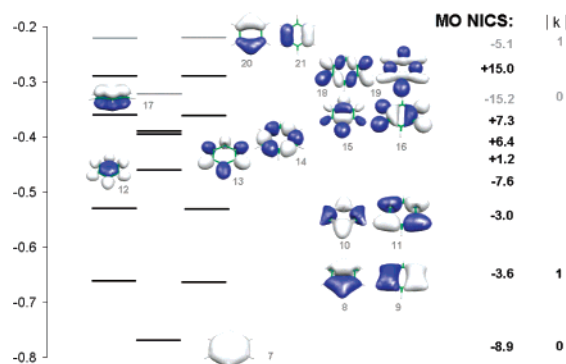
The recently proposed CMO–NICS analysis is not well-established yet but already has augmented the understanding of the magnetic response of well-known molecules<sup>81b</sup> or reactions.<sup>116</sup> Additionally, CMO–NICS has been applied to rationalize the stability of inorganic clusters<sup>117</sup> and systems contain-



ing a planar tetracoordinate carbon.<sup>118</sup> The next section describes CMO–NICS applications in more detail.

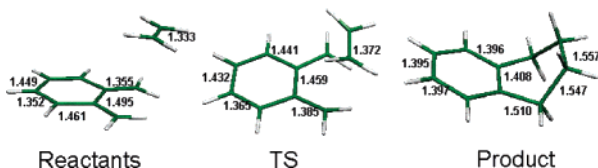
### 2.3.2.1. Applications of CMO–NICS Method.

The first illustrative application of the CMO–NICS analysis on  $[n]$ annulenes<sup>81b</sup> revealed that the lowest-energy  $\pi$  orbital gives the largest contributions to NICS. It was shown that the character and magnitude of the CMO–NICS contribution of both  $\sigma$  and  $\pi$  orbitals depend on the number of nodes along the ring as expected by the London–Hückel susceptibilities (Figure 5). However, these results seem to contradict those of Steiner, Fowler, and co-workers,<sup>77</sup> who found that only the frontier orbitals of  $[n]$ -annulenes exhibit a ring current density when an external magnetic field is applied and that the lower energy orbitals hardly contribute to the ring current at all. Actually, both CMO–NICS and ring current interpretations can be reconciled when the tensor components are interpreted instead of the isotropic NICS (see section 2.3.2.2 for details).



**Figure 5.** Occupied valence molecular orbitals of  $D_{6h}$  benzene, their energies in hartrees (in gray for  $\pi$  MOs and in black for  $\sigma$  orbitals), and MO–NICS contributions. Reprinted with permission from ref 81b. Copyright 2003 American Chemical Society.

The CMO–NICS technique has also been recently applied to study a Diels–Alder reaction involving *o*-quinodimethanes (Figure 6).<sup>116</sup> The *o*-quinodimethanes are highly reactive in the presence of dienophile because a Diels–Alder cycloaddition re-establishes a benzenoid ring, which results in aromatic stabilization.



**Figure 6.** The reactant, transition state, and product for the Diels–Alder cycloaddition. Reprinted with permission from ref 116. Copyright 2003 American Chemical Society.

The degree of aromaticity of this benzenoid ring along the geometries of the Diels–Alder reaction path and the role of the  $\pi$  orbitals has been studied in terms of orbital shape, energies, and magnetic aromaticity contributions.  $\delta$   $^{13}\text{C}$  NMR and CMO–NICS calculations showed, for instance, that the aromatic character of the benzenoid ring increases along the Diels–Alder reaction path, especially between the

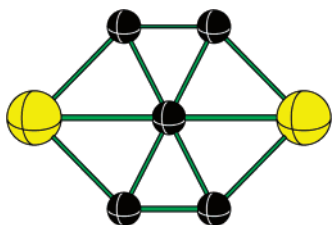
transition state and the formation of the product, even though the number of  $\pi$  orbitals drops from five for the reactants to three for the products.

In addition, CMO–NICS has been demonstrated to be a useful tool for analyzing aromaticity in metal ring and highly symmetrical clusters. For instance, the diatropic contribution of the  $\sigma$  system of the very recently reported gas-phase ( $C_s$ )  $\text{Al}_4\text{Li}_3^-$  species<sup>119</sup> is found to overcome antiaromatic character of the  $\pi$ -system.<sup>117a</sup> Analyzing the individual  $\pi$ -orbital MO–NICS contributions reveals that the lower-lying  $\pi$ -MO is diamagnetic (–12.9 ppm) but the higher-lying  $\pi$ -MO is paramagnetic (+27.1 ppm). The much stronger paramagnetic effect dominates; hence, the  $4e^-$   $\pi$ -system of  $\text{Al}_4\text{Li}_3^-$  is antiaromatic, in agreement with Boldyrev and Wang's expectation.<sup>119</sup> However, this  $\pi$ -antiaromaticity (14.2 ppm) is overcome by the diamagnetic contributions of all the  $\sigma$  orbitals together (NICS(0) $_{\sigma}$  –16.8 ppm). The total NICS(0) of –4.8 ppm at GIAO-PW91/IGLO-III discussed in ref 117a characterizes the overall weakly aromatic character of  $\text{Al}_4\text{Li}_3$  ( $C_s$ ) and contradicts the Boldyrev–Wang conclusions. This debate over aromaticity–antiaromaticity of these all-metal systems is discussed in more detail in section 3.6 and refs 120 and 121.

However, truly antiaromatic all-metal clusters do exist. The octahedral Zintl ion,  $\text{Sn}_6^{2-}$  ( $O_h$ ), prepared as a complex in the solid phase in 1993,<sup>122</sup> has a paratropic NICS(0) value at the cage center, +18.8 ppm at the GIAO-B3LYP/LanL2DZp/B3LYP/LanL2DZp level (+26.8 at the GIAO MP2/LanL2DZp//MP2/LanL2DZp level), providing evidence of its strongly antiaromatic character. Using CMO–NICS,<sup>117b</sup> the remarkable antiaromaticity of its silicon analogue,  $\text{Si}_6^{2-}$  ( $O_h$ ), and the larger  $\text{Si}_{12}^{2-}$  ( $I_h$ ) cluster has been shown recently to be related to the high symmetry. The contrasting magnetic behavior of the isoelectronic octahedral  $\text{B}_6\text{H}_6^{2-}$  and  $\text{Si}_6^{2-}$ , as well as their icosahedral analogues  $\text{B}_{12}\text{H}_{12}^{2-}$  and  $\text{Si}_{12}^{2-}$  is perfectly reflected by their CMO–NICS contributions. The *complete offset* of diatropicity by the very paratropic 3-fold degenerate  $t_{1u}$  orbitals (HOMO) in  $\text{Si}_6^{2-}$  ( $t_{1u}$ -NICS = +34.2 ppm) contrasts with the *partial offset* in  $\text{B}_6\text{H}_6^{2-}$  ( $t_{1u}$ -NICS = +14.4 ppm). The energy lowering of the  $t_{1u}$  orbital (HOMO – 1) in  $\text{B}_6\text{H}_6^{2-}$  is due to mixing with the orbitals of the external hydrogens, resulting in a decrease of the paratropicity.<sup>123</sup> The behavior of the  $\text{Si}_{12}^{2-}$  and  $\text{B}_{12}\text{H}_{12}^{2-}$  icosahedrons is analogous, but the contrast is even more pronounced due to the 5-fold degeneracy of the  $h_g$  frontier orbitals.

Finally, in a recent study of molecules based on the smallest carbon cluster containing a tetracoordinate carbon ( $\text{C}_5^{2-}$ ), NICS, HOMO–NICS, and  $^{13}\text{C}$  NMR chemical shifts were calculated to complement reactivity indexes and molecular scalar fields.<sup>118</sup> This theoretical analysis indicated that the lithium salt,  $\text{C}_5\text{Li}_2$ , is the most plausible candidate for experimental detection (see Figure 7) due to Coulomb stabilization. For instance, the paratropic character of the HOMO in neutral  $\text{C}_5\text{Li}_2$  is found to be reduced by 10 ppm as compared to the dianion,  $\text{C}_5^{2-}$ .

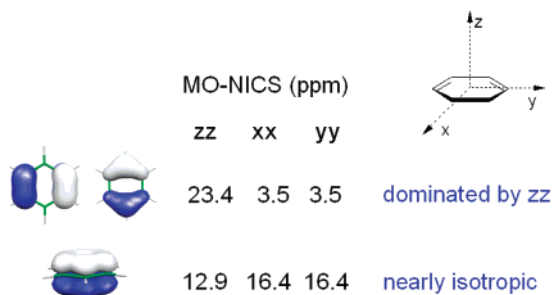
**2.3.2.2. Reconciliation between NICS and Current Density Plots.** CMO–NICS analysis on  $[n]$ -



**Figure 7.** Schematic representation of  $C_5M_2$  structures, where M is the metal cation.

annulenes<sup>81b</sup> concludes that the NICS contributions of the lowest-energy  $\sigma$  and  $\pi$  orbitals are the largest. The  $\pi$  contributions are dominated by the lowest-energy  $\pi$  orbital (with no nodes in going around the ring) in agreement with the Hückel energies and the London–Hückel magnetic susceptibility expression.<sup>124</sup> However, this conclusion appears to contradict Fowler et al.,<sup>77b</sup> who find that the *frontier*  $\pi$  orbitals of  $[n]$ -annulenes (rather than the lowest-energy  $\pi$  orbital) are mainly responsible for the ring current density when an external magnetic field is applied perpendicularly to the molecular ring plane, “In all cases [annulenes], the HOMO contribution to the ring current density map is almost indistinguishable from the total  $\pi$  current!”<sup>77b</sup>

Steiner and Fowler<sup>77b</sup> are discussing ring current densities parallel to the molecular plane arising from a perpendicular magnetic field. In contrast, (CMO–)NICS corresponds to one-third of the trace of the shielding tensor at the ring center, which takes into account the magnetic field applied in all three space directions. Therefore, important features inherent to each component are masked when considering the average isotropic values of NICS. Indeed, analysis of the NICS tensor components show that the contributions of the frontier orbitals are dominated by the  $zz$ -component of the shielding tensor (or the NICS tensor), which arises from a current density in the  $xy$  plane, while the zero-node orbitals have considerable contributions from all components of the shielding tensor (see Figure 8).<sup>81c</sup> Hence, the analysis of the CMO–NICS tensor components rather than the isotropic values is in agreement with orbital current density plots, which suggest that the ring current density arises mostly from HOMO contribution.

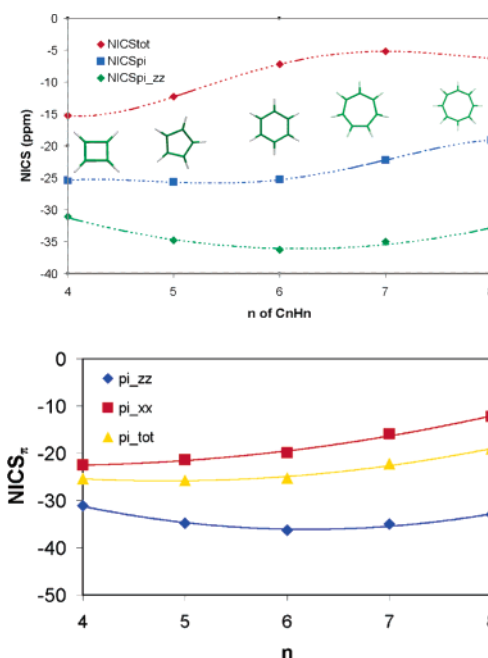


**Figure 8.** Components of the  $\pi$  MO contributions to the NICS tensor of benzene at the ring center.

Another motivation for analyzing the NICS tensor components lies in the apparent underestimation of the aromatic character of the benzene molecule as compared to other  $D_{nh}$   $[n]$ annulenes using NICS. For

a chemist, benzene is the prime example for an aromatic compound, and no other single, neutral ring molecule is considered to be more aromatic than benzene. According to the harmonic oscillator model,<sup>48a</sup> an aromatic compound should have C–C bond lengths of 1.388 Å and bond angles of 120° rationalized by the  $sp^2$  hybridization of the participating carbon atoms. The compound with the most compatible structure to this requirement is  $D_{6h}$   $C_6H_6$ . Therefore, benzene should represent the ideal aromatic molecule.

The behavior of the isotropic NICS,  $NICS_\pi$ , as well as the  $NICS_\pi$  tensors, suggests that the components parallel to the molecule,  $NICS_{xx}$  and  $NICS_{yy}$ , monotonically decrease with the ring size. But interestingly  $NICS_{\pi zz}$  versus the ring size has a nearly parabolic form, with a minimum, as expected, at benzene. These results confirm  $NICS_{\pi zz}$  to be a superior NICS-based aromaticity index compared to the isotropic NICS (see Figure 9). Most recently Ruiz-Morales<sup>125</sup> employed the total  $NICS_{zz}$  in and above the ring plane to characterize the aromaticity of polycyclic aromatic hydrocarbons and to validate their new topological aromatic criteria, so-called the Y-rule.



**Figure 9.** (a) Isotropic NICS,  $NICS_\pi$ , and  $NICS_{\pi zz}$  component, and (b)  $NICS_\pi$  tensor components against the ring size  $n$  in a series of six  $\pi$  electron annulenes at the ring centers (in ppm).

## 2.4. Comparison of NICS-Based Methods

The comparison of the NICS,  $NICS_\pi$ , and CMO–NICS performance for a series of small molecules is summarized in Table 4. The results are nicely complementary, and all aromatic compounds exhibit negative NICS. However, a careful examination of the results reveals subtle discrepancies. (i) The  $NICS(0)$  of benzene complexed by  $Cr(CO)_3$  is larger than the  $NICS(0)$  of benzene. However,  $NICS_\pi$  concludes that the  $\pi$  systems of these two molecules exhibit a very similar diatropicity. (ii) For the transition metal-

**Table 4.** The Molecular Radius,  $R_{\text{mol}}$  (in Å), NICS, NICS $_{\pi}$ , and MO-NICS ( $\sigma$  and  $\pi$  Contributions with 0 and 1 Nodes along the Ring, Respectively)<sup>a</sup>

	$R_{\text{mol}}$	NICS(0)						NICS(1)	
		NICS	NICS $_{\pi}$	NICS $_{\sigma 0}$	NICS $_{\sigma 1}$	NICS $_{\pi 0}$	NICS $_{\pi 1}$	NICS	NICS $_{\pi}$
C <sub>6</sub> H <sub>6</sub> ( $D_{6h}$ )	1.386	−8.9	−20.7	−8.9	−15.2	−3.6	−5.1	−10.6	−9.7
C <sub>4</sub> H <sub>4</sub> ( $D_{2h}$ )	1.033	+21.5	+0.9	−17.8	−23.8	−2.6	+25.2	+13.3	+14.8
Cr(CO) <sub>3</sub> C <sub>6</sub> H <sub>6</sub> ( <b>21</b> , $C_{3v}$ )	1.407	−24.2	−21.0					−12.0	−7.4
C <sub>5</sub> H <sub>5</sub> <sup>−</sup> ( $D_{5h}$ )	1.204	−15.0	−22.1	−12.6	−18.9	−3.8	−3.4	−11.0	−6.6
C <sub>7</sub> H <sub>7</sub> <sup>+</sup> ( $D_{7h}$ )	1.609	−6.7	−17.5	−6.1	−11.2	−3.6	−5.5	−9.5	−9.7
C <sub>8</sub> H <sub>9</sub> <sup>+</sup> ( <b>22</b> , $C_s$ )	1.718	−10.9	+1.3 <sup>a</sup>	−6.7 <sup>b</sup>	−4.2/−4.0 <sup>b</sup>	+4.6 <sup>b</sup>	−3.2/−0.1 <sup>b</sup>	−14.0	+0.5

<sup>a</sup> All values at the IGLO–PW91/IGLO-III level, except MO–NICS at GIAO–PW91/IGLO-III level of theory. All data were from ref 126. <sup>b</sup> For C<sub>8</sub>H<sub>9</sub><sup>+</sup>, a clear classification of  $\sigma$  and  $\pi$  contributions is impossible due to strong mixing of the contributions.

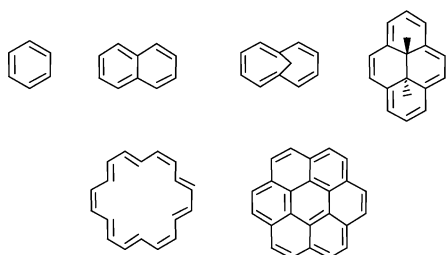
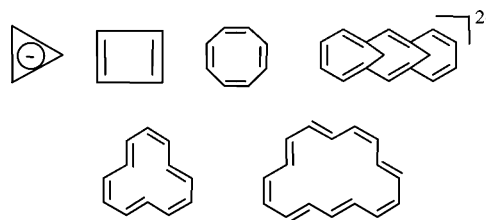
containing compounds, the falloff of the  $\pi$  contributions is much faster than in benzene itself. (iii) NICS(0) debatably suggests a stronger diatropic ring current in nonplanar homotropylium cation C<sub>8</sub>H<sub>9</sub><sup>+</sup> (**22**) than in benzene itself (−10.9 vs −8.9 ppm). However, NICS $_{\pi}$  and MO–NICS analysis conclude that the diatropic character of this molecules is mainly due to its  $\sigma$  framework. The  $\pi$ -like orbitals of **22** give very small contributions to the total NICS, resulting in a nearly zero NICS $_{\pi}$ . Note that a clear separation between  $\sigma$  and  $\pi$  MOs is not possible for a nonplanar molecule, thus the dissection into  $\sigma$  and  $\pi$  contributions is only qualitative.

In summary, every approach has its own drawback. It is therefore essential to combine various approaches before reaching appropriate conclusions. In addition, the systematic examination of the out-of-plane component of NICS $_{\pi}$  is strongly recommended.

### 3. Selected Applications

#### 3.1. Aromaticity in Annulenes

Annulenes are higher (CH)<sub>*n*</sub> ring homologues of benzene. The unusual chemical and physical properties of aromatics as compared to their linear counterparts (unsaturated straight chains) can be attributed to the presence of complete cyclic conjugation in the former structures. The major breakthrough to the understanding of the nature of cyclic conjugated compounds came from Hückel,<sup>33</sup> who predicted that the structures involving  $(4n + 2)$   $\pi$  electrons would have special benzene-like properties. Hence the name *aromatic* was coined for structures depicted in Figure 10. The analogous compounds having  $4n$   $\pi$  electrons and contrasting properties to those of benzene were termed *antiaromatic* (structures as in Figure 11).<sup>7</sup> However, the name annulenes was suggested for all conjugated cyclic structures irrespective of their properties. Thus, benzene is the smallest neutral and stable annulene and is hence sometimes referred to

**Figure 10.** Examples of aromatic molecules.**Figure 11.** Examples of antiaromatic molecules.

as [6]annulene. In general, the application of NICS to characterize simple and complex annulenes as aromatic or antiaromatic, based on the ring currents, has been successful.<sup>75,81,103,128</sup>

##### 3.1.1. Aromatic Annulenes

Longuet-Higgins and Salem,<sup>129</sup> as well as later Coulson and Dixon,<sup>130</sup> predicted that the smaller cyclic fully conjugated polyenes would have delocalized structures while the higher analogues would have localized structures with significant CC bond alternation. The first stable and neutral compound belonging to Hückel series, benzene, prefers a delocalized structure with equal CC bond lengths.<sup>131</sup> Shaik and Hiberty have stressed that  $\sigma$  frameworks favor regular geometries while the tendency of  $\pi$  orbitals is to prefer bond alternation.<sup>14,132</sup> The unusual  $D_{6h}$  benzene is thus due to its CC  $\sigma$  framework. As Shaik and co-workers<sup>132e</sup> pointed out, the preference for CC bond alternation or delocalization in larger annulenes depends on a “fine balance between  $\sigma$  resistance and  $\pi$  distortivity.” Obviously, the bond length alternation in [*n*]annulenes should set in beyond a certain size. However, the critical value of “*n*” had not been established with certainty till recently.

In 1959, Longuet-Higgins and Salem predicted a bond alternating structure for [30]annulene.<sup>129</sup> However, in 1965, Dewar showed that the preference for localized structure starts at  $n = 22$ .<sup>133</sup> The 1972 and 1995 X-ray structures of [14]annulene<sup>134</sup> and [18]annulene,<sup>135</sup> respectively, showed small CC bond alternation in these structures. Yoshizawa’s semiempirical method with appropriate corrections for electron correlation showed that the tendency of annulenes toward CC bond alternation starts at  $n = 30$ .<sup>136</sup> Kertesz and Choi further verified these results at the B3LYP density functional level.<sup>137</sup> Schleyer and Schaefer disagreed with these results and stated that the level of theory used by Kertesz and by Yoshizawa was inadequate and that a highly correlated method is required for studying these large annulenes.<sup>138</sup>



**Table 5. Relative Energies ( $E_{\text{rel}}$ , kcal/mol), Isomerization Stabilization Energies<sup>21</sup> (ISE, kcal/mol), Total NICS(0) and Dissected  $\pi$  Contributions (at the Ring Centers), Magnetic Susceptibility Exaltations ( $\Lambda$ , cgs-ppm), and Averaged Inner and Outer <sup>1</sup>H NMR Chemical Shifts of the  $[n]$ Annulenes**

$[n]$	symm	method	$E_{\text{rel}}$	ISE <sup>a</sup>	NICS(0)	NICS( $\pi$ )	$\Lambda^b$ ( $\Lambda^c$ )	$\delta$ H <sub>inner</sub>	$\delta$ H <sub>outer</sub>
6	$D_{3h}$	B3/HF	4.5 <sup>d</sup>		-8.3	-20.1			7.5
	$D_{6h}$	B3/B3	0.0	34.7	-8.8	-20.7	-17.9 (-15.8)		7.5
10	$C_s$	B3/HF	2.9	31.1	-28.8	-17.7	-52.8 (-54.0)	-5.7	8.4
	$C_{2v}$	B3/B3	0.0	32.6	-28.6	-17.7	-56.6 (-64.2)	-5.9	8.7
14	$C_{2v}$	B3/HF	10.4	20.9	-7.5	-10.7	-71.8 (-79.9)	-1.8	8.5
	$D_{2h}$	B3/B3	0.0	26.7	-13.4	-15.7	-120.5 (-137.3)	-7.5	10.1
18	$D_{3h}$	B3/HF	12.0	21.9	-5.9	-8.4	-99.7 (-105.9)	-1.6	8.8
	$D_{6h}$	B3/B3	0.0	27.4	-15.9	-15.9	-235.9 (-257.4)	-11.2	11.8
22	$C_{2v}$	B3/HF	13.1	21.2	-4.9	-6.8	-114.8 (-122.1)	-0.8	8.8
	$D_{2h}$	B3/B3	0.0	26.3	-15.2	-16.2	-394.3 (-416.7)	-14.1	13.3
26	$C_{2v}$	B3/HF	13.9	20.5	-3.9	-5.0	-124.3 (-131.4)	0.1	8.7
	$D_{2h}$	B3/B3	0.0	24.9	-15.8	-16.1	-636.4 (-599.1)	-17.0	15.2
30	$D_{3h}$	B3/HF	14.8	20.1	-3.0	-3.9	-126.9 (-133.2)	1.1	8.5
	$D_{3h}$	B3/B3	0.0	23.6	-13.8	-14.4	-760.8 (-741.2)	-16.1	15.6
42	$D_{6h}$	B3/B3	0.3		-16.2	-16.5	-979.2	-20.0	17.2
	$D_{3h}$	B3/HF	18.6	20.7	-1.1		-91.0 (-89.3)	3.6	7.7
54	$D_{3h}$	B3/B3	0.0	22.9	-5.6		-924.2 (-940.9)	-6.5	10.8
	$D_{6h}$	B3/B3	1.9		-16.7		-2637.9	-28.8	21.7
66	$D_{3h}$	B3/HF	23.3	20.8	0.0		-54.0 (-46.7)	4.8	4.9
	$D_{3h}$	B3/B3	0.0	22.5	-2.6		-903.6 (-900.0)	-1.3	8.7
66	$D_{6h}$	B3/B3	3.8		-17.0		-5567.0	-37.2	28.0
	$D_{3h}$	B3/HF	28.3	20.8	0.1		-32.6 (-21.1)	5.0	4.8
66	$D_{3h}$	B3/B3	0.00	22.4	-1.2		-770.2 (-760.3)	1.7	7.2
	$D_{6h}$	B3/B3	6.1		-17.1		-10127.6	-45.0	34.5

<sup>a</sup> Evaluated using the  $[n]$ annulene derivatives in Scheme 1. <sup>b</sup>  $\Lambda = \chi_M - \chi'_M$ . Magnetic susceptibilities of aromatic annulenes,  $\chi_M$ , at CSGT-B3LYP/6-31+G\*\*/(for  $n \leq 30$ ) and at CSGT<sup>145</sup>-B3LYP/6-31G\*\*/ (for  $n > 30$ ); magnetic susceptibilities of nonaromatic annulenes,  $\chi'_M$ , evaluated by using increments.<sup>146</sup> <sup>c</sup> Values in parentheses are  $\Lambda$  based on Scheme 1 at CSGT-B3LYP/6-31+G\*\*/ for  $n \leq 30$  and at CSGT-B3LYP/6-31G\* for  $n > 30$ . <sup>d</sup> With fixed 1.449 and 1.350 CC lengths.

Their results obtained at the KMLYP/6-311+G\*\* matched those at the CCSD(T) level and confirmed that the bond alternation in annulenes takes preference over the delocalized structure for  $n = 14$  ([14]-annulene). They further stated that the X-ray structures of [14]- and [18]annulene were incorrect because their associated <sup>1</sup>H NMR chemical shifts are in disagreement with the experimentally measured  $\delta$  values. Thus, the presently accepted critical value of  $n$ , at which the bond alternation sets in, is 14. Since nearly equal CC bond lengths are not expected for larger annulenes, the following questions arise:

How does bond alternation affect aromaticity?

Are the largest annulenes, such as [66]annulene, still aromatic?

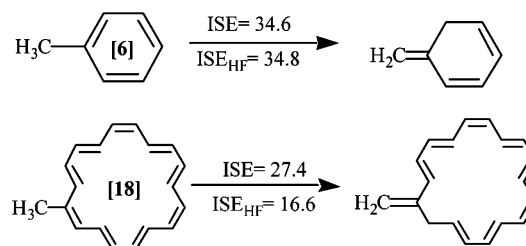
Do the diatropic properties of aromatics disappear gradually or suddenly?

Since several authors<sup>36e,139</sup> have criticized geometric, energetic, and magnetic criteria without providing alternative means for characterizing diatropic currents in cyclic conjugated structures, the effects of bond alternation on the aromaticity of large annulenes are best evaluated by focusing on all of the above criteria with special emphasis on magnetic properties (NICS, NICS( $\pi$ ), magnetic susceptibility exaltations, and <sup>1</sup>H NMR chemical shifts).

**3.1.1.1. Geometric and Energetic Criteria.** At the Hartree–Fock (HF) level,  $[n \geq 10]$ annulenes prefer a bond alternating structure, while the B3LYP optimization leads to a delocalized structure for  $n \geq 30$ .<sup>137b,140</sup> However, the energy difference between the highly symmetrical structure ( $D_{6h}$ ) and lower symmetry ( $D_{3h}$ ) for  $n \geq 30$  (i.e., [30]-, [42]-, [54]-, and [60]-annulene) increases steadily from 0.26 to 6.1 kcal/mol at the B3LYP level. Schaefer et al. have indicated

that the neither B3LYP nor HF (and MP2) level is appropriate to study annulenes because these methods, respectively, overestimate and underestimate energies.<sup>141</sup> Nevertheless careful calibration shows that HF geometries (but not the energies) agree with that given by the highly correlated CCSD(T). However, KMLYP,<sup>142</sup> a hybrid functional containing a greater HF component, gives not only geometries but also energies in agreement with that of CCSD(T).<sup>138</sup> KMLYP optimization of the cyclic conjugated structures indicates that the bond alternation starts at [14]annulene. However, we restrict to the results obtained from Hartree–Fock (HF) and B3LYP levels in the following discussions on annulenes.

Dewar predicted that large annulenes reach a stabilization energy of 2.8 kcal/mol.<sup>41d</sup> In contrast to his prediction, data in Table 5 indicated that at the HF as well as at the B3LYP level the ASEs (evaluated using the equations from Scheme 1) of large

**Scheme 1**

annulenes reach a plateau of 20 and 22 kcal/mol, respectively. Also evident from Table 5 is that *ISE per  $\pi$ -electron* decreases with the increasing ring size. However, a sharp decrease in ASE at the HF level



indicates that the aromaticity of  $[4n + 2]$ annulenes decreases rapidly with size. Nevertheless, the steady decrease of ASEs (at the B3LYP/6-31G\* level) for  $n \geq 30$  annulenes shows that bond localization, in large annulenes, does not result in major loss in aromaticity.

**3.1.1.2. Magnetic Criteria.** In general, criteria based on magnetic properties, although sometimes criticized,<sup>36e,100,139</sup> very well support the conclusions given by the ASE data.<sup>59b,98,143</sup> The magnetic susceptibility exaltations,<sup>44</sup>  $\Lambda$ , increase with increasing ring size up to  $n \leq 30$  (Table 5). The curve then falls off for the realistic B3LYP-optimized  $D_{3h}$  geometries. However,  $\Lambda$  of the larger annulenes ( $n > 30$ ) continues to rise for the higher symmetry structures. The increase in  $\Lambda$  for larger annulenes does not necessarily indicate an increase in aromaticity because the dependence of magnetic susceptibility exaltation on the product of ASE and the square of ring area is well established.<sup>144</sup> Moreover, Table 5 also indicates that the aromatic character retained in the B3LYP-optimized annulene geometries is larger than that for the HF ones.

Similar to  $\Lambda$ , the computed proton chemical shifts are also quite sensitive to the bond alternation effects. The  $\delta$   $^1\text{H}$ 's of the inner and the outer protons in annulenes differ dramatically (Table 5) from those of normal alkenes ( $\delta = 5.6$  for cyclohexene). The chemical shifts of outer H's are shifted downfield (also from those of benzene,  $\delta = 7.2$ ) whereas the inner H's resonate further upfield, indicating the presence of strong diatropic ring currents in these annulenes. The  $\delta$   $^1\text{H}$ 's computed on the most symmetrical B3LYP geometries (Table 5) show steady increase to very large negative ( $H_{\text{inner}}$ ) and positive ( $H_{\text{outer}}$ ) chemical shift values, but these do not correlate with the experimental<sup>134,147</sup>  $\delta$   $^1\text{H}$ 's (e.g., for [14]-, [18]-, and [22]-annulene).

The behavior of the computed  $\delta$   $^1\text{H}$ 's using the bond localized HF-optimized annulene geometries is quite different. The inner–outer  $\delta$   $^1\text{H}$  difference is largest for  $n = 10$  but then decreases with increasing ring size, slowly at first and then rapidly to the vanishing point. There is no  $\delta$   $^1\text{H}$  difference between the olefin-like outer and the inner proton for [54]- and [66]-annulene using the  $D_{3h}$  HF geometries. The less bond length-alternating B3LYP-optimized  $D_{3h}$  [ $n > 30$ ]-annulene geometries result in an intermediate behavior: the inner–outer  $\delta$   $^1\text{H}$  differences decrease steadily with ring size.

The NICS (NICS(0) as well as its dissected  $\pi$  contribution, NICS( $\pi$ ), in Table 5) values, which depend markedly on the geometry for [ $n > 10$ ], correlate very well with the behavior of  $^1\text{H}$  NMR chemical shifts. For example, the magnitudes of NICS are largest for the  $D_{6h}$  geometries, moderate for the B3LYP  $D_{3h}$  minima, and smallest to negligible for the HF geometries.

Table 5 indicates that NICS correlates well with energies (as well as with geometries and with other magnetic criteria). The negative NICS(0) and NICS( $\pi$ ) values (Table 5) denote that the highest symmetry (bond equalized) annulene geometries are all aromatic. NICS(0) reaches a constant value of about  $-17$

(Table 5) for these largest annulenes. The NICS(0) values for the HF-optimized do not agree with those for  $D_{3h}$  B3LYP minima. These values decrease rather rapidly with increasing size, sooner along the HF than the B3LYP series. NICS(0) follows the ISE per  $\pi$ -electron behavior and also  $\Lambda$  and the  $^1\text{H}$  chemical shifts trend. However, the  $\Lambda$ , ISE, and  $^1\text{H}$  NMR chemical shift but not NICS(0) predict that the B3LYP-optimized  $D_{3h}$  bond alternating structure of [66]annulene retains significant aromatic character. Although the HF-optimized bond alternating [54]- and [66]annulenes have large ISEs, the  $\Lambda$ 's,  $^1\text{H}$  NMR chemical shift differences, and NICS (Table 5) are very small; evidently these annulenes behave more like long chain cyclic polyenes.

Despite the divergence in the data at different levels and geometries, the best interpretations of all the criteria investigated generally agree in revealing the major trends along the [ $n$ ]annulene series. Structurally, the trend toward greater bond alternation follows the increases with ring size; its onset for partial localization occurs at  $n = 10$  at HF/6-31G\* but at  $n = 30$  at B3LYP/6-31G\*. The ASE per  $\pi$ -electron decreases to very small values with increasing ring size of annulenes. The magnetic criteria are very sensitive to the geometries. Thus  $\Lambda$ , NICS, and the  $^1\text{H}$  NMR chemical shifts show marked changes with small changes in annulene geometry; however, more realistic lower-symmetry structures follow the trend to smaller aromaticity. The effect of bond localization on benzene is negligible; magnetic properties are hardly changed. The HF  $D_{3h}$  forms of the largest annulenes show nonaromatic  $\delta$   $^1\text{H}$  behavior; also, their ISE/ $\pi$ -electron,  $\Lambda$ , and NICS values are quite small.

### 3.1.2. Antiaromatic Annulenes

[ $4n$ ]Annulenes in the earlier days were described as pseudoaromatic<sup>148</sup> because they lacked benzene-like stabilization and their behavior closely resembled that of polyenes. Breslow coined the term antiaromatic based on the evidence that the  $\pi$ -electron interactions in small  $4\pi$  systems (like cyclopropenium anion and cyclobutadiene) are destabilizing.<sup>7</sup> Wiberg's 2001 review<sup>149</sup> on aromaticity concluded that "when the ring size becomes larger, the antiaromatic character is decreased and is small even with cyclooctatetraene" However due to complications arising from ring strain, Wiberg did not evaluate destabilization energies in [ $4n$ ]annulenes. The destabilization energies in [ $4n$ ]annulenes were uniformly evaluated using the Hückel theory and its subsequent refinements. Using Dewar's concept of "resonance energy per electron" (REPE), Hess and Schaad<sup>41e,46a</sup> showed that the antiaromatic character in [ $4n$ ]annulenes decreases (REPE becomes less and less negative) as the size increases and that cyclobutadiene has the largest negative REPE. Consequently, it is of interest to evaluate the [ $4n$ ]annulenes ring size effect on various aromaticity criteria.

**3.1.2.1. Geometric and Energetic Criteria.** The difference in the length between the smallest and the longest bonds ( $\Delta r$ ) provides a measure of geometric aromaticity index in forced planar [ $4n$ ]annulenes.

**Table 6. The Difference between Shortest and Longest [4*n*]Annulene Bond Length ( $\Delta r$ ), Syn–Anti Corrected<sup>150</sup> Isomerization Stabilization Energies (kcal/mol) Evaluated by the Schleyer–Pühlhofer Method (ISE<sub>Spcorr</sub>, Scheme 2), Magnetic Susceptibility Exaltations ( $\Lambda$ , cgs·ppm), and Averaged Inner ( $\delta H_{\text{inner}}$ ) and Outer ( $\delta H_{\text{outer}}$ ) <sup>1</sup>H NMR Chemical Shifts of the Antiaromatic [4*n*]Annulenes in Planar Bond Alternating Geometries<sup>a</sup>**

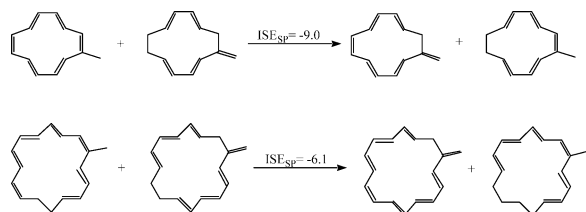
[ <i>n</i> ]	symm	$\Delta r$ (Å)	ISE <sub>Spcorr</sub>	$\Lambda$	NICS(0)	NICS(0) <sub>π</sub>	$\delta H_{\text{inner}}$	$\delta H_{\text{outer}}$
6	<i>D</i> <sub>6h</sub>	0.000	33.2	−17.6	−8.8	−20.7		7.5
4	<i>D</i> <sub>2h</sub>	0.243	−35.2	13.0	20.8	−0.2		5.9
8	<i>D</i> <sub>4h</sub>	0.130	0.6	79.4	35.9	28.4		2.0
12	<i>D</i> <sub>2h</sub>	0.174	−9.0	98.8	24.5	19.2	32.4	2.8
16	<i>D</i> <sub>2h</sub>	0.129	−6.1	187.7	23.4	20.2	33.1	0.9
20	<i>D</i> <sub>2h</sub>	0.110	−4.8	296.6	21.5	19.5	33.3	1.4
24	<i>C</i> <sub>s</sub>	0.087	−3.1	407.3	19.3	18.1	33.0	−1.9

<sup>a</sup> ISE<sub>Spcorr</sub> was evaluated at B3LYP/6-31G\* + ZPE (B3LYP/6-31G\*) + syn–anti corrections (Scheme 2).  $\Lambda = \chi_M - \chi'_M$ . Magnetic susceptibilities of parent [4*n*]annulenes,  $\chi_M$ , were calculated at CSGT-B3LYP/6-31+G\*/B3LYP/6-31+G\*; magnetic susceptibilities of nonaromatic models,  $\chi'_M$ , were evaluated using increments. NICS(0), NICS(0)<sub>π</sub>,  $H_{\text{outer}}$ , and  $H_{\text{inner}}$  were calculated at IGLO/TZ2P/B3LYP/6-31G\*.

With the exception of cyclooctatetraene ( $\Delta r = 0.130$  Å), there is a regular decrease in the  $\Delta r$  value from cyclobutadiene (0.243 Å) to [24]annulene (0.087 Å). The  $\Delta r$  value for the interior of long chain conjugated polyene is 0.078 Å. Thus based on the geometric aromaticity criteria, as the ring size increases [4*n*]annulenes tend to behave like polyenes.

Table 6 indicates that all the [4*n*]annulenes are destabilized and that the larger ones are destabilized only to a small extent. Surprisingly, but in accordance with experimental results<sup>147b,151</sup> and molecular mechanics calculations,<sup>152</sup> cyclooctatetraene's (COT) ISE is close to zero, indicating that this antiaromatic annulene is destabilized minimally. In general, the ISE values, computed using Scheme 2 and indicated in Table 6, show that all the [4*n*]annulenes, with the exception of cyclobutadiene,<sup>153</sup> are not destabilized appreciably.

#### Scheme 2



**3.1.2.2. Magnetic Criteria.** In contrast to energies, more sensitive measures of [4*n*]annulene antiaromaticity are provided by the  $\Lambda$  and the <sup>1</sup>H NMR chemical shifts, as well as NICS and its dissection. These properties are influenced directly by the special ring current effects attributable to the cyclic  $\pi$ -electron conjugation.

The magnetic susceptibility exaltation,  $\Lambda$ , is known experimentally for only a few [4*n*]annulenes.<sup>44</sup> The computed  $\Lambda$  of *D*<sub>4h</sub> COT is large and positive (79.4 cgs·ppm, Table 6). The data in Table 6 show an increase in  $\Lambda$  from [8]- to [24]annulene. The large and positive [24]annulene  $\Lambda$  indicates unfavorable cyclic  $\pi$ -electron interactions and antiaromaticity in [4*n*]annulenes.

The computed proton chemical shifts (Table 6) are extremely sensitive to the geometries and to the cyclic  $\pi$ -electron currents. In contrast to the large antiaromatic destabilization energy of cyclobutadiene, its protons ( $\delta$  5.9) appear in the olefinic region.<sup>154</sup> Planar cyclooctatetraene ( $\delta$  2.0) and the outer H's of [12]-,

[16]-, [20]-, and [24]annulene are shifted further upfield ( $\delta$  −1.9 to +2.8), while the inner protons are strongly deshielded (downfield) and resonate at  $\delta$  ~33. The computed downfield chemical shifts of the inner H's and the upfield chemical shifts of the outer H's indicate strong paratropic ring currents in [4*n*]annulenes supporting an “antiaromatic” behavior.

NICS mirrors the behavior of the chemical shifts of the inner protons. The [4*n*]annulene NICS(0) values are large and positive due to the strong induced paratropic ring currents arising from cyclic  $\pi$ -electron interaction. *D*<sub>4h</sub> cyclooctatetraene exhibits the largest NICS(0) value among the [4*n*]annulenes set, Table 6. NICS(0) decreases, but only slightly, with increasing ring size. The large positive NICS(0) values, also comparable to  $\Lambda$  data, indicate strong paratropic ring currents in [4*n*]annulenes. Dissected NICS values are more instructive in assigning the paratropic  $\pi$ -bond contributions. The cyclobutadiene NICS(0)<sub>π</sub> value (−0.2) is exceptional in showing no net  $\pi$  contributions, but a strong but hidden paratropic influence is revealed by a more careful examination.<sup>65b</sup> The other [4*n*]annulenes have large and positive  $\pi$  contributions. Like NICS(0), NICS(0)<sub>π</sub> also is the largest at the center of planar cyclooctatetraene, but the NICS(0)<sub>π</sub> values of the other [4*n*]annulenes remain nearly the same with increasing ring size.

The [4*n*]annulene antiaromaticity criteria give somewhat inconsistent results; cyclobutadiene is exceptional in having a uniquely large destabilization energy<sup>153</sup> and positive  $\Lambda$  but exhibiting olefinic proton chemical shifts and a near-zero NICS(0)<sub>π</sub> value. The next higher analogue, planar cyclooctatetraene, has a near-zero stabilization energy, but the largest NICS(0) and NICS(0)<sub>π</sub> values. For the rest of the [4*n*]annulenes, there is regular progression in degree of bond alternation with ring size, but no notable differences in the remaining properties listed in Table 6.

The small destabilization energies in larger [4*n*] systems undermine definitions of antiaromaticity based on energy at least for systems with more than four  $\pi$  electrons. The degree of bond alternation of the antiaromatics is larger than that for conjugated olefins. While ASE does not reveal significant antiaromatic behavior of the larger [4*n*]annulenes, the computed proton chemical shifts,  $\Lambda$ , and NICS reveal

strong paratropic ring currents in these larger  $[4n]$ -annulenes.

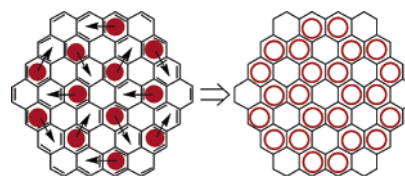
Consequently, the  $[4n]$ annulene aromaticity can be regarded as statistically multidimensional (eg. ref 98d). The larger  $[4n]$ annulenes ( $n > 1$ ) are non-aromatic energetically but exhibit an upfield chemical shift ( $\delta$  2.0) for outer protons and a positive NICS. The term “antiaromaticity,” applied to  $[4n]$ annulenes with  $n > 1$ , is better supported by their magnetic behavior, rather than by their energetic destabilization.

### 3.2. Aromaticity in Polycyclic Aromatic Hydrocarbons (PAHs)

Polycyclic aromatic hydrocarbons (PAHs) (or polycyclic benzenoid hydrocarbons (PBHs)) constitute another important class of organic molecules, which consist of two or more unsaturated rings. The aromaticity of PAHs permit their application in various field of chemistry such as conducting polymers,<sup>155</sup> organic (photo)conductors,<sup>156</sup> solar cell research,<sup>157</sup> or pigments for dyes.<sup>158</sup> In polycyclic aromatic compounds, the delocalization is not expected to be as ideal as in benzene, because of the fusion of two or more aromatic rings that perturbs the delocalization of the electrons. This, of course, leads to the question about the degree of aromaticity in PAHs.

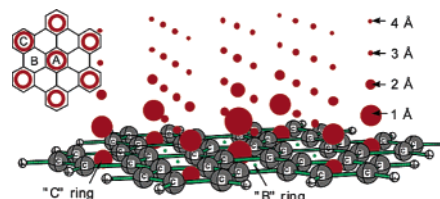
A simple and practical method to understand the aromatic stability and behavior of PAHs was developed by Clar.<sup>47</sup> In Clar's model the  $\pi$ -electrons are localized favorably in sextets as in benzene rings. The stability of the structure increases with the number of  $\pi$ -electron sextets. For instance, PAHs that can be regarded as cross-linked purely benzenoid partial systems, such as triphenylene are the most stable known.<sup>159</sup> Although Clar's model predicts many of the chemical and physical properties of PAHs (e.g., reactive positions in electrophilic aromatic substitution and bond lengths) correctly, the physical basis for its representation remains somewhat unclear.

The NICS values represent a strong theoretical support for Clar's picture of aromatic  $\pi$ -sextets. For



**Figure 12.** C<sub>96</sub>H<sub>24</sub> (27) Kekulé structure (left): the arrows show Clar sextet (solid red dot) migration, which is responsible for the NICS aromaticity pattern on the right.

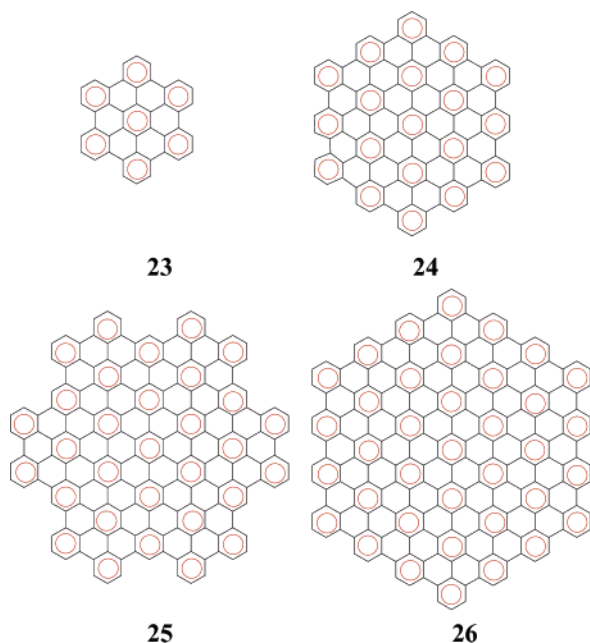
instance, Schleyer and his collaborators recently computed ring values of NICS for a series of large polybenzenoid hydrocarbons.<sup>160</sup> They concluded that only the four fully polybenzenoid hydrocarbons (i.e., all carbon atoms are members of a single sextet), C<sub>42</sub>H<sub>18</sub> (23, hexabenzocoronene), C<sub>114</sub>H<sub>30</sub> (24), C<sub>186</sub>H<sub>42</sub> (25), and C<sub>222</sub>H<sub>42</sub> (26), show the extreme NICS values, while compounds having migrating  $\pi$ -sextets (e.g., 27) show intermediate values for several rings (Figure 12). Though clear differentiated Clar sextet ring patterns occur in the molecular planes of  $D_{6h}$  PBHs (23–26), above molecular planes, uniform magnetic fields develop and graphite-like properties appear, although graphite-like PBH dimensions have not been approached. Figure 13 shows that NICS values placed above the PBH surface tend to a uniform value for even the relatively small PBH 23. Extensive studies of NICS and Clar models of the PAHs were also reported by Ruiz-Morales.<sup>125</sup>



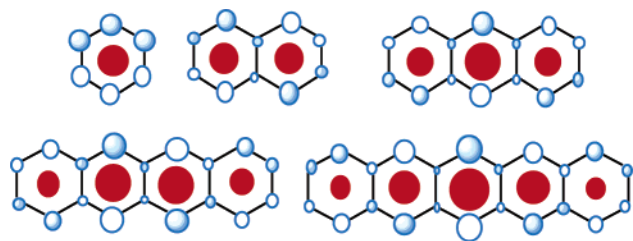
**Figure 13.** C<sub>42</sub>H<sub>18</sub> (23) NICS grid. Extending to 4 Å, the grid shows the trend toward a uniform magnetic field (i.e., NICS points develop uniform size) above PBH ring planes.

On the other hand, Schleyer et al. made a comprehensive study on the properties of linear polyacenes.<sup>161</sup> Although the chemical and physical properties of these systems seem to support a loss of benzenoid character when the number of rings increases,<sup>162</sup> it was finally concluded that the stabilization resonance energies per  $\pi$  electrons remain essentially constant from benzene to heptacene. Also, NICS calculations<sup>161</sup> along the series indicated that the inner rings actually are more aromatic than the outer rings and even more aromatic than benzene itself (Figure 14), whereas the opposite trend is observed in the case of angular polyacenes.<sup>162</sup> The more aromatic inner rings are more reactive to the Diels–Alder reaction than the less aromatic outer rings. However, the reactivities (computed activation energies) of the individual acene rings, which depend on the activation energies and the product stabilities, are not a ground-state phenomenon.

Gomes and Mallion<sup>52c</sup> summarized the relative ring currents and the relative NICS values for several middle to small conjugated hydrocarbons including anthracene, phenanthrene, and triphenylene. They



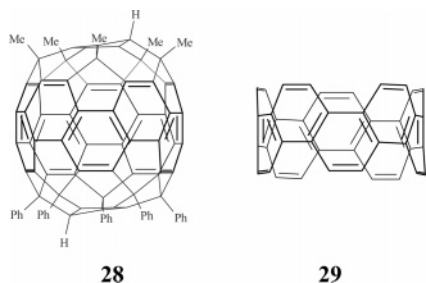




**Figure 14.** NICS(0) at the ring centers of linear arenes. The sizes of the red dots indicate that the more reactive inner rings actually are more aromatic than the less reactive outer rings and even more aromatic than benzene itself.

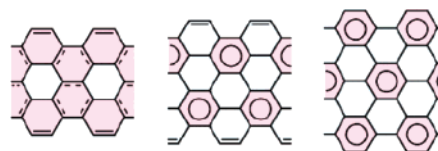
showed an overall parallelism between the results of ring currents and chemical shifts at the center of a ring of conjugated hydrocarbons. For instance, it was confirmed that the central rings in phenanthrene and triphenylene have substantially smaller ring currents and relative NICS in comparison with the peripheral rings in the same molecules. Obviously, the opposite is true for anthracene.

Besides the planar structures discussed above, PAHs also include belt- or hoop-shaped structures made of laterally fused benzenoid hydrocarbons. Such novel molecular architectures are expected to possess exciting physical and chemical properties, such as nanotube precursors. For example, the first hoop-shaped benzenoid derived from [10]cyclophenacene (**28**) was recently synthesized and studied theoreti-



cally by Nakamura and collaborators.<sup>163</sup> The NICS computation reveals a clear aromatic behavior for both the six-membered rings of cyclophenacene (−11.46 to −11.99 ppm) and its cage center (−11.58 ppm), while other rings are found to be nonaromatic (−1.27 to 0.30 ppm). This molecule represents the shortest [5,5] carbon nanotube (CNT) (**29**).

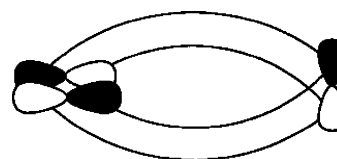
In recent studies, Nakamura et al.<sup>164</sup> extended Clar's aromatic sextet valence bond (VB) model to predict properties and reactivity of single-walled carbon nanotubes (CNTs). Using NICS analysis, Nakamura et al.<sup>165</sup> show that the chemical structures of finite-length armchair [5,5] and [6,6] CNTs fall into three different classes that maybe referred to Kelulé, incomplete Clar, and complete Clar, depending on the exact length of the tube (Figure 15). Ormsby and King<sup>166</sup> convincingly showed that the NICS values calculated for three types of short CNTs (e.g., CNTs with different roll-up vectors<sup>167</sup> ( $m,n$ )) agree perfectly with the best-constructed Clar VB models associated with each of the possible CNTs. These observations are also confirmed by the patterns exhibited by SMT images, which are consistent with the model predicted by Clar.



**Figure 15.** Chemical structure of finite-length armchair tubes: (a) Kelulé; (b) incomplete Clar; (c) complete Clar.

### 3.3. Möbius Aromaticity

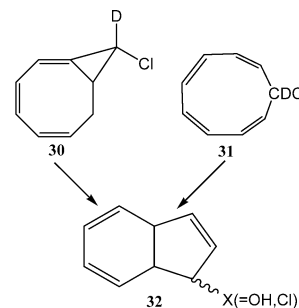
After the synthesis of large Hückel annulenes around 1964, Heilbronner suggested that singlet  $[4n]$  cyclic  $\pi$  conjugated rings of about 20 carbon members or more could incorporate a  $180^\circ$  twist and be aromatic if characterized by a Möbius topology (Figure 16).<sup>6</sup> Zimmerman soon accepted Heilbronner's idea in formulating selection rules of pericyclic reactions and generalized the Möbius–Hückel concept for the transition states.<sup>168</sup>



**Figure 16.** Schematic representation of the Möbius type overlapping p orbitals in  $(\text{CH})_9^+$ . The  $\text{C}_2$  axis lies horizontally; the carbon atom on it (right) is across from the phase inversion (left).

For ground-state molecules, generally, the ring has to be large enough to accommodate the small dihedral angle “twists” going from one carbon p orbital to the next around the annulene cycle. For example, eight- $\pi$ -electron *trans*-cyclooctatetraene does not have a Möbius-like p-orbital topology due to the reduced overlap between the p-orbitals and is nonaromatic (NICS −1.9 ppm).<sup>169</sup> However, the eight-membered ring is big enough for an eight  $\pi$  Möbius aromatic transition state;<sup>168</sup> Rzepa even designed stable seven-membered Möbius aromatic rings (see later section for details, as well as ref 170 appearing in this special issue).

In 1971, Schleyer et al. postulated a short-lived intermediate, monocyclic  $(\text{CH})_9^+$  cation, which allowed isotope label scrambling, in the solvolysis of exo-9-chlorobicyclo [6.1.0]nona-2,4,6-triene in aqueous acetone at  $75^\circ\text{C}$ .<sup>171</sup> Starting from **30**, which

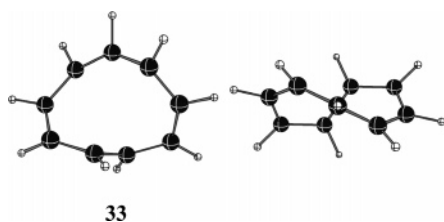


contained deuterium at C9, the bicyclic product **31** ( $\text{X} = \text{OH}$ ), containing uniformly scrambled deuterium, was isolated. Subsequently, Anastassiou and Yakali succeeded in preparing 9-chlorocyclononatriene, **32**, which (deuterated) under ionizing conditions gave uniformly scrambled deuterium product,

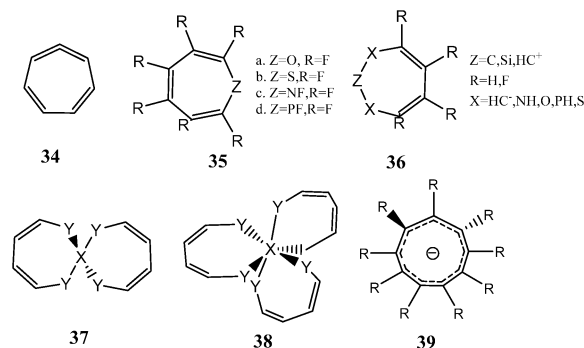


**32.**<sup>172</sup> In anticipation of antiaromatic planar cyclo-nonatetraenyl cation, Anastassiou and Yakali wondered why the ion forms so easily and how the positions could become equivalent. They represented the involved intermediate (of conversion from **31** and **32**) in a coiled conformation, which minimized the antiaromatic destabilizations.

In 1998, Schleyer et al.<sup>173</sup> reported that the computationally most stable conformation of  $(\text{CH})_9^+$  was indeed a helical  $C_2$  symmetrical structure. It was recognized for the first time that a Möbius system can exist for such a small system. Schleyer further confirmed the aromaticity of the Möbius topology structure **33** by reporting a large NICS(0) value of  $-13.4$  ppm at the ring center. Additionally, **33** represented remarkably equalized CC bond lengths and a large magnetic susceptibility value,  $-188.8$  cgs·ppm.

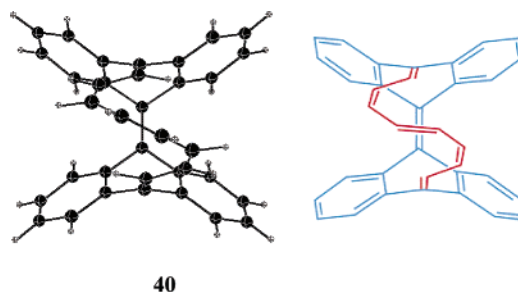


Rzepa and co-workers have discussed the electronic properties of small ring compounds containing a strained allene bond as having a Möbius topology.<sup>174</sup> However, these twisted cyclic molecules may sometimes be destabilized due to ring strain. But cyclic allene structures can adopt Möbius topology only if ring size is large. Thus, Rzepa and co-workers have designed several Möbius topology systems, e.g., **34**,<sup>175</sup>



and categorized them as aromatic based on the NICS values. Möbius heteropines<sup>176</sup> (**35**) and carbeno[8]-heteroannulenes<sup>177</sup> (**36**) with eight  $\pi$  electrons also were characterized as aromatic. The aromaticity of bis and tris spiro systems (**37** and **38**), in which each ring exhibits Möbius  $4n$   $\pi$ -electrons, was also investigated.<sup>178</sup> Several examples, like **39**, of triplet state annulenes containing  $4n + 2$   $\pi$  electrons were also predicted to be aromatic.<sup>177</sup> Schleyer and Karney have predicted several Möbius local minima of [12]-, [16]-, and [20]annulene. On the basis of the computed NICS value, they showed evidence for the presence of diatropic ring currents in these molecules.<sup>179</sup> However, they also recognized that Möbius topology in [12]-, [16]-, and [20]annulene is not the most stable isomer due to counterbalancing strain effects.

Recently, Herges et al. have synthesized the first stable neutral hydrocarbon (**40**) that possesses



Möbius topology.<sup>180</sup> Compound **40** contains a flexible polyene bridge that twists to connect the ends of a rigid bianthraquinodimethane moiety. Although **40** shows significant CC bond alternation (up to 0.157 Å) along the C16 ring perimeter, Herges et al. characterized this molecule being moderately aromatic. However, critical analysis<sup>181</sup> showed that delocalization in this core is inhibited by large dihedral angles, which hinders effective  $\pi$  overlap. Consequently, the [16]annulene core of **40** is non-aromatic and any aromatic character of **40** is confined to the benzene rings. This conclusion is supported by computed geometric ( $\Delta r$ ,  $\Delta r_m$ , Julg A, HOMA), magnetic (NICS, magnetic susceptibility exaltation), and energetic criteria of aromaticity.

### 3.4. Aromaticity in Hydrocarbon Pericyclic Reaction Transition States

Reactions in which all the first-order changes in the bonding relationships take place concertedly around a ring are called pericyclic reactions. Woodward and Hoffmann classified such processes further into five categories: sigmatropic shifts, cycloaddition, electrocyclic, cheletropic, and group transfer reactions.<sup>182</sup> A few reactions that do not fall under any category were classified as “miscellaneous” by Houk et al.<sup>183</sup> Reetz introduced yet another class, dyotropic shifts.<sup>184</sup> Recently, Herges pointed out another group of concerted transformations, “coarctate reactions”.<sup>185</sup>

Molecular rearrangements with no net change in the number of  $\pi$  and  $\sigma$  bonds ( $\Delta H \approx 0$ ) include group transfers and sigmatropic shifts. Electrocyclization and ene reactions involve transformations of a  $\pi$  bond into a  $\sigma$  bond, while under cycloadditions and cheletropic, reactions exemplify  $2\pi$  bond to  $2\sigma$  bond processes. Besides their synthetic utility,<sup>186</sup> pericyclic reactions have attracted even more attention due to the controversies over the mechanistic possibilities. Such processes can proceed stepwise involving biradical intermediates or in a concerted fashion involving synchronous formation and breaking of bonds.

As early as 1938, Evans and Warhurst<sup>3</sup> recognized the analogy between the  $\pi$  electrons of benzene and the six delocalized electrons in the cyclic transition state (TS) of the Diels–Alder reaction<sup>187</sup> of butadiene and ethylene. Evans also pointed out that “the more the enhanced mobility of the  $\pi$  electrons in the transition state, the greater will be the lowering of the activation energy.”<sup>73</sup> Thermally allowed pericyclic

reactions, based on the Woodward–Hoffmann rules, can be considered to take place preferentially through concerted<sup>188</sup> aromatic transition states, which are energetically favored.

Schleyer and co-workers,<sup>58d,60</sup> as well as others,<sup>116,189</sup> have systematically analyzed the aromaticity of pericyclic transition states on the basis of geometric, energetic, and magnetic criteria. Geometric and energetic evidence indicated that aromatic transition states have delocalized structures and large resonance stabilization (energies of concert). In addition, these structures exhibited exalted magnetic susceptibilities, magnetic susceptibility anisotropies, and abnormal <sup>1</sup>H NMR chemical shifts. NICS also has been used to characterize the delocalization in the pericyclic transition states. For instance, Schleyer et al. showed that for TSs NICS agrees well with the energetic, geometric, and various other magnetic criteria.<sup>59d,161,190</sup> Since the pericyclic TSs involve reorganization of bonds, Schleyer et al. employed the term *mobile electrons* to denote the contribution of formal  $\pi$  and  $\sigma$  bond electrons (taking part in rearrangement) to the total NICS(0) value.<sup>189k</sup> For example, the TS involved in the Diels–Alder reaction of butadiene with ethylene, **51**, has six  $\pi$  electrons. While four electrons belong to the C1–C2 and the C3–C4 of butadiene (diene) and the other two to the C5–C6 of ethylene (dienophile) in the starting reactants, these electrons are transformed to two  $\sigma$  bonds (C1–C5 and C4–C6) and a  $\pi$  bond (C2–C3) of the product, cyclohexene. Hence all these six  $\pi$  electrons, as shown by dotted line in **51** (Figure 17), are termed as mobile electrons. The following sections discuss the evidence of delocalized ring currents in different types of pericyclic reactions.

### 3.4.1. Sigmatropic Shifts

Sigmatropic rearrangements (molecular reorganizations with no change in the number of  $\pi$  or  $\sigma$  bonds) involve the movement of bonds over a conjugated system. Rearrangement can occur through a concerted mechanism (one step) or via a two-step alternative involving a biradical intermediate, as proposed by Woodward and Hoffmann. In a few cases, the stepwise mechanism dominates over the concerted alternative.

**3.4.1.1. [1,5] Sigmatropic Shifts.**<sup>191</sup> The [1,5] transition states of sigmatropic hydrogen shifts have been shown to be aromatic based mainly on energetic and magnetic criteria.<sup>60c,192</sup> We have reexamined two cases here: (*Z*)-1,3-pentadiene and cyclopentadiene (**41** and **42**).

**3.4.1.1.1. (*Z*)-1,3-Pentadiene.** Structure **41** summarizes various data pertinent to the aromaticity evaluation. The C–C bond lengths in the six-membered TS ring show little alternation (0.020 Å). The large energy of concert, 40 kcal mol<sup>−1</sup>, reported by Schleyer et al., implies a large preference for the concerted over a stepwise (biradical) mechanism<sup>60c,192</sup> The reported magnetic susceptibility exaltation, −9.9 cgs·ppm, is close to the benzene value, −13.4 cgs·ppm.

Structure **41** also shows the computed NMR proton chemical shifts. For example,  $\delta$  <sup>1</sup>H attached to C2,

C3, and C4 are in the aromatic region (7.0–7.3 ppm), downfield shifted compared to olefinic H's. The axial protons attached to C1 and C5 are much upfield (2.3 ppm) compared to the equatorial protons at C1 and C5 (4.9 ppm). Hence the NMR chemical shifts of the protons show a strong delocalized diatropic ring current in the aromatic TS, **41**. The  $\delta$  <sup>1</sup>H bridging H is more difficult to interpret because the combined contributions of the partial (C···H) bonds are less than that of a normal C–H bond.

The GIAO and IGLO–NICS in the center of the six-membered TS, −13.5 and −14.2 ppm, respectively, illustrate the general agreement between the two methods. The total contributions of the six mobile electrons (dotted line in **41**), given by the NICS dissection, −16.9 ppm, indicates a pronounced diatropic ring current and a concerted mechanism.

**3.4.1.1.2. Cyclopentadiene.** The [1,5] sigmatropic shift in cyclopentadiene shows a much lower activation barrier of 25.6 kcal/mol (Table 1) than pentadiene (36.4 kcal/mol).<sup>60c,191,192</sup> The energy of concert, 50 kcal/mol, also is larger and favors the concerted over a stepwise mechanism. Notably the magnetic susceptibility exaltation, −8.9 cgs·ppm, of the TS is lower than that of the pentadiene TS (−9.9 cgs·ppm).

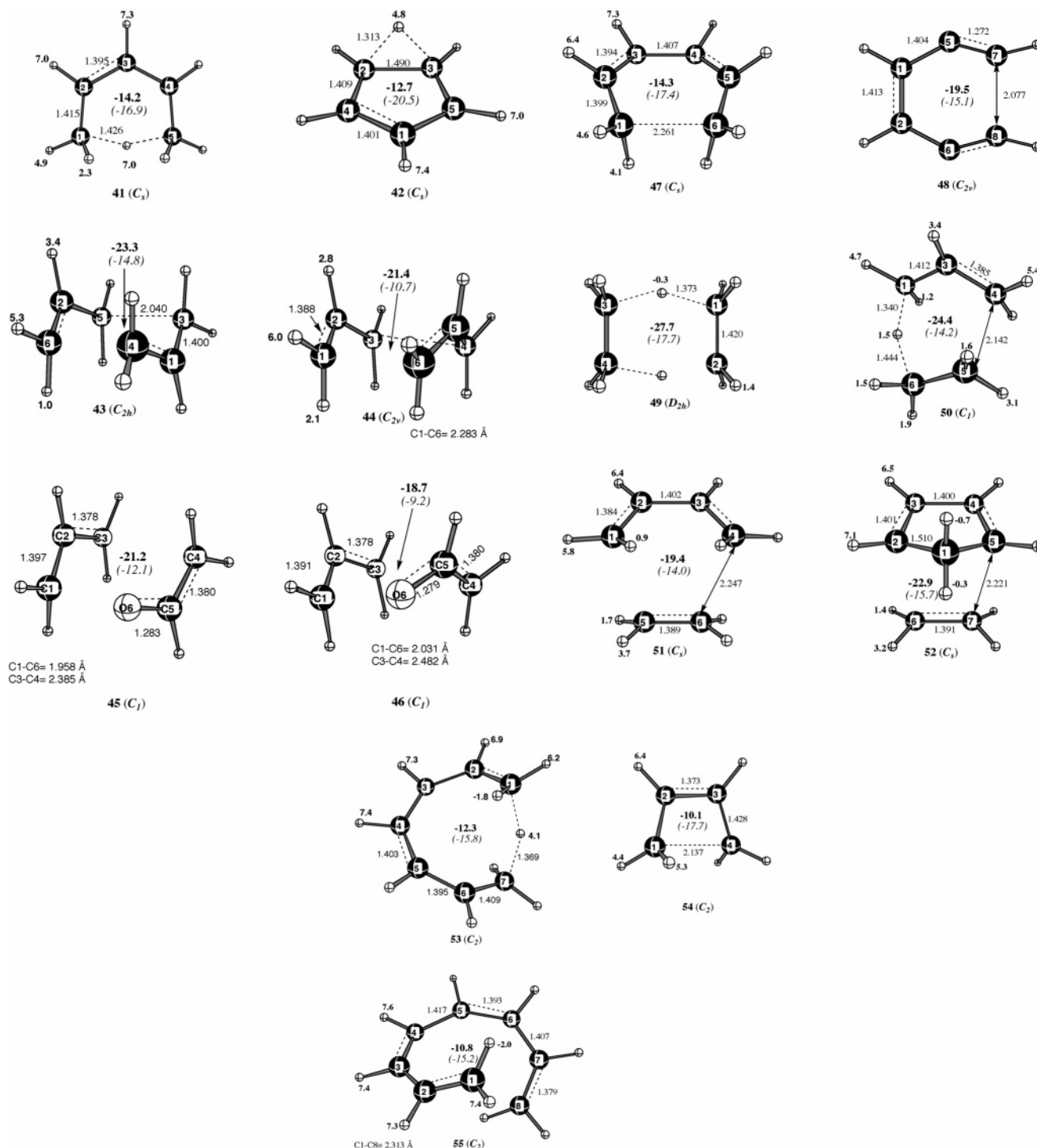
The GIAO and IGLO–NICS, −11.5 and −12.7, respectively, in the center of the five-membered TS, **42**, are slightly smaller than those in **41**. Because of the small size of the five-membered cyclopentadiene TS ring, the paratropic contributions from the  $\sigma$  electrons are slightly larger than those in the pentadiene TS (GIAO and IGLO–NICS differences between the Figure 1.1 and 1.2). The dissected NICS of **42** show that the six mobile electrons in the aromatic transition state contribute substantially, −20.5, to the total value.

The chemical shifts of the protons attached to C1, C4, and C5 are in the aromatic region (7.0–7.4 ppm) implying a strong diatropic ring current and a concerted mechanism.

### 3.4.2. Cope and Claisen Rearrangements:

**3.4.2.1. [3,3] Cope Rearrangements.**<sup>60e,188,193</sup> The detailed nature of the mechanism of the [3,3] sigmatropic shift, Cope rearrangement, of parent 1,5-hexadiene was debated for almost a half century. The controversy was the preference of this rearrangement to occur in a stepwise fashion involving an intermediate or a concerted single step. Does the transition state have a diradicaloid (singlet) or aromatic character?<sup>58d</sup> Evidence now classifies most Cope [3,3] rearrangements as a concerted reaction proceeding through a chairlike aromatic transition state.<sup>194</sup> Hence we intend to limit our [3,3] Cope rearrangement discussion to include only a concerted transition state.

The chair, **43** (*C*<sub>2h</sub>), and boat, **44** (*C*<sub>2v</sub>), form TSs have been located for the Cope rearrangement of 1,5-hexadiene, though the former is preferred by 5.8 kcal/mol over the latter at the B3LYP/6-311+G\*\* level.<sup>192b</sup> When more refined experimental data<sup>195</sup> was used to estimate energies, notably the concerted chair TS was found to be 9 kcal/mol more stable than the diyl intermediate, 1,4-cyclohexanediyl. Since the Cope



**Figure 17.** Geometries of the transition states (41–47 and 49–55) optimized at the B3LYP/6-311+G\*\* and that of 48 at the BLYP/6-311+G\*\*. The values in the center are the NICS(0) value (in bold) and the delocalized mobile electron (in italics, shown by dotted lines) contribution computed at the geometric center consisting of heavy atoms with the IGLO-III TZ2P basis set at the SOS-DFPT-IGLO level with the PW91 exchange functional using the deMon NMR program. The  $^1\text{H}$  NMR chemical shifts (in  $\delta$  ppm) are also shown next to the protons and are computed as the difference from proton shieldings of TMS.

rearrangement involves six mobile electrons ( $2\sigma$  and  $4\pi$ ), the transition state is expected to be aromatic. Indeed, the computed magnetic properties showed pronounced ring current effects close to benzenoid structures and other aromatic molecules. Magnetic susceptibility exaltations,  $-19.9$  for **43** and  $-17.4$  for **44**, show a delocalized ring current in the synchronous TS.<sup>192b</sup> The  $^1\text{H}$  NMR shifts of the axial protons in **43** and **44** are upfield (1.0–3.4 ppm), while the

equatorial protons are downfield (5.3–6.0 ppm), thus showing a delocalized ring current. In addition NICS(0) values in the center of **43** ( $-23.0$ ) and **44** ( $-21.4$ ) show the aromatic character of the concerted TSs. Dissected NICS(0),  $-14.8$  (chair TS) and  $-10.7$  (boat TS), also indicated pronounced diatropic ring currents due to six mobile electrons.

**3.4.2.2. Claisen Rearrangement.**<sup>196</sup> The [3,3] sigmatropic arrangement of allyl vinyl ether to form



4-pentalen is known as the Claisen rearrangement. This mechanism, which also may occur via a chair (45) or a boat (46) transition state, involving a heterocyclic ring is closely related to the previously discussed Cope rearrangement.<sup>c</sup> Houk and co-workers have indicated that the energies given by B3LYP are in excellent agreement with the experimental values.<sup>194c,d</sup> The computed NICS and  $\Lambda$  characterize the existence of diatropic ring currents in the transition states. The GIAO-B3LYP/6-31G\* NICS value computed at the geometrical central point of the six heavier atoms is  $-21.2$  for chairlike (45) and  $-18.5$  for boatlike transition state structures (46). Likewise, the dissected NICS(0) value in 45,  $-12.1$ , and in 46,  $-10.2$ , further establishes the aromatic nature of these concerted TSs. In agreement with the NICS data, the computed magnetic susceptibility exaltations indicate that the chair TS,  $-15.8$  cgs·ppm, is more aromatic than the boat TS,  $-13.3$  cgs·ppm. Note that  $\Lambda$  values of 45 and 46 are closer to that of benzene,  $-13.4$  cgs·ppm.

### 3.4.3. Electrocyclic Reactions

The cyclization of conjugated  $\pi$  systems or the reverse ring-opening process is termed as electrocyclic reactions. These reactions may proceed via a disrotatory or conrotatory mode.

**3.4.3.1. Ring Closure of 1,3,5-Hexatriene.**<sup>193p,197</sup> Woodward–Hoffmann rules predict that the disrotatory ring closure of 1,3,5-hexatriene to form 1,3-cyclohexadiene is thermally allowed. Doering et al. predicted 42–45 kcal/mol activation energy for hexatriene ring closure assuming a diradical non-concerted transition state.<sup>198</sup> The barrier for the stepwise process is thus much larger than that (30.7 kcal/mol evaluated at the B3LYP/6-311+G\*\*) for the concerted transition state, 47. The aromaticity of 47 has been very well established on the basis of geometric, energetic, and magnetic criteria.<sup>58d,192b</sup> The above energetic data clearly indicate that the energy of concert is ca. 12–15 kcal/mol. The computed magnetic susceptibility exaltation of 47,  $-17.4$  cgs·ppm, is close to the benzene value of  $-13.4$  cgs·ppm. In addition, the NICS(0) of  $-14.3$  and dissected NICS( $\pi$ ) of  $-17.4$  are indicative of diatropic ring currents in the concerted TS 47. Schleyer and Jiao also noted that 1,3,5-hexatriene ring closure showed considerable acceleration on complexation with various metal cations.<sup>58d</sup> They also characterized the aromaticity of the concerted TS by computing  $\text{Li}^+$  chemical shift, which was largely upfield shifted to  $-7.8$  ppm.

**3.4.3.2. Electrocyclization of Hexenediyne–Bergman Cyclization.** Singlet biradical benzene-1,4-diyl is formed on thermal six- $\pi$ -electron cyclization of hex-3-ene-1,5-diyne. Various other versions of this reaction have been extensively studied by Bergman et al.<sup>199</sup> Although considered as an “aromatization reaction”, the extent of cyclic electron delocalization in the Bergman reaction is not understood satisfyingly. Based on valence bond (VB) description, Shaik and Schreiner have developed a view suggesting that the transition state involved in this cyclization, 48, is essentially  $\pi$ -nonaromatic but  $\sigma$ -aromat-

ic.<sup>200</sup> Their conclusions were based on detailed analysis of energetic criteria. Additionally, the transition state involved in Bergman cyclization essentially does not contain multireference character; activation energies, 25.2 kcal/mol, given by pure density functional methods (e.g., BLYP) reproduce the value of 28.2 kcal/mol for the parent system.<sup>201</sup>

The aromatic character of transition state 48 involved in Bergman cyclization of hex-3-ene-1,5-diyne is confirmed by the large and negative NICS(0) value of  $-19.5$ . The dissected NICS( $\pi$ ),  $-15.1$ , also supports the existence of diatropic ring currents in 48. The IGLO computations indicate that the triple-bond in-plane components also make small contributions,  $-3.3$  ppm, to the total NICS(0). Schreiner et al.<sup>201s</sup> pointed out that the results obtained from the dissected NICS analysis for 48 are in contradistinction with those obtained by using a VB approach and that “it is unclear at this point why there is a discrepancy”.

### 3.4.4. Group Transfers

Group transfer reactions are molecular reorganizations involving no change in the number of  $\pi$  and  $\sigma$  bonds.

**3.4.4.1. Dihydrogen Transfer between Ethene and Ethane.** In 1982, Feller, Schmidt, and Ruedenberg reported ab initio studies on the concerted transition state in dihydrogen transfer between ethene and ethane.<sup>202</sup> The concerted TS 49 has a  $D_{2h}$  symmetry with  $\text{C}\cdots\text{H}$  bonds stretched to 1.37 Å. Note that the  $\text{C}\cdots\text{C}$  separations, 1.42 Å, are typical of aromatic systems. McKee et al. have reported<sup>203</sup> an activation barrier of 48.1 kcal/mol at the MP2/6-31G\* level, which is in reasonable agreement with that, 46.7 kcal/mol, evaluated at the B3LYP/6-311+G\*\* level.

Since this reaction is classified as  $2\sigma_s + 2\pi_s + 2\sigma_s$  type, there are six mobile electrons in the synchronous transition state, 49. In agreement with our expectation, the large negative IGLO NICS(0) value of  $-27.7$  ppm confirms the aromatic character of the concerted transition state. The dissected NICS value,  $-17.7$  ppm, corresponding to the mobile electron contributions also validates strong diatropic ring currents in 49. In addition, upfield shift (ranging from  $-0.3$  ppm) of the central protons in  $^1\text{H}$  NMR confirms the aromaticity in 49.

### 3.4.5. Ene Reactions

The ene reaction,<sup>204</sup> also known as homodienyl[1,5]-shift, involves a hydrogen atom transfer when there is simultaneous conversion of one  $\pi$  bond to a  $\sigma$  bond.

**3.4.5.1. Ene Reaction between Propene and Ethylene.**<sup>205</sup> The activation barrier for ene reaction between propene and ethylene is estimated to be 35 kcal/mol.<sup>205a</sup> In agreement with this value, B3LYP/6-311+G\*\* predicts the reaction barrier, involving a concerted transition state (50), to be 35.9 kcal/mol. The transition state, 50, has an envelope conformation with C1–C3, C3–C4, and C6–C5 bond lengths in the range of  $\sim 1.4$  Å. The NICS(0) value,  $-24.4$  ppm, in the center is supportive of aromatic character in 50. Additionally, large and negative NICS,  $-14.4$ ,



originating from the six mobile electrons indicate that the concerted transition state sustains significant diatropic character.

### 3.4.6. Cycloaddition Reactions

**3.4.6.1. Diels–Alder Reactions.**<sup>187,188</sup> This reaction, perhaps, not only is central in the development of theoretical models of concerted mechanisms but also is the most widely used synthetic method for the construction of six-membered rings. Many *ab initio* and semiempirical calculations on the [4 + 2] cycloadditions have been reported.<sup>206</sup> The prototype Diels–Alder reaction of 1,3-butadiene with ethene has been theoretically computed at different levels, and a well-defined synchronous transition state (**51**),  $C_s$ , which is 2–7 kcal/mol more stable than the stepwise alternatives, is predicted to be favored.

Both **51** and **52** (involved in cycloaddition of cyclopentadiene and ethene) have  $\sim 1.4$  Å C–C bond lengths in the diene and in the dienophile moieties. Schleyer et al. have verified Evan's suggestion that **51** is aromatic by using geometric, energetic, and magnetic ( $^1\text{H}$  NMR chemical shifts, magnetic susceptibility exaltations, and NICS) criteria. Herges et al.<sup>60d</sup> showed that the change in the  $^1\text{H}$  NMR chemical shift along the reaction coordinate of the inner and the outer protons attached to ethene and 1,3-butadiene in **51** provides a firm basis for the aromaticity concept of the pericyclic transition state. The NICS(0) values in the center of the six heavy atoms forming the TS in **51** and **52** are  $-19.4$  and  $-22.9$ , respectively. The large and negative NICS contributions ( $-14.0$  and  $-15.7$ , respectively) from the six mobile electrons indicate large aromatic character in both transition states. Moreover, the computed magnetic susceptibility exaltation ( $-14.0$  and  $-17.7$ , respectively) of both these transition states further supports the conclusions given by NICS.

### 3.4.7. Pericyclic Reactions Involving Möbius Transition States

**3.4.7.1. [1,7] Sigmatropic Hydrogen Shifts in 1,3,5-Heptatriene.** In contrast to [1,5] sigmatropic shifts, which have a Hückel topology, [1,7] hydrogen<sup>191f,h,207</sup> migration TSs, involving eight mobile electrons as in 1,3,5-heptatriene, have a Möbius twist.<sup>208</sup> The Möbius aromatic transition state, **53**, ( $C_2$  symmetry) in 1,3,5-heptatriene has a relatively low activation barrier (24.7 kcal/mol)<sup>209</sup> as compared to 36.4 kcal/mol for [1,5] hydrogen shift in 1,3-pentadiene. This may be due to the greater flexibility of the triene, which permits better overlap in **53** at the cost of relatively less distortion energy.<sup>188a</sup> Schleyer et al.<sup>60a</sup> evaluated a large energy of concert, 60.0 kcal/mol, indicating a preference for concerted TS **53** over a stepwise diradical intermediate. The  $^1\text{H}$  NMR shifts of protons attached to C1 and C7 and lying on the inner side are shifted upfield to  $-1.8$  ppm, while the protons attached to C2, C3, C4, C5, and C6 are downfield shifted (to 6.9–7.4 ppm); this behavior is characteristic if diatropic ring currents are present. The magnetic susceptibility exaltation of **53** ( $-23.1$  cgs·ppm) is greater than that of benzene. In addition, the Möbius aromaticity of the transition state is

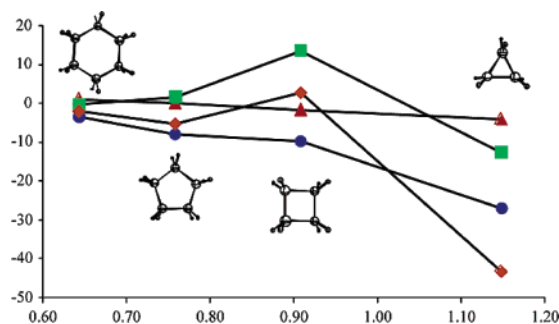
confirmed by NICS: GIAO ( $-11.7$ ) and IGLO ( $-12.3$ ) NICS(0). Further more the presence of strong ring currents in the TS with a Möbius topology, **53**, is supported by large and negative contributions,  $-15.8$  ppm, from the eight delocalized electrons to the total NICS.

**3.4.7.2. Ring Opening of Cyclobutene to Butadiene.** This electrocyclic reaction, like the Diels–Alder reaction, of cyclobutene to butadiene has been extensively studied<sup>210</sup> using different levels of theory.<sup>211</sup> There are four delocalized electrons involved in the TS (**54**) in the conrotatory ring opening of cyclobutene. Although the geometry of the Möbius transition state, **54**, is largely method-independent, only correlated levels best reproduce the experimental thermochemistry.<sup>197i</sup> Schaefer et al.<sup>211d</sup> pointed out that there is no concerted  $C_s$  transition state for the symmetry-forbidden disrotatory process. The MP2/6-31G\* transition-state geometry of **54**, reported by Houk,<sup>188a</sup> is in good agreement with that computed at the B3LYP/6-311+G\*\*. The existence of diatropic ring currents in **54** not only is displayed by a negative magnetic susceptibility exaltation value,  $-5.2$  ppm but also is supported by large negative NICS(0) of  $-10.1$ . Moreover the significant contribution of the four mobile electrons,  $-17.7$  ppm, toward total NICS also shows aromatic character in **54**.

**3.4.7.3. Ring Closure of 1,3,5,7-Octatetraene.** Since the conrotatory (thermal) ring closure in 1,3,5,7-octatetraene involves eight electrons, a Möbius transition state is predicted on the basis of Woodward–Hoffmann rules. The twisted topology of the transition state, **55**, permits excellent  $\pi$  overlap throughout the ring, as well as at the C···C termini, where the new  $\sigma$  bond is formed. Unlike structure **54**, the Möbius transition state **55** shows large geometry variations with the change in computational methods;<sup>212</sup> optimization at HF/6-31G\* level gives a structure with smaller bond alternation (0.034 Å) and hence with greater aromaticity than those at B3LYP or MP2/6-31G\* methods (0.072 Å).<sup>60b,192b</sup> The same conclusion can also be deduced from the calculated magnetic susceptibility exaltation, which is  $-12.6$  cgs·ppm for the MP2 and  $-28.4$  cgs·ppm for the HF geometry. The NICS(0) value and the contributions of the eight mobile electrons toward total shielding,  $-10.8$  and  $-15.2$  ppm, respectively, further establish the presence of diatropic ring currents in **55**.

## 3.5. $\sigma$ -Aromaticity and $\sigma$ -Antiaromaticity

Although aromaticity was initially confined to systems with  $\pi$  delocalized electrons, the concept of  $\sigma$ -aromaticity has been invoked to rationalize properties of saturated cyclic hydrocarbons.<sup>11</sup> In this context, three-membered rings (3MRs) have drawn much of the interest among experimental<sup>213</sup> and theoretical chemists<sup>214</sup> for many decades. The stability and reactivity of these small rings is dictated by an interplay of steric and electronic influences, which can give rise to aromatic or antiaromatic (de)-stabilization, as well as inductive, mesomeric, and hyperconjugative effects. The  $\sigma$ -aromaticity of cyclopropane that was first suggested by Dewar<sup>11</sup> was further supported by many electronic studies.<sup>215,216</sup>



**Figure 18.** Saturated 3-, 4-, 5-, and 6MR MO–NICS showing  $\pi$  CH<sub>2</sub> (red triangles), Walsh (green squares), and lowest energy (blue circles) MO contributions to NICS (total).

For instance, the upfield shift of its <sup>1</sup>H NMR signals,<sup>217</sup> as well as the negative value of NICS<sup>216</sup> located above the ring, indicates the presence of a strong diatropic current in the  $\sigma$ -plane of the molecule. On the other hand, 4MRs have been shown to be destabilized by  $\sigma$ -antiaromaticity and are characterized by paratropic values of NICS (Figure 18).<sup>218</sup>

These large magnetic effects appear even magnified in some 3- and 4MR cages that have been qualified as “super  $\sigma$ -(anti)aromaticity” by Schleyer et al.<sup>218</sup> The large negative NICS(0) at the cage and face centers of the tetrahedrane cages<sup>218,219</sup> (greater than –40 ppm) contrast remarkably with the paratropic ring current effect<sup>218,220</sup> occurring in cubane (NICS = +23.1 (cage) and +13.1 ppm (4MR)<sup>218</sup>).

Aromaticity in systems without  $\pi$ -electrons (with only  $\sigma$ -electrons) received much less attention. Such an important concept has only been addressed to limited number of hydrogen clusters<sup>221</sup> and, very

recently, to small (three- and four-atom) lithium and magnesium clusters<sup>222</sup> and small saturated inorganic rings such as (SiH<sub>2</sub>)<sub>n</sub>, (GeH<sub>2</sub>)<sub>n</sub>, (NH)<sub>n</sub>, (PH)<sub>n</sub>, (AsH)<sub>n</sub>, O<sub>n</sub>, S<sub>n</sub> and Se<sub>n</sub> ( $n = 3–6$ ).<sup>223</sup> The existing results show that the  $D_{mh}$  H<sub>x</sub><sup>q</sup> rings with  $4n + 2$   $\sigma$ -electrons are aromatic,<sup>221</sup> as are two- $\sigma$ -electron Li<sub>3</sub><sup>+</sup> and six- $\sigma$ -electron Li<sub>2</sub>Mg<sub>2</sub> rings.<sup>222</sup> For the small saturated inorganic rings, simple counting of the ring  $\sigma$ -bond electrons also fits well with the Hückel  $(4n + 2)/4n$  rule for planar  $\sigma$ -systems: three- and five-membered saturated rings are aromatic, while four- and six-membered rings are antiaromatic.<sup>223</sup>

To investigate  $\sigma$ -aromaticity of planar hydrogen and lithium clusters,  $D_{nh}$  symmetrical H<sub>n</sub><sup>q</sup> and Li<sub>n</sub><sup>q</sup> ( $n = 3–70$ ) rings with  $4n + 2$   $\sigma$ -electrons were computed; their structural data and NICS(0) values are summarized in Table 7. According to the frequency analysis, only the triatomic systems (H<sub>3</sub><sup>+</sup> and Li<sub>3</sub><sup>+</sup>) are local minima ( $N_{\text{imag}} = 0$ ), and very few species (H<sub>6</sub>, H<sub>10</sub>, H<sub>14</sub>, Li<sub>4</sub><sup>2+</sup>, Li<sub>8</sub><sup>2+</sup>) are transition states ( $N_{\text{imag}} = 1$ ), while the majority of the hydrogen and lithium rings are higher-order saddle points. NICS values at the ring centers (Table 7) show that all the rings with  $4n + 2$   $\sigma$ -electrons have very negative NICS values, indicating their significant aromatic character. Moreover, it is interesting to notice that the NICS values become invariable for larger rings, as found for the trend of the bond lengths.

However, a different opinion on the aromaticity of Li<sub>3</sub><sup>+</sup> was raised by Havenith et al.<sup>224</sup> on the basis of the ring-current map computations. Although H<sub>3</sub><sup>+</sup> shows a marked diatropic ring current and can be considered  $\sigma$  aromatic on the magnetic criterion, it was found that Li<sub>3</sub><sup>+</sup> shows no global current and thus

**Table 7.** Number of Imaginary Frequencies ( $N_{\text{imag}}$ ), Bond Length ( $R$ , Å) and NICS Values (ppm)<sup>a</sup> of Planar Hydrogen and Lithium Rings<sup>225</sup>

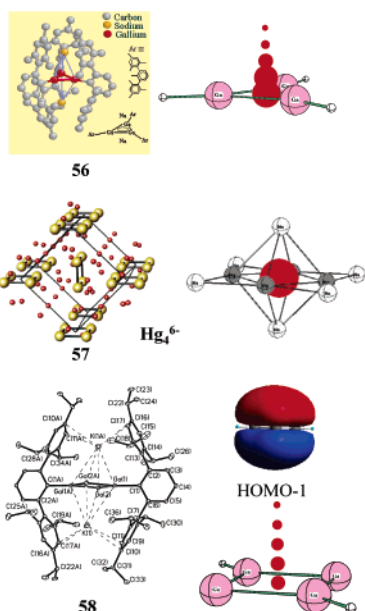
species	symm	$N_{\text{imag}}$	$R$	NICS(0) <sup>a</sup>	species	symm	$N_{\text{imag}}$	$R$	NICS(0) <sup>b</sup>
H <sub>3</sub> <sup>+</sup>	$D_{3h}$	0	0.880	–33.8	Li <sub>3</sub> <sup>+</sup>	$D_{3h}$	0	2.952	–11.1
H <sub>4</sub> <sup>2+</sup>	$D_{4h}$	4	1.208	–23.1	Li <sub>4</sub> <sup>2+</sup>	$D_{4h}$	2	3.356	–9.7
H <sub>4</sub> <sup>2–</sup>	$D_{4h}$	3	1.371	–12.7	Li <sub>4</sub> <sup>2–</sup>	$D_{4h}$	1	3.038	–3.5
H <sub>5</sub> <sup>–</sup>	$D_{5h}$	2	1.131	–16.4	Li <sub>5</sub> <sup>–</sup>	$D_{5h}$	2	2.979	–4.8
H <sub>7</sub> <sup>+</sup>	$D_{7h}$	2	0.948	–24.6	Li <sub>7</sub> <sup>+</sup>	$D_{7h}$	8	3.003	–6.5
H <sub>8</sub> <sup>2+</sup>	$D_{8h}$	6	0.988	–23.5	Li <sub>8</sub> <sup>2+</sup>	$D_{8h}$	10	3.196	–5.9
H <sub>8</sub> <sup>2–</sup>	$D_{8h}$	3	1.196	–20.6	Li <sub>8</sub> <sup>2–</sup>	$D_{8h}$	1	3.119	–6.9
H <sub>9</sub> <sup>–</sup>	$D_{9h}$	2	1.065	–23.8	Li <sub>9</sub> <sup>–</sup>	$D_{9h}$	8	2.996	–6.9
H <sub>6</sub>	$D_{6h}$	1	0.992	–21.9	Li <sub>6</sub>	$D_{6h}$	6	2.937	–6.3
H <sub>10</sub>	$D_{10h}$	1	0.980	–26.0	Li <sub>10</sub>	$D_{10h}$	14	2.963	–6.7
H <sub>14</sub>	$D_{14h}$	1	0.979	–27.6	Li <sub>14</sub>	$D_{14h}$	22	2.971	–6.7
H <sub>18</sub>	$D_{18h}$	3	0.980	–28.4	Li <sub>18</sub>	$D_{18h}$	30	2.974	–6.8
H <sub>22</sub>	$D_{22h}$	3	0.980	–29.2	Li <sub>22</sub>	$D_{22h}$	38	2.982	–7.1
H <sub>26</sub>	$D_{26h}$	3	0.980	–29.3	Li <sub>26</sub>	$D_{26h}$	46	2.983	–7.1
H <sub>30</sub>	$D_{30h}$	3	0.980	–29.4	Li <sub>30</sub>	$D_{30h}$	54	2.984	–7.1
H <sub>34</sub>	$D_{34h}$	5	0.981	–29.4	Li <sub>34</sub>	$D_{34h}$	60	2.983	–7.1
H <sub>38</sub>	$D_{38h}$	5	0.981	–29.5	Li <sub>38</sub>	$D_{38h}$	62	2.985	–7.1
H <sub>42</sub>	$D_{42h}$	5	0.981	–29.5	Li <sub>42</sub>	$D_{42h}$	66	2.985	–7.1
H <sub>46</sub>	$D_{46h}$	7	0.981	–29.5	Li <sub>46</sub>	$D_{46h}$		2.986	–7.1
H <sub>50</sub>	$D_{50h}$	7	0.981	–29.5	Li <sub>50</sub>	$D_{50h}$		2.986	–7.1
H <sub>54</sub>	$D_{54h}$	7	0.981	–29.5	Li <sub>54</sub>	$D_{54h}$		2.986	–7.1
H <sub>58</sub>	$D_{58h}$	7	0.981	–29.5	Li <sub>58</sub>	$D_{58h}$		2.986	–7.1
H <sub>62</sub>	$D_{62h}$	9	0.981	–29.5	Li <sub>62</sub>	$D_{62h}$		2.986	–7.1
H <sub>66</sub>	$D_{66h}$	9	0.981	–29.5	Li <sub>66</sub>	$D_{66h}$		2.986	–7.1
H <sub>70</sub>	$D_{70h}$	9	0.981	–29.5	Li <sub>70</sub>	$D_{70h}$		2.986	–7.1

<sup>a</sup> At GIAO–B3LYP/6-311++G(d,3pd)//B3LYP/6-311++G(d,3pd) for H<sub>n</sub><sup>q</sup> ( $n < 20$ ); at GIAO–B3LYP/6-31G\*\*//B3LYP/6-31G\*\* for H<sub>n</sub> ( $n \geq 20$ ). <sup>b</sup> At GIAO–B3LYP/6-311+G\*//B3LYP/6-311+G\* for Li<sub>n</sub><sup>q</sup> ( $n < 20$ ); at GIAO–B3LYP/6-31G\*//B3LYP/6-31G\* for Li<sub>n</sub> ( $n \geq 20$ ).

is nonaromatic on this criterion, despite its electron count and negative NICS value.

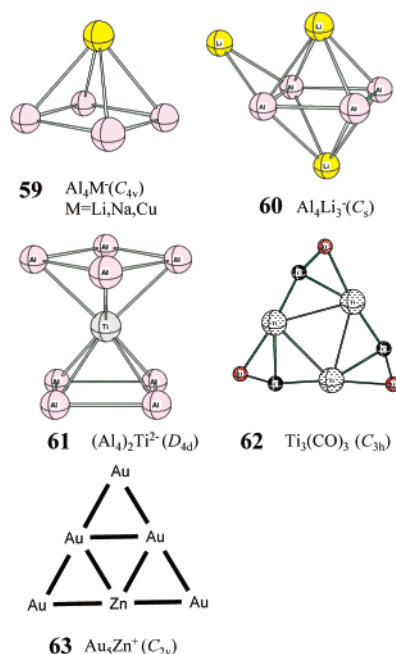
### 3.6. Aromaticity in Metal Clusters

The applicability of the aromaticity concept has also been recently expanded to all-metal clusters.<sup>120,226</sup> Readers interested in aromaticity of metal clusters are encouraged to read the Boldyrev and Wang review<sup>120</sup> in this issue. The first good evidence of metal aromaticity was recognized by Robinson in 1995 in the  $\text{Ga}_3^{2-}$  ring (**56**).<sup>227</sup> A year later, the aromatic character of the gallium ring was supported by NICS calculations<sup>228</sup> (NICS(0)  $-45.4$  ppm and NICS(1)  $-23.5$  ppm at the GIAO-B3LYP/6-311+G\*\*//B3LYP/6-311+G\* level).



Despite its long time existence, the importance of aromaticity has not been generally recognized in inorganic chemistry. For instance, mercury amalgams  $\text{Hg}_4^{6-}$  (**57**) (with two  $\pi$  electrons and square-planar structure), used since ancient times, were not considered as aromatic up to 2001.<sup>229</sup> Since then, various well-known clusters including  $\text{P}_4$  and its isoelectronic analogues, namely, Zintl ions have been characterized as aromatic by NICS.<sup>230</sup> Sometimes the aromatic character was simply overlooked. One example is the  $\text{Ga}_4\text{R}_2^{2-}$  (**58**,  $\text{R} = \text{C}_6\text{H}_3\text{-}2,6\text{-Trip}_2$ ,  $\text{Trip} = \text{C}_6\text{H}_2\text{-}2,4,6\text{-iPr}_3$ ), which has a square-planar gallium ring.<sup>231</sup> Our computation on the model compound  $\text{Ga}_4\text{H}_2^{2-}$  ( $D_{2h}$ ), at the B3LYP/6-311+G\*\* level, shows that its HOMO  $-1$  is a  $\pi$ -orbital, and the highly negative NICS values (NICS(0)  $-19.9$  ppm and NICS(1)  $-17.4$  ppm at GIAO-B3LYP/6-311+G\*\*//B3LYP/6-311+G\*\*) denote its aromaticity. Thus, though not recognized in the original paper,<sup>231</sup>  $\text{Ga}_4\text{R}_2^{2-}$  is actually a two  $\pi$  electron aromatic molecule.

One remarkable achievement is the gas-phase observation of all-metal aromatic clusters  $\text{Al}_4\text{M}^-$  ( $\text{M} = \text{Li}, \text{Na}, \text{or Cu}$ ) (**59**).<sup>232</sup> The origin of the aromaticity in  $\text{Al}_4^{2-}$  has attracted extensive theoretical interest,<sup>233</sup> and it is recognized that “the  $\text{Al}_4^{2-}$  dianion can be considered as  $\pi$ -aromatic and doubly

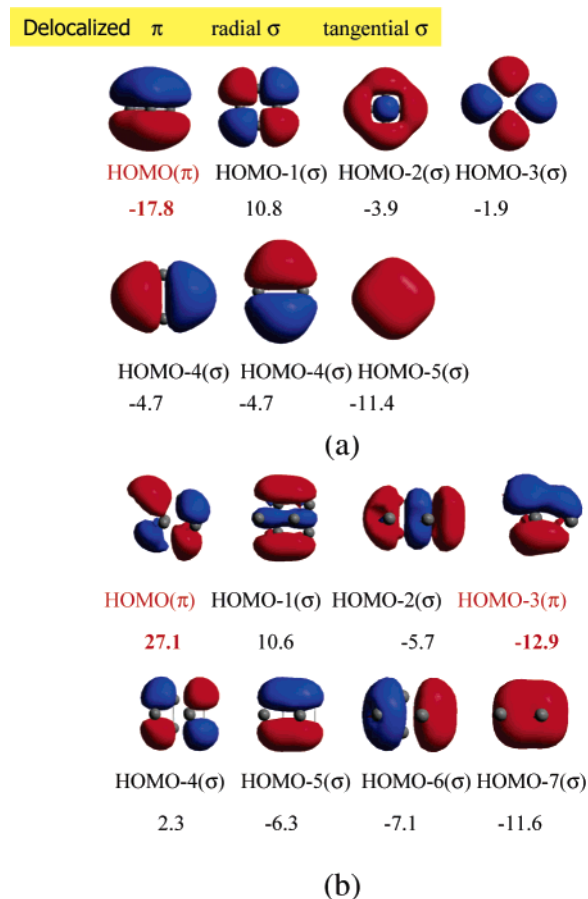


$\sigma$ -aromatic” due to delocalized  $\pi$  and  $\sigma$  orbitals.<sup>119</sup> Recent valence bond study shows that the resonance energy of the  $\sigma$  system is significantly higher than that of the  $\pi$  system (123 vs 40 kcal/mol).<sup>233e</sup> The  $\pi$  resonance energy is indeed substantially lower than that of the  $\pi$  isoelectronic hydrocarbon  $\text{C}_4\text{H}_4^{2+}$  (167 kcal/mol).<sup>233e</sup> Dissected NICS techniques such as LMO-NICS<sup>65</sup> or CMO-NICS<sup>81</sup> constitute very good tools to separate  $\sigma$  from  $\pi$  contributions. The CMO-NICS(0) analysis of  $\text{Al}_4^{2-}$  shows, for instance, both strong diatropic  $\pi$  ( $-17.8$  ppm) and  $\sigma$  MO (sum =  $-11.1$  ppm) contributions (Figure 19), thus confirming the double aromatic character of  $\text{Al}_4^{2-}$  ( $D_{4h}$ ). However, the delocalized radial  $\sigma$  orbital, as termed in ref 232, has a paratropic contribution to the total NICS (Figure 19a).<sup>117a</sup>

The  $\text{Al}_4\text{Li}_3^-$  cluster (**60**)<sup>119</sup> was also observed in the gas phase, and the  $\text{Al}_4^{4-}$  ring was claimed to be “antiaromatic”. This claim was exclusively based on the number of  $\pi$  electrons (four  $\pi$   $e^-$ ) and on the distortion of the  $\text{Al}_4^{4-}$  ring from a square to a rectangular geometry. However, the  $\pi$ -antiaromaticity of  $\text{Al}_4^{4-}$  ( $+14.2$  ppm) is overcome by the diamagnetic  $\sigma$ -contributions ( $-16.8$  ppm), which leads to a net weak overall aromaticity ( $-4.8$  ppm) in  $\text{Al}_4\text{Li}_3^-$  (Figure 19b).<sup>117a</sup> Although it is established that  $\text{Al}_4\text{Li}_3^-$  cluster is  $\sigma$ -aromatic and  $\pi$ -antiaromatic, the net aromatic character is still controversial. Readers are referred to refs 120 and 121 for the debate. However, note that  $\text{Al}_4\text{Li}_3^-$  has many isomers very close in energy; if  $\text{Al}_4\text{Li}_3^-$  were really antiaromatic, it should not adopt the  $\text{C}_s$  structure as shown in **60** at all.

Further  $\text{Al}_4^{2-}$ -based sandwich-like complexes such as  $\text{Al}_4\text{TiAl}_4^{2-}$  (**61**) have been recently designed.<sup>234</sup> The rather negative values at and 1 Å above the  $\text{Al}_4$  square center ( $-39$  and  $-17$  ppm, respectively) support the aromatic-metal-aromatic structure of **61**. Moreover, regardless of the aromatic character of  $\text{Al}_4\text{Li}_4$ , its stable transition metal complexes were





**Figure 19.** CMO–NICS analysis at the ring center of  $\text{Al}_4^{2-}$  ( $D_{4h}$ ) and  $\text{Al}_4\text{Li}_3^-$  ( $C_s$ ).

designed, and it was found that  $\text{Al}_4\text{Li}_4$  can be stabilized by complexation with 3d transition metals.<sup>235</sup>

Very recently, *cyclo*- $\text{Ti}_3[\eta^2-(\mu_2\text{-C,O})]_3$  (**62**), a side-on-bonded polycarbonyl titanium cluster, was prepared in rare-gas matrixes and its windmill-like structure was characterized by FTIR spectroscopy.<sup>236</sup> Although **62** has six  $\pi$  electrons and equal Ti–Ti bond length in the central titanium ring, the significant positive NICS values at the ring center (23.4 ppm) and at 1 Å above the ring center (14.8 ppm) indicate that **62** has “*potentially antiaromatic character*”.<sup>236</sup> However, it should be pointed out that NICS points further away from the ring center are better aromaticity probes for heavy element rings. More detailed studies, such as current density plots and dissected NICS analysis, may help to characterize its aromatic/antiaromatic character.

Besides, the planar cluster  $\text{Au}_5\text{Zn}^+$  (**63**) constitutes the first example of a bimetallic cluster involving  $\sigma$  orbitals only. The lowest-energy isomer was described by Tanaka et al.<sup>237</sup> as being triangular with the zinc atom located at the edge of the triangle. The NICS calculations performed on this cluster confirmed the presence of a diatropic ring current. The delocalization of the six  $\sigma$  electrons in its planar geometry is consistent with the high stability of  $\text{Au}_5\text{Zn}^+$  (**63**) and its abundance in gas-phase experiments.

#### 4. The Relationship among Geometric, Energetic, and Magnetic Aromaticity Criteria

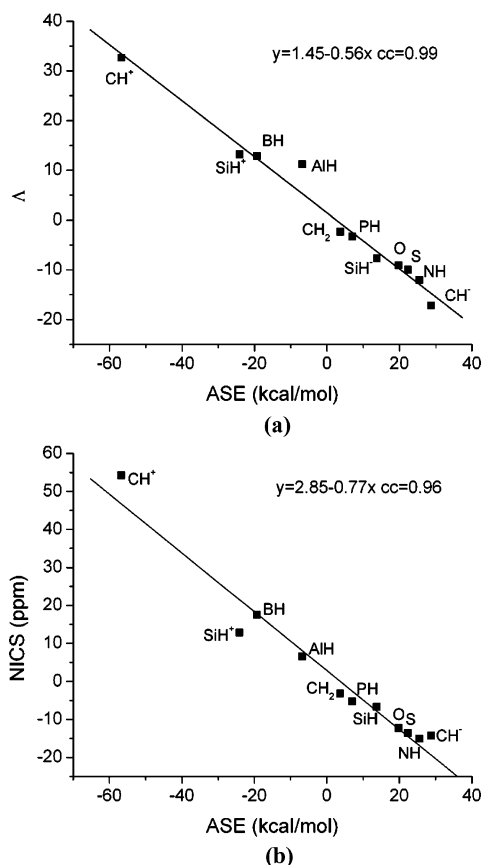
Aromaticity is widely characterized by different quantitative criteria, typically divided into three categories, geometric, energetic, and magnetic. In some cases, these various criteria do not agree. This occurs when an individual property is dominated or is perturbed by influences other than aromaticity (note the discussion above concerning RE and ASE evaluations of benzene; such evaluations for heterocycles and strained systems are even more complicated). For example, a recent pertinent study analyzed the aromaticity of Hückel  $[4n + 2]$  and  $[4n]$   $\pi$  electron annulenes based on computed geometries, energies, and magnetic properties. Changes in geometry from equalized to alternating CC bond lengths only affected the energy to a minor extent, but influenced the magnetic properties enormously.<sup>138,140,150</sup> The extent to which these various aromaticity criteria are related is of scientific interest. Is aromaticity a uniform or a statistically multidimensional phenomenon? In other words, can aromaticity be fully described by a single criterion?

Aromaticity is not a physical observable and cannot be defined precisely. But it can be described depending on the criterion or criteria chosen for analysis. The NICS view (and those of other magnetic criteria) implicates the presence of an induced ring current; other views favor interpretations based on extra stability or the geometry. If all these criteria correlate well (as they do with the five-heteroatom-substituted cyclopentadienes  $(\text{CH})_4\text{X}$ ,<sup>98a</sup> aromaticity can be defined operationally by a “fully aromatic” description including all the criteria. If correlations among two or more categories are lacking, the definition is arbitrary: systems of this type have been termed “partially aromatic” by Krygowski.<sup>1d</sup>

Hess, Schaad, and Nakagawa already demonstrated in the 1970s that resonance energy and chemical shifts can correlate.<sup>238a</sup> A few years later, Haddon derived a relationship connecting the induced ring current with the resonance energy.<sup>238b</sup>

However, in 1989, Katritzky et al.<sup>239a</sup> asserted, on the basis of a principal component analysis, that at least two principal components, identified with “classical (geometric and energetic)” and “magnetic” aromaticity, were required to describe a set of 12 common quantitative aromaticity criteria. Thus, they concluded that aromaticity is at least a statistically two-dimensional phenomenon.<sup>239a</sup> Their original conclusion was based on a statistical survey of only nine compounds, but this was extended later to 59 mono- and bicyclic compounds.<sup>239b</sup> The statistical multidimensionality of aromaticity has been supported by others.<sup>240</sup>

In 1991, Jug and Köster<sup>241</sup> reexamined this concept using SINDO1 calculations (eight aromaticity criteria and 12 compounds) and concurred with Katritzky’s conclusion that “aromaticity is at least a [statistically] two-dimensional phenomenon” and “energetic and magnetic criteria appear to be dominant”. Jug et. al. concluded that energetic and magnetic criteria such as ring current criterion,  $\text{RC}_v$ ,<sup>53</sup> and its alternative  $\text{RC}_v$  based on the bond valence<sup>241</sup> are orthogonal to



**Figure 20.** The correlation between different aromaticity criteria for a set of five-membered ring heterocycles,  $C_4H_4X$  (X as shown): (a) magnetic susceptibility exaltation ( $\Delta$ , ppm·cgs) vs aromatic stabilization energy (ASE, kcal/mol); (b) NICS (ppm) vs aromatic stabilization energy (ASE, kcal/mol), correlation coefficient 0.96.

each other. However, in contrast to Kartritzky, Jug et al. found that the magnetic criteria  $\Delta$  and  $\chi_m$  correlate with the energy criteria for the set of compounds examined.

On the basis of a set of 11 five-membered  $(CH)_4X$  ring systems, Schleyer et. al.<sup>59b</sup> demonstrated in 1995 that “linear relationships exist among the energetic, geometric and magnetic criteria of aromaticity, and these relationships can be extended even to antiaromatic systems”. They implied that aromaticity actually can be “one-dimensional” statistically and that any of the available criteria can describe aromaticity completely. As an example, Figure 20a shows an excellent correlation between the magnetic susceptibility exaltation and aromatic stabilization energy. Correlations involving this  $(CH)_4X$  set were later extended to NICS<sup>98a</sup> and to proton chemical shift differences.<sup>242</sup>

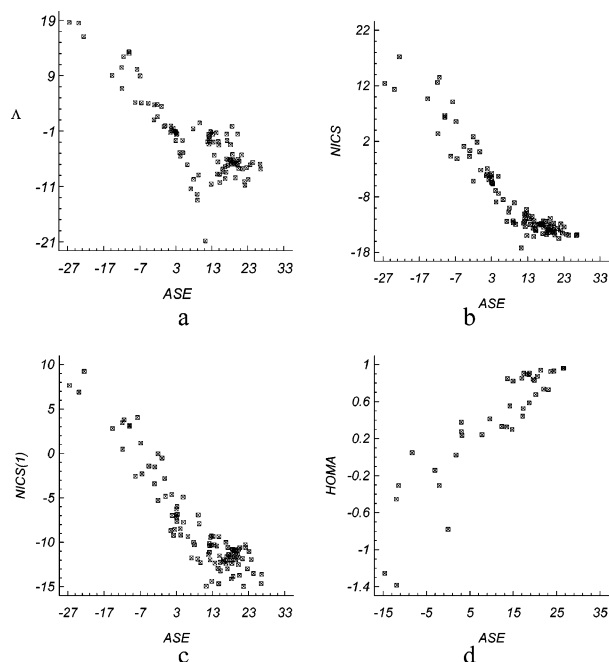
In 1996, Bird<sup>243</sup> showed that good linear relationships exist between experimental diamagnetic susceptibility enhancements for ca. 50 aromatic and heteroaromatic ring structures and their corresponding resonance energies. He further clarified that “consequently there is no apparent justification for separate ‘classical’ and ‘magnetic’ concepts of aromaticity”. In the same year, Schleyer and co-workers showed that linear relationship does exist between computed NICS values and ASEs for a series of five-membered ring compounds  $C_4H_4X$  (Figure 20b).<sup>26</sup>

Katritzky published a rebuttal entitled “Aromaticity Reaffirmed as a Multidimensional Characteristic” in 1998,<sup>19</sup> defending his initial 1989 paper.<sup>239a</sup> This new study extended Schleyer’s set by including many more types of five-membered heteroatom derivatives. While the plots showed a great deal of scatter and were useless for fine-tuned comparisons of one type of molecule with another, acceptable correlations were found between NICS and other criteria (HOMA, ASE) for related series of compounds.<sup>98a,162,244,245</sup> The 2002 paper of Quiñonero et al., “Quantification of Aromaticity in Oxocarbons: The Problem of the Fictitious in Nonaromatic Reference System”,<sup>245</sup> concluded “Oxocarbon acids and their anions are examples where the criteria of aromaticity that use reference systems are unsuccessful, only NICS criterion gives satisfactory results”.

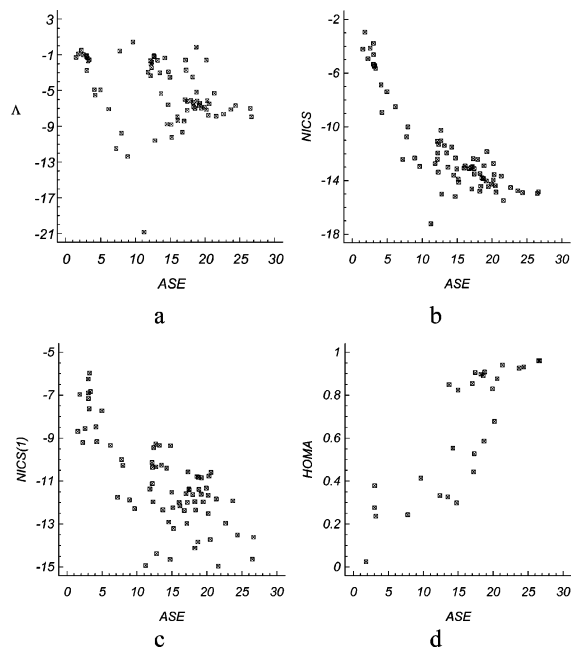
A joint 2002 paper, “To what extent can aromaticity be defined uniquely”,<sup>98d</sup> by the protagonists in the controversy was “intended to present an authoritative assessment” of the dimensionality of aromaticity. This study employed a set of 75 five-membered  $\pi$ -electron systems: aza and phospho derivatives of furan, thiophene, pyrrole, and phosphole (aromatic systems), and a set of 30 ring-monosubstituted compounds (aromatic, nonaromatic, and antiaromatic systems). Statistical analyses of quantitative definitions of aromaticity, ASE (aromatic stabilization energies), magnetic susceptibility exaltation, NICS, and HOMA revealed statistically significant correlations among the various aromaticity criteria, provided the whole set of compounds was involved. Hence, broadly considered, the various manifestations of aromaticity are related and aromaticity can be regarded statistically as a one-dimensional phenomenon (as shown in Figure 21). In contrast, when comparisons are restricted to smaller groups of compounds, for example, aromatic compounds with  $ASE > 5$  kcal/mol or polyhetero five-membered rings, the correlations deteriorate in quality or even vanish. In practical applications, energetic, geometric, and magnetic descriptors of aromaticity are not equivalent (as shown in Figure 22). In such cases, the phenomenon of aromaticity can be thus be regarded as being statistically multidimensional. Consequently, the most reliable comparisons are restricted to closely related sets of aromatic compounds, such as the five-membered  $(CH)_4X$  ring systems.<sup>59b</sup> Recommendations to employ several aromaticity criteria, or as many as possible, are well founded.

The investigations related to the dimensionality of aromaticity still continue. Using the recently introduced isomerization method of Schleyer and Pühlhofer,<sup>21</sup> De Proft and Geerlings<sup>57f</sup> computed aromatic stabilization energies, magnetic susceptibilities, and hardnesses for a series of five-membered  $C_4H_4X$  compounds, ranging from antiaromatic to highly aromatic. They found that the hardness is linearly correlated to other aromaticity criteria, such as ASE and NICS.

Poater et al.<sup>246</sup> examined the local aromaticity of a series of carbazole derivatives using three different aromaticity criteria, NICS, HOMA, and para-delocalized index (PDI).<sup>79</sup> In these series of compounds,



**Figure 21.** Dependence of  $\Delta$ , NICS, NICS(1), and HOMA vs ASE for all 105 structures: (a) exaltation of susceptibility vs ASE (correlation coefficient =  $-0.8280$ ; 102 data); (b) NICS vs ASE (correlation coefficient =  $-0.9406$ ; 102 data); (c) NICS computed 1 Å above the ring centers vs ASE (correlation coefficient =  $-0.9223$ ; 102 data); (d) HOMA vs ASE (correlation coefficient =  $0.9001$ ; 39 data).



**Figure 22.** Dependence of  $\Delta$ , NICS, NICS(1), and HOMA vs ASE for all aza and phosphorus derivatives of furan, thiophene, pyrrole, and phosphole (including parent systems): (a) exaltation of magnetic susceptibility vs ASE (correlation coefficient =  $-0.3447$ ; 72 data); (b) NICS vs ASE (correlation coefficient =  $-0.8588$ ; 72 data); (c) NICS computed 1 Å above the ring centers vs ASE (correlation coefficient =  $-0.7456$ ; 72 data); (d) HOMA vs ASE (correlation coefficient =  $0.8360$ ; 28 data).

the three measures of local aromaticity vary in a rather narrow range (with small difference). As far as the relative aromaticity of the different derivatives is concerned, there is a clear divergence among the

three methods used to quantify the local aromaticity.

Even more recently, Sadlej-Sosnowska<sup>247</sup> investigated the aromaticity of three sets of compounds, various five-membered heterocycles, derivatives of 2*H*-tetrazole, and six-membered heterocycles, using a number of aromaticity indices, especially the magnetic ones. Mutual relationships among these aromaticity criteria were claimed to depend on the choice of molecules included in the set subjected to statistical analysis. Magnetic characteristics themselves may be orthogonal to one another: “the properties calculated here cannot be thoroughly accounted for by the corresponding ring currents, and that other effects, despite the lack of identification yet, have also intruded upon the properties being calculated”.

**Our Recommendation.** Attempts to rationalize and quantify the concept of aromaticity should employ as many criteria as possible. Each category of criteria has its limitations and ambiguities. While aromaticity is now more closely associated with magnetic (ring current) criteria, we recommend comparisons of several indexes to better identify and characterize aromatic molecules.

## 5. Concluding Remarks

Since its introduction in 1996, the NICS magnetic criteria of aromaticity has been validated, refined, and improved considerably. NICS is widely used to characterize aromaticity and antiaromaticity not only of cyclic molecular systems but also of transition states, transition metal complexes, three-dimensional clusters, etc. The popularity of NICS as a quantitative aromaticity index is due to several advantages. NICS is easy and inexpensive to compute and is implemented in the many quantum mechanics programs used to compute chemical shifts of atoms in molecules. Since not much CPU time is required, larger molecules may be examined. Many computed NICS points or surfaces may be used to characterize the shielding environment of molecules more fully. NICS is not restricted to planar compounds. In particular, NICS can characterize three-dimensional clusters and cage molecules. Being a local property calculated relatively distant from the nuclei, NICS is relatively insensitive to the level of theory employed (basis set and method). NICS is an absolute measure of aromaticity in the sense that its evaluation does not require the use of reference compounds. NICS often (but not always) correlates very well with other quantitative or qualitative aromatic indexes, which may be much more difficult to obtain or to define reliably.

The limitations of NICS must also be appreciated. Manifestations of magnetic phenomena, such as NICS or the chemical shifts of atoms, are defined as one-third of the sum of the three diagonal shielding components (the trace) and take the magnetic field applied in all three space directions into account. Because the response to a magnetic field applied along each of the three principal directions may be quite different, important features inherent to each direction (tensor components) can be masked when considering the averaged isotropic values of NICS. Although dipole moments, polarizabilities,  $g$  and



hyperfine tensors, etc. are also vector or tensor quantities, discussions of their tensor components are less familiar to chemists (except spectroscopists) than straightforward analyses of scalar properties (geometries, energies, etc.). In particular, the commonly computed isotropic NICS values, especially in ring centers, do not exclusively reflect the “ring currents”. While the ring currents are most closely associated with cyclic  $\pi$  electron delocalization, they arise primarily from a magnetic field applied in the direction perpendicular to the ring. For these reasons, the NICS $_{\pi\text{-out-of-plane}}$  component has been recommended to be a superior NICS-based aromaticity index rather than the isotropic NICS.<sup>81c</sup> Moreover, isotropic NICS values are influenced by their immediate environment,  $\sigma$  as well as  $\pi$ . Because  $\sigma$  contributions fall off faster than  $\pi$  ones normal to a ring, isotropic NICS(1) values (1 Å away from the center), which are often dominated by the  $\pi$  contribution to the tensor component perpendicular to the ring, are also recommended.<sup>65</sup> Because contributions from remote parts of molecules are small, NICS is a local, rather than a global, aromatic index. NICS characterizes individual rings in a polycycle, rather than the aromaticity of the entire molecule. It is not immediately clear whether NICS in the center of clusters reflects “globular aromaticity” or only the sum of the influences of the remote rings comprising the cage.

New interpretive insights into magnetic aromaticity are now provided by refined NICS-based criteria, which reveal the individual diatropic and paratropic contributions not only of the  $\sigma$  and  $\pi$  systems of

planar ring systems, but also of parts of three-dimensional molecules. NICS has been refined by LMO and CMO dissections, as well as by the aromatic ring current shielding (ARCS) method.<sup>72</sup> More detailed examinations of the contributions of orbitals and tensor components to NICS in the future will surely lead to refined predictions and further progress in the understanding of electron delocalization in molecules.

The purpose of quantifying aromaticity is not restricted to the classification of known compounds. More importantly, the aim is to design novel molecules, find general trends, and understand the intrinsic nature of unusual chemical systems.

Aromaticity is like the icing on a cake. Icing contributes only a little to holding the cake together, but it is the most delicious part.


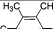
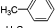
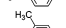
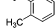
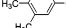
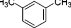
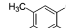
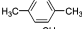
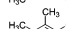
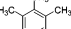
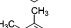
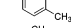
## 6. Acknowledgment

We thank the US National Science Foundation (Grant CHE-0209857). Z.C. thanks Prof. Andreas Hirsch and Prof. Walter Thiel for support and the Alexander von Humboldt foundation for supporting the 2004 summer visit in Germany. C.C. thanks Dr. Thomas Heine for fruitful discussions.

## 7. Appendix

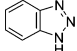
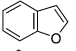
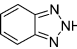
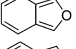
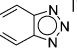
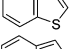
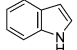
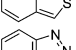
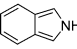
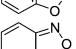
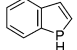
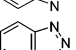
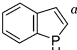
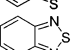
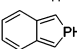

Tables 8–48 summarize NICS(0) and NICS(1) data at the uniform GIAO–B3LYP/6-311+G\*\*//B3LYP/6-311+G\* level of theory. Note that NICS values are somewhat method and basis set dependent.

**Table 8. NICS(total) RB3LYP/6-311+G\*\* Values for Methylbenzenes<sup>a</sup>**

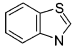
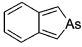
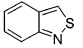
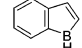
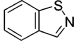
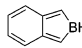
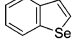
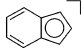
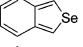
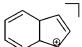
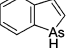
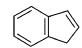
		NICS(0)	NICS(1)			NICS(0)	NICS(1)
Benzene		-8.03	-10.20	1,2,3,4- Tetramethylbenzene		-7.82	-9.78
Methylbenzene		-8.01	-10.07	1,2,3,5- Tetramethylbenzene		-7.70	-9.59
1,2-Dimethylbenzene		-8.15	-10.16	1,2,4,5- Tetramethylbenzene		-7.96	-9.82
1,3-Dimethylbenzene		-7.94	-9.84	1,2,3,4,5- Tetramethylbenzene		-7.24	-9.25
1,4-Dimethylbenzene		-8.01	-9.89	Hexamethylbenzene		-7.32	-9.37
1,2,3- Trimethylbenzene		-7.80	-9.83				
1,2,4- Trimethylbenzene		-8.06	-9.91				
1,3,5- Trimethylbenzene		-9.78	-9.54				

<sup>a</sup> All structures are fully optimized local minima (RB3LYP/6-311+G\*\*).

**Table 9. NICS(total) RB3LYP/6-311+G\*\* Values for Indol Derivates<sup>a</sup>**

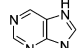
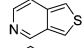
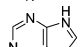
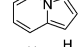
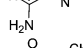
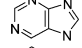
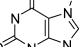
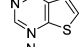
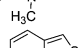
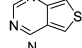
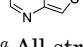
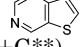
	NICS(0) 6 membered ring	NICS(1) 6 membered ring	NICS(0) 5 membered ring	NICS(1) 5 membered ring		NICS(0) 6 membered ring	NICS(1) 6 membered ring	NICS(0) 5 membered ring	NICS(1) 5 membered ring
	-9.76	-10.94	-12.94	-12.68		-9.96	-10.99	-9.56	-8.26
	-7.76	-9.64	-15.44	-14.26		-4.92	-7.03	-15.00	-12.27
	-9.03	-10.26	-13.14	-15.19		-9.10	-10.63	-10.35	-8.85
	-9.69	-10.83	-12.43	-10.18		-5.06	-7.62	-14.86	-12.61
	-6.72	-8.63	-16.21	-12.82		-9.43	-10.65	-12.22	-10.65
	-7.82	-10.55	-2.15	-4.72		-5.30	-7.53	-15.64	-14.30
	-8.32	-10.09	-14.94	-10.77		-9.12	-10.63	-10.85	-10.89
	-7.07	-9.33	-17.23	-12.83		-5.42	-8.45	-15.81	-14.21

**Table 9. (Continued)**

	NICS(0) 6 membered ring	NICS(1) 6 membered ring	NICS(0) 5 membered ring	NICS(1) 5 membered ring		NICS(0) 6 membered ring	NICS(1) 6 membered ring	NICS(0) 5 membered ring	NICS(1) 5 membered ring
	-9.43	-10.77	-9.91	-9.35		+2.15	-1.92	-4.23	-5.41
	-5.54	-8.22	-14.77	-13.03		-1.59	-5.04	+18.06	+9.10
	-10.77	-9.67	-9.12	-10.72		+42.46	+32.79	+84.26	+66.77
	-8.74	-10.41	-9.29	-7.75		-7.93	-9.26	-14.20	-13.13
	-4.12	-6.86	-13.94	-11.93		+20.91	+14.06	+43.81	+30.98
	-7.65	-1.04	-9.89	-2.67		-8.11	-10.17	-0.50	-3.37

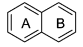
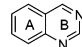
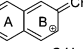
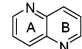
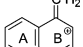

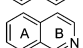
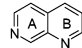
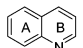
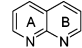
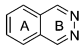
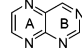
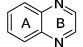
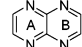
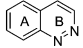

<sup>a</sup> All structures are fully optimized local minima (RB3LYP/6-311+G\*\*). <sup>b</sup> Planar,  $N_{\text{imag}} = 1$ .

**Table 10. NICS(total) RB3LYP/6-311+G\*\* Values for Selected Substituted Hetero Inden Derivates<sup>a</sup>**

	NICS(0) 6 membered ring	NICS(1) 6 membered ring	NICS(0) 5 membered ring	NICS(1) 5 membered ring		NICS(0) 6 membered ring	NICS(1) 6 membered ring	NICS(0) 5 membered ring	NICS(1) 5 membered ring
	-8.47	-11.13	-11.55	-10.40		-4.41	-7.75	-15.22	-12.90
	-6.57	-8.47	-11.22	-9.61		-5.23	-6.61	-16.23	-13.40
	-3.10	-2.69	-11.22	-9.24		-8.11	-10.84	-11.39	-10.17
	-4.15	-7.68	-15.02	-12.77		-7.36	-10.51	-10.78	-9.12
						-3.60	-7.80	-15.52	-13.03
						-7.10	-10.42	-10.79	-9.27

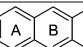
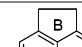
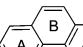
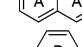
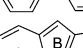
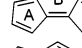
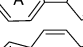
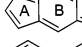
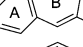
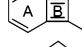
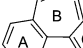
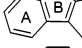
<sup>a</sup> All structures are fully optimized local minima (RB3LYP/6-311+G\*\*).

**Table 11. NICS(total) RB3LYP/6-311+G\*\* Values for Selected Substituted and Hetero Naphtahlene Derivates<sup>a</sup>**

	NICS(0) A ring	NICS(1) A ring	NICS(0) B ring	NICS(1) B ring		NICS(0) A ring	NICS(1) A ring	NICS(0) B ring	NICS(1) B ring
	-8.55	-10.71	-8.55	-10.71		-8.83	-10.91	-6.24	-10.30
	-3.33	-7.16	-0.82	-4.75		-7.52	-10.68	-7.52	-10.68
	-6.42	-9.56	0.43	-4.19		-7.69	-10.72	-7.33	-10.54
	-8.68	-10.83	-7.50	-10.58		-7.50	-10.67	-7.47	-10.69
	-8.81	-10.85	-7.47	-10.52		-7.75	-10.73	-7.75	-10.73
	-9.23	-11.28	-5.61	-10.13		-6.25	-10.66	-6.72	-10.59
	-8.83	-10.92	-5.94	-10.47		-6.70	-10.86	-6.70	-10.86
	-8.76	-10.85	-6.81	-11.50					

<sup>a</sup> All structures are fully optimized local minima (RB3LYP/6-311+G\*\*).

**Table 12. NICS(total) RB3LYP/6-311+G\*\* Values for Selected Systems with Three Fused Rings<sup>a</sup>**

	NICS(0) A ring	NICS(1) A ring	NICS(0) B ring	NICS(1) B ring	NICS(0) C ring	NICS(1) C ring		NICS(0) A ring	NICS(1) A ring	NICS(0) B ring	NICS(1) B ring	NICS(0) C ring	NICS(1) C ring
	-7.50	-9.80	-11.47	-13.06				-8.28	-10.36	1.79	-0.63		
	-8.53	-10.71	-5.72	-8.40				23.69	17.32	14.43	9.77		
	-2.89	-5.56	-11.49	-13.13	-9.81	-11.68		21.50	15.35	18.07	12.87		
	-8.52	-10.38	-5.51	-2.92	-13.74	-14.87		-2.45	-4.76	19.25	9.50		
	-7.04	-9.24	-2.91	-5.44	-13.83	-14.96		-7.31	-9.54	1.25	-2.33		
	-6.68	-8.86	4.18	0.15				-5.26	-7.46	+14.24	+8.84		

<sup>a</sup> All structures are fully optimized local minima (RB3LYP/6-311+G\*\*).

**Table 13. NICS(total) RB3LYP/6-311+G\*\* Values for Selected Systems with Three Fused Rings<sup>a</sup>**

	NICS(0) A ring	NICS(1) A ring	NICS(0) B ring	NICS(1) B ring	NICS(0) C ring	NICS(1) C ring		NICS(0) A ring	NICS(1) A ring	NICS(0) B ring	NICS(1) B ring	NICS(0) C ring	NICS(1) C ring
	-7.16	-9.32	9.60	2.48				1.42	-1.58	0.91	-1.75		
	-7.48	-9.90	-10.05	-12.39				-7.81	-10.13	-6.45	-8.83	5.71	0.23
	-5.06	-9.57	12.38	-13.40				-10.49	-10.83	-9.25	-6.40	-11.85	-9.62
	-6.51	-8.36	-10.74	-11.66	-7.64	-10.25		-10.10	-10.63	-9.62	-6.95	-11.37	-9.08
	-7.58	-10.81	-5.58	-8.36				-9.52	-10.67	-9.27	-8.45		
	-7.40	-10.62	-5.81	-8.56	-7.42	-10.67		-9.74	-10.72	-6.97	-6.74		
	-7.46	-10.65	-5.72	-8.58				-8.55	-10.21	-7.33	-6.72		
	-7.26	-8.23	-5.07	-6.60				-8.09	-9.91	-6.43	-5.76		
	-3.20	-7.85	-9.96	-11.73	-16.85	-15.18							
	-15.99	-14.40	-9.81	-11.33									
	4.86	0.15											

<sup>a</sup> All structures are fully optimized local minima (RB3LYP/6-311+G\*\*).**Table 14. NICS(total) RB3LYP/6-311+G\*\* Values for Selected Seven-Membered Ring Derivates<sup>a</sup>**

	NICS(0) 7 membered ring	NICS(1) 7 membered ring	NICS(0) second ring	NICS(1) Second ring		NICS(0) 7 membered ring	NICS(1) 7 membered ring	NICS(0) second ring	NICS(1) Second ring
	-3.68	-6.96				11.60	6.68	-1.59	-3.34
	-1.09	-4.54	-9.04	-10.89		-5.63	-7.82	-17.11	-17.77
	0.54	-3.88				-6.80	-8.98	-14.59	-16.34
	2.27	-2.20				15.25	10.26	-0.94	0.40
	1.52	-2.27							

<sup>a</sup> All structures are fully optimized local minima (RB3LYP/6-311+G\*\*).**Table 15. NICS(total) RB3LYP/6-311+G\*\* Values for Selected Systems with Oligo Fused Hetero Rings<sup>a</sup>**

	NICS(0) A ring	NICS(1) A ring	NICS(0) B ring	NICS(1) B ring	NICS(0) C ring	NICS(1) C ring	NICS(0) D ring	NICS(1) D ring		NICS(0) A ring	NICS(1) A ring	NICS(0) B ring	NICS(1) B ring	NICS(0) C ring	NICS(1) C ring	NICS(0) D ring	NICS(1) D ring
	-6.64	-9.19	-10.61	-11.55						-5.44	-10.28	-1.18	-5.00				
	-11.30	-8.54	-8.89	-6.90						-8.34	-10.50	-6.93	-11.05	1.11	-3.36	-6.17	-10.09
	-11.71	-8.90	-9.93	-6.75						-10.26	-10.57	1.57	-0.95				

<sup>a</sup> All structures are fully optimized local minima (RB3LYP/6-311+G\*\*).



Table 16. NICS(total) RB3LYP/6-311+G\*\* Values for Selected Phenylene Derivates<sup>a</sup>

	NICS(0) A ring	NICS(1) A ring	NICS(0) B ring	NICS(1) B ring	NICS(0) C ring	NICS(1) C ring	NICS(0) D ring	NICS(1) D ring		NICS(0) A ring	NICS(1) A ring	NICS(0) B ring	NICS(1) B ring	NICS(0) C ring	NICS(1) C ring	NICS(0) D ring	NICS(1) D ring
	-8.03	-10.20								-2.91	-5.24	17.30	7.73	-1.51	-3.87	-3.52	-6.33
	-0.50	-2.80	23.67	13.66						-2.90	-5.14	17.35	7.79	-2.21	-4.15	-5.29	-7.69
	-2.45	-4.76	19.25	9.50													
	-4.60	-6.51	14.16	5.05	2.30	0.31											
	-2.28	-4.29	18.04	9.09	0.98	-1.54				-9.40	-13.42	-8.23	-9.57				
										-9.18	-13.31	-6.72	-9.10				
	5.12	-1.81	-1.30	-1.33						8.17	0.27	4.21	1.20	9.80	0.71		
	2.49	1.61	9.67	1.46	-6.21	-7.98											

<sup>a</sup> All structures are fully optimized local minima (RB3LYP/6-311+G\*\*).

Table 17. NICS(total) RB3LYP/6-311+G\*\* Values for Selected Aromatic Poly Cyclic Hydrocarbons Derivates<sup>a</sup>

	NICS(0) A	NICS(1) A	NICS(0) B	NICS(1) B	NICS(0) C	NICS(1) C	NICS(0) D	NICS(1) D		NICS(0) A	NICS(1) A	NICS(0) B	NICS(1) B	NICS(0) C	NICS(1) C	NICS(0) D	NICS(1) D
	-8.03	-10.20								-5.69	-8.24	8.00	2.96				
	-8.55	-10.71								-7.24	-9.56	-0.16	-3.79	-4.08	-7.00	-9.87	-11.70
	-7.50	-9.80	-11.47	-13.06						-8.87	-11.01	-10.05	-11.97	-1.21	-4.76	-4.98	-7.97
	-6.58	-9.06	-11.22	-12.69						-5.26	-7.46	-14.24	-8.84				
	-11.27	-13.03	-3.88	-6.62						-3.07	-5.60	18.50	12.47	7.36	3.19		
	1.56	-1.71	17.58	11.63													

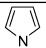
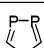
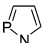
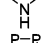
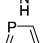
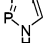
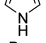
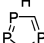
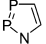
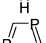
<sup>a</sup> All structures are fully optimized local minima (RB3LYP/6-311+G\*\*). <sup>b</sup> NICS(0) E ring, -10.70; NICS(1) E ring, -12.54.

Table 18. NICS(total) RB3LYP/6-311+G\*\* Values for Aza Pyrroles<sup>a</sup>

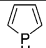
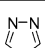
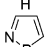
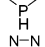
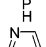
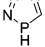
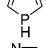
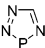
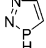
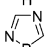
		NICS(0)	NICS(1)			NICS(0)	NICS(1)
Pyrrole		-13.62	-10.09	3,4- Diazapyrrole		-13.95	-12.76
2-Azapyrrole		-13.61	-11.30	2,3,4-Triazapyrrole		-14.33	-13.49
3-Azapyrrole		-13.10	-10.55	2,3,5-Triazapyrrole		-14.46	-13.89
2,3-Diazapyrrole		-13.97	-12.73	2,3,4,5-Tetraazapyrrole		-16.72	-15.76
2,4- Diazapyrrole		-13.09	-11.57				
2,5- Diazapyrrole		-13.64	-11.28				

<sup>a</sup> All structures are fully optimized local minima (RB3LYP/6-311+G\*\*).

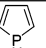
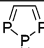
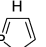
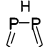
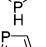
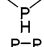
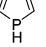
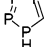
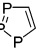
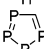
**Table 19. NICS(total) RB3LYP/6-311+G\*\* Values for Phospha Pyrroles<sup>a</sup>**

		NICS(0)	NICS(1)			NICS(0)	NICS(1)
Pyrrole		-13.62	-10.09	3,4- Diphosphapyrrole		-13.18	-10.90
2-Phosphapyrrole		-12.96	-10.47	2,3,4-Triphosphapyrrole		-14.44	-12.24
3-Phosphapyrrole		-13.45	-10.86	2,3,5-Triphosphapyrrole		-12.93	-11.77
2,3-Diphosphapyrrole		-13.55	-11.28	2,3,4,5-Tetraphosphapyrrole		-15.46	-13.42
2,4- Diphosphapyrrole		-12.85	-11.19				
2,5- Diphosphapyrrole		-11.95	-10.78				

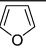
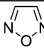
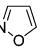
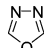
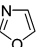
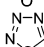
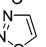
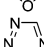
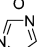
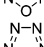
<sup>a</sup> All structures are fully optimized local minima (RB3LYP/6-311+G\*\*).**Table 20. NICS(total) RB3LYP/6-311+G\*\* Values for Aza Phospholes<sup>a</sup>**

		NICS(0)	NICS(1)			NICS(0)	NICS(1)
Phosphole		-5.35	-5.94	3,4- Diazaphosphole		-4.57	-7.48
2-Azaphosphole		-5.96	-7.01	2,3,4-Triazaphosphole		-5.86	-9.77
3-Azaphosphole		-4.46	-6.63	2,3,5-Triazaphosphole		-6.89	-10.20
2,3-Diazaphosphole		-4.56	-8.37	2,3,4,5-Tetraazaphosphole		---	---
2,4- Diazaphosphole		-5.88	-7.86				
2,5- Diazaphosphole		-6.63	-8.03				

<sup>a</sup> All structures are fully optimized local minima (RB3LYP/6-311+G\*\*).**Table 21. NICS(total) RB3LYP/6-311+G\*\* Values for Phospha Phospholes<sup>a</sup>**

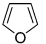
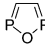
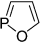
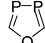
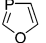
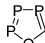
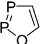
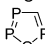
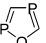
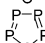
		NICS(0)	NICS(1)			NICS(0)	NICS(1)
Phosphole		-5.35	-5.94	2,5- Diphosphaphosphole		-8.46	-9.01
2-Phosphaphosphole		-6.60	-7.60	3,4- Diphosphaphosphole		-6.53	-8.19
3-Phosphaphosphole		-5.62	-7.05	2,3,4-Triphosphaphosphole		-10.14	-10.43
2,3-Diphosphaphosphole		-7.81	-8.58	2,3,5-Triphosphaphosphole		-10.97	-11.00
2,4- Diphosphaphosphole		-7.63	-8.72	2,3,4,5-Tetraphosphaphosphole		-17.70	-15.15

<sup>a</sup> All structures are fully optimized local minima (RB3LYP/6-311+G\*\*).**Table 22. NICS(total) RB3LYP/6-311+G\*\* Values for Aza Furans<sup>a</sup>**

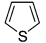
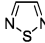
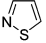
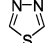
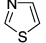
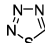
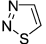
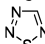
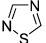
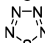
		NICS(0)	NICS(1)			NICS(0)	NICS(1)
Furan		-11.88	-9.38	2,5- Diazafuran		-11.11	-10.29
2-Azafuran		-12.23	-10.51	3,4- Diazafuran		-13.40	-12.29
3-Azafuran		-11.43	-9.72	2,3,4-Triazafuran		-14.03	-12.13
2,3-Diazafuran		-13.70	-11.62	2,3,5-Triazafuran		-15.34	-13.58
2,4- Diazafuran		-11.85	-10.64	2,3,4,5-Tetraazafuran		-18.87	-16.20

<sup>a</sup> All structures are fully optimized local minima (RB3LYP/6-311+G\*\*).

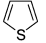
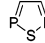
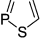
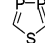
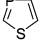
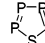
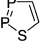
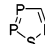
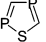
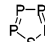
**Table 23. NICS(total) RB3LYP/6-311+G\*\* Values for Phospha Furanes<sup>a</sup>**

		NICS(0)	NICS(1)			NICS(0)	NICS(1)
Furane		-11.88	-9.38	2,5- Diphosphafurane		-11.16	-9.88
2-Phosphafurane		-11.57	-9.59	3,4- Diphosphafurane		-12.90	-11.40
3-Phosphafurane		-11.99	-10.35	2,3,4-Triphosphafurane		-13.90	-12.00
2,3-Diphosphafurane		-12.35	-10.66	2,3,5-Triphosphafurane		-12.51	-11.19
2,4- Diphosphafurane		-11.98	-10.61	2,3,4,5-Tetraphosphafurane		-15.41	-13.20

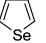
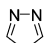
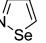
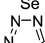
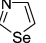
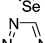
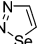
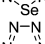
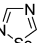
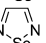
<sup>a</sup> All structures are fully optimized local minima (RB3LYP/6-311+G\*\*).**Table 24. NICS(total) RB3LYP/6-311+G\*\* Values for Aza Thiophenes<sup>a</sup>**

		NICS(0)	NICS(1)			NICS(0)	NICS(1)
Thiophene		-12.87	-10.24	2,5- Diazathiophene		-13.63	-12.20
2-Azathiophene		-13.19	-11.15	3,4- Diazathiophene		-14.15	-12.35
3-Azathiophene		-12.82	-11.07	2,3,4-Triazathiophene		-15.53	-13.92
2,3-Diazathiophene		-13.69	-12.66	2,3,5-Triazathiophene		-15.72	-14.23
2,4- Diazathiophene		-13.69	-11.92	2,3,4,5-Tetraazathiophene		-18.87	-16.20

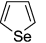
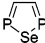
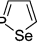
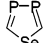
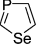
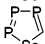
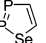
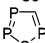
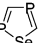
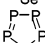
<sup>a</sup> All structures are fully optimized local minima (RB3LYP/6-311+G\*\*).**Table 25. NICS(total) RB3LYP/6-311+G\*\* Values for Phospha Thiophenes<sup>a</sup>**

		NICS(0)	NICS(1)			NICS(0)	NICS(1)
Thiophene		-12.87	-10.24	2,5- Diphosphathiophene		-12.95	-11.74
2-Phosphathiophene		-12.91	-10.92	3,4- Diphosphathiophene		-12.83	-11.96
3-Phosphathiophene		-12.50	-11.10	2,3,4-Triphosphathiophene		-14.17	-13.05
2,3-Diphosphathiophene		-13.41	-11.81	2,3,5-Triphosphathiophene		-13.96	-12.94
2,4- Diphosphathiophene		-12.83	-11.86	2,3,4,5-Tetraphosphathiophene		-15.62	-14.62

<sup>a</sup> All structures are fully optimized local minima (RB3LYP/6-311+G\*\*).**Table 26. NICS(total) RB3LYP/6-311+G\*\* Values for Aza Selenophenes<sup>a</sup>**

		NICS(0)	NICS(1)			NICS(0)	NICS(1)
Selenophene		-12.02	-9.51	3,4- Diazaselenophene		-13.40	-11.67
2-Azaselenophene		-11.95	-10.03	2,3,4-Triazaselenophene		-14.34	-12.58
3-Azaselenophene		-12.17	-10.49	2,3,5-Triazaselenophene		-14.13	-12.50
2,3-Diazaselenophene		-12.52	-11.30	2,3,4,5-Tetraazaselenophene		---	---
2,4- Diazaselenophene		-12.62	-10.90				
2,5- Diazaselenophene		-12.48	-10.87				

<sup>a</sup> All structures are fully optimized local minima (RB3LYP/6-311+G\*\*).**Table 27. NICS(total) RB3LYP/6-311+G\*\* Values for Phospha Selenophenes<sup>a</sup>**

		NICS(0)	NICS(1)			NICS(0)	NICS(1)
Selenophene		-12.02	-9.51	2,5- Diphosphaselenophene		-12.76	-11.63
2-Phosphaselenophene		-12.53	-10.60	3,4- Diphosphaselenophene		-11.96	-11.29
3-Phosphaselenophene		-11.67	-10.33	2,3,4-Triphosphaselenophene		-13.73	-12.73
2,3-Diphosphaselenophene		-13.00	-11.45	2,3,5-Triphosphaselenophene		-13.64	-12.76
2,4- Diphosphaselenophene		-12.46	-11.57	2,3,4,5-Tetraphosphaselenophene		-15.21	-14.38

<sup>a</sup> All structures are fully optimized local minima (RB3LYP/6-311+G\*\*).

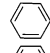
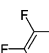
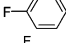
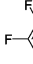
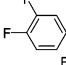
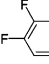
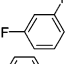
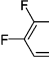
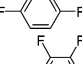
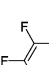
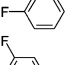
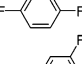
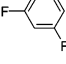


**Table 28. NICS(total) RB3LYP/6-311+G\*\* Values for Mono-Substituted Benzene X–C<sub>6</sub>H<sub>5</sub><sup>a</sup>**

X	NICS(0)	NICS(1)	X	NICS(0)	NICS(1)	X	NICS(0)	NICS(1)	X	NICS(0)	NICS(1)
H	-8.03	-10.20	PH <sub>3</sub> <sup>+</sup>	-7.68	-9.87	CBr <sub>3</sub>	-8.51	-10.03	CH=CH <sub>2</sub>	-7.26	-9.60
Li	-6.64	-9.76	SH	-7.83	-9.48	C(CH <sub>3</sub> ) <sub>3</sub>	-8.11	-10.20	CH=CH <sub>2</sub> <sup>b</sup>	-8.20	-9.99
HBe	-7.31	-10.20	S <sup>-</sup>	-4.45	-6.86	CCH	-8.12	-10.04	CO–NH <sub>2</sub>	-8.16	-10.39
BH <sub>2</sub>	-6.86	-9.83	Cl	-8.81	-10.05	CC <sup>-</sup>	-6.02	-8.11	COH=CH <sub>2</sub>	-7.72	-10.05
BH <sub>2</sub> <sup>b</sup>	-7.20	-9.62	K	-6.76	-9.79	CN	-9.44	-10.23	CO–CH <sub>3</sub>	-7.86	-10.14
BH <sub>3</sub> <sup>-</sup>	-6.54	-9.27	CaH	-7.24	-10.21	CP	-8.29	-9.90	=CH <sub>2</sub> <sup>+</sup>	-1.41	-6.09
CH <sub>3</sub>	-8.01	-10.08	GaH <sub>2</sub>	-7.37	-10.06	CHO	-7.68	-10.11	=CH <sub>2</sub> <sup>-</sup>	+1.41	-1.13
NH <sub>2</sub>	-7.84	-8.93	GeH <sub>3</sub>	-7.10	-9.96	CHO <sup>b</sup>	-8.75	-10.35	=CH <sub>2</sub> <sup>-b</sup>	-7.54	-9.86
NH <sub>2</sub> <sup>1</sup>	-8.67	-10.21	AsH <sub>2</sub>	-7.71	-9.92	COOH	-7.95	-10.15	N <sub>2</sub> <sup>+</sup>	-8.51	-9.64
NH <sub>3</sub> <sup>+</sup>	-9.52	-10.43	SeH	-7.65	-9.55	COOH <sup>b</sup>	-8.83	-10.34	(Z)-N <sub>2</sub> -Ph	-8.17	-9.80
OH	-9.06	-9.82	Se <sup>-</sup>	-4.67	-7.16	COO <sup>-</sup>	-8.02	-10.41	(E)-N <sub>2</sub> -Ph	-6.84	-9.15
O <sup>-</sup>	-4.18	-5.92	Br	-8.52	-9.88	COCl	-8.04	-10.16	N(CH <sub>3</sub> ) <sub>2</sub>	-7.94	-9.38
OH <sub>2</sub> <sup>+</sup>	-10.95	-10.98	OCH <sub>3</sub>	-8.94	-9.94	COCl <sup>b</sup>	-9.06	-10.33	NH(CH <sub>3</sub> ) <sub>2</sub> <sup>+</sup>	-9.60	-10.54
F <sup>-</sup>	-9.98	-10.39	O(CH <sub>3</sub> ) <sub>2</sub> <sup>+</sup>	-10.65	-10.79	COOOH	-7.93	-10.18	N(CH <sub>3</sub> ) <sub>3</sub> <sup>+</sup>	-9.65	-10.59
Na	-6.83	-9.71	OOH	-9.21	-9.98	CH <sub>2</sub> NH <sub>2</sub>	-7.85	-10.07	MgCl	-7.10	-9.97
MgH	-7.07	-9.99	NO <sub>2</sub>	-9.03	-10.30	CH <sub>2</sub> CH <sub>3</sub>	-8.14	-10.10	MgBr	-7.04	-9.93
AlH <sub>2</sub>	-7.16	-10.10	NO <sub>2</sub> <sup>1</sup>	-9.97	-10.47	C <sub>6</sub> H <sub>5</sub> (phenyl)	-7.54	-9.63	SO <sub>2</sub> OH	-9.20	-10.62
SiH <sub>3</sub>	-7.36	-9.94	CF <sub>3</sub>	-8.69	-10.51	1-adamantyl	-8.17	-10.23	SO <sub>3</sub> <sup>-</sup>	-8.69	-10.51
PH <sub>2</sub>	-7.81	-10.05	CCl <sub>3</sub>	-8.57	-10.17	tetrahedryl	-7.30	-9.52	SO <sub>2</sub> Cl	-9.56	-10.64

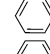
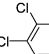
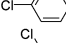
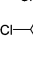
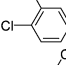
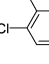
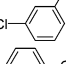
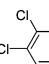
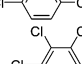
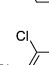
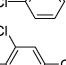
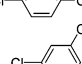
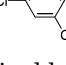
<sup>a</sup> All structures are fully optimized (RB3LYP/6-311+G\*\*) and local minima (if not otherwise noted). <sup>b</sup> 90° rotated, transition state,  $N_{\text{imag}} = 1$ .

**Table 29. NICS(total) RB3LYP/6-311+G\*\* Values for Fluorinated Benzenes<sup>a</sup>**

	NICS(0)	NICS(1)		NICS(0)	NICS(1)
Benzene		-8.03 -10.20	1,2,3,4-Tetrafluorobenzene		-15.19 -11.17
Fluorobenzene		-9.98 -10.39	1,2,3,5-Tetrafluorobenzene		-14.94 -10.79
1,2-Difluorobenzene		-11.76 -10.67	1,2,4,5-Tetrafluorobenzene		-15.22 -11.01
1,3-Difluorobenzene		-11.70 -10.40	1,2,3,4,5-Pentafluorobenzene		-16.74 -11.40
1,4-Difluorobenzene		-11.60 -10.43	1,2,3,5-Hexafluorobenzene		-18.23 -11.93
1,2,3-Trifluorobenzene		-13.39 -10.85			
1,2,4-Trifluorobenzene		-13.43 -10.69			
1,3,5-Trifluorobenzene		-13.16 -10.25			


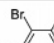
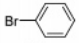
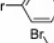
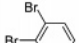
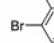
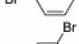
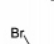
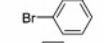
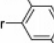
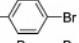
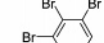
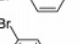
<sup>a</sup> All structures are fully optimized local minima (RB3LYP/6-311+G\*\*).

**Table 30. NICS(total) RB3LYP/6-311+G\*\* Values for Chlorinated Benzenes<sup>a</sup>**

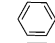
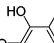
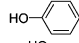
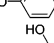
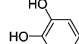
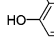
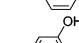
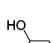
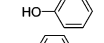
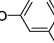
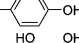
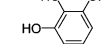
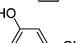
	NICS(0)	NICS(1)		NICS(0)	NICS(1)
Benzene		-8.03 -10.20	1,2,3,4-Tetrachlorobenzene		-10.15 -9.57
Chlorobenzene		-8.81 -10.05	1,2,3,5-Tetrachlorobenzene		-9.93 -9.30
1,2-Dichlorobenzene		-9.22 -9.89	1,2,4,5-Tetrachlorobenzene		-9.99 -9.35
1,3-Dichlorobenzene		-9.35 -9.75	1,2,3,4,5-Pentachlorobenzene		-10.21 -9.35
1,4-Dichlorobenzene		-9.33 -9.74	Hexachlorobenzene		-10.61 -9.51
1,2,3-Trichlorobenzene		-9.50 -9.66			
1,2,4-Trichlorobenzene		-9.67 -9.54			
1,3,5-Trichlorobenzene		-9.72 -9.36			

<sup>a</sup> All structures are fully optimized local minima (RB3LYP/6-311+G\*\*).

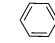
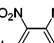
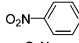
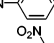
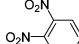
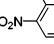
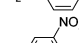
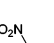
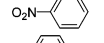
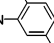
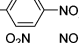
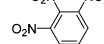
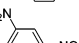
**Table 31. NICS(total) RB3LYP/6-311+G\*\* Values for Brominated Benzenes<sup>a</sup>**

		NICS(0)	NICS(1)			NICS(0)	NICS(1)
Benzene		-8.03	-10.20	1,2,3,4-Tetrabromobenzene		-8.92	-8.97
Bromobenzene		-8.52	-9.88	1,2,3,5-Tetrabromobenzene		-8.92	-8.80
1,2-Dibromobenzene		-9.10	-9.65	1,2,4,5-Tetrabromobenzene		-8.94	-8.79
1,3-Dibromobenzene		-8.84	-9.49	1,2,3,4,5-Pentabromobenzene		-9.06	-8.71
1,4-Dibromobenzene		-8.79	-9.45	Hexabromobenzene		-9.35	-8.76
1,2,3-Tribromobenzene		-9.26	-9.34				
1,2,4- Tribromobenzene		-8.88	-9.13				
1,3,5- Tribromobenzene		-9.01	-9.03				

<sup>a</sup> All structures are fully optimized local minima (RB3LYP/6-311+G\*\*).**Table 32. NICS(total) RB3LYP/6-311+G\*\* Values for Hydroxy Benzenes<sup>a</sup>**


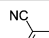
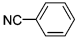
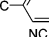
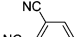
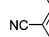
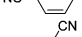
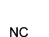
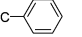
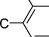
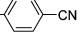
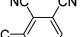

		NICS(0)	NICS(1)			NICS(0)	NICS(1)
Benzene		-8.03	-10.20	1,2,3,4-Tetrahydroxybenzene		-12.98	-10.11
Hydroxybenzene		-9.06	-9.82	1,2,3,5-Tetrahydroxybenzene		-12.12	-9.25
1,2-Dihydroxybenzene		-10.39	-9.97	1,2,4,5-Tetrahydroxybenzene		-12.63	-9.76
1,3-Dihydroxybenzene		-9.73	-9.26	1,2,3,4,5-Pentahydroxybenzene		-14.03	-10.10
1,4-Dihydroxybenzene		-10.19	-9.63	Hexahydroxybenzene		-15.52	-10.70
1,2,3-Trihydroxybenzene		-11.49	-9.88				
1,2,4- Trihydroxybenzene		-11.34	-9.58				
1,3,5- Trihydroxybenzene		-10.20	-8.36				

<sup>a</sup> All structures are fully optimized local minima (RB3LYP/6-311+G\*\*).**Table 33. NICS(total) RB3LYP/6-311+G\*\* Values for Nitro Benzenes<sup>a</sup>**


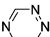
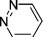
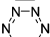
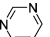
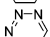
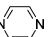
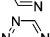
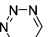
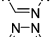
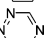
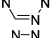
		NICS(0)	NICS(1)			NICS(0)	NICS(1)
Benzene		-8.03	-10.20	1,2,3,4-Tetranitrobenzene		-13.54	-10.33
Nitrobenzene		-9.03	-10.30	1,2,3,5-Tetranitrobenzene		-13.27	-10.65
1,2-Dinitrobenzene		-10.74	-10.33	1,2,4,5-Tetranitrobenzene		-13.39	-10.21
1,3-Dinitrobenzene		-10.02	-10.53	1,2,3,4,5-Pentanitrobenzene		-14.84	-10.28
1,4-Dinitrobenzene		-10.15	-10.53	Hexanitrobenzene		-16.34	-10.06
1,2,3-Trinitrobenzene		-12.10	-10.47				
1,2,4- Trinitrobenzene		-11.87	-10.45				
1,3,5- Trinitrobenzene		-11.27	-10.84				

<sup>a</sup> All structures are fully optimized local minima (RB3LYP/6-311+G\*\*).

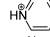
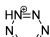
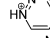
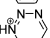
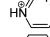
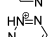
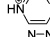
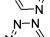
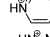
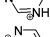
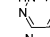
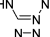
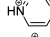
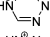
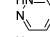
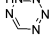
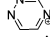
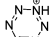
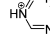
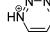
**Table 34. NICS(total) RB3LYP/6-311+G\*\* Values for Cyano Benzenes<sup>a</sup>**

		NICS(0)	NICS(1)			NICS(0)	NICS(1)
Benzene		-8.03	-10.20	1,2,3,4-Tetracyanobenzene		-9.29	-9.78
Cyanobenzene		-9.44	-10.23	1,2,3,5-Tetracyanobenzene		-9.28	-9.76
1,2-Dicyanobenzene		-8.71	-10.06	1,2,4,5-Tetracyanobenzene		-9.36	-9.75
1,3-Dicyanobenzene		-8.77	-10.07	1,2,3,4,5-Pentacyanobenzene		-9.49	-9.59
1,4-Dicyanobenzene		-8.82	-10.12	Hexacyanobenzene		-9.49	-9.30
1,2,3-Tricyanobenzene		-8.92	-9.90				
1,2,4-Tricyanobenzene		-9.08	-9.90				
1,3,5-Tricyanobenzene		-9.17	-9.98				

<sup>a</sup> All structures are fully optimized local minima (RB3LYP/6-311+G\*\*).**Table 35. NICS(total) RB3LYP/6-311+G\*\* Values for Azapyridines<sup>a</sup>**

		NICS(0)	NICS(1)			NICS(0)	NICS(1)
Pyridine		-6.82	-10.17	3,5-Diazapyridine		-4.04	-9.65
2-Azapyridine		-5.33	-10.53	2,3,4-Triazapyridine		-2.67	-10.78
3-Azapyridine		-5.51	-9.99	2,3,5-Triazapyridine		-2.37	-10.36
4-Azapyridine		-5.30	-10.24	2,4,5-Triazapyridine		-1.80	-10.58
2,3-Diazapyridine		-4.32	-10.80	2,3,4,5-Tetraazapyridine		-0.62	-10.64
2,4-Diazapyridine		-3.77	-10.36	Pentaazapyridine		+1.86	-10.24

<sup>a</sup> All structures are fully optimized local minima (RB3LYP/6-311+G\*\*).**Table 36. NICS(total) RB3LYP/6-311+G\*\* Values for Monoprotonated Azapyridines<sup>a</sup>**

		NICS(0)	NICS(1)			NICS(0)	NICS(1)
Protonated Pyridine		-7.75	-9.89	2-Protonated 2,3,4-Triazapyridine		-4.05	-10.76
Protonated 2-Azapyridine		-6.82	-10.28	1-Protonated 2,3,5-Triazapyridine		-3.28	-9.65
Protonated 3-Azapyridine		-6.13	-9.52	2-Protonated 2,3,5-Triazapyridine		-5.03	-10.94
Protonated 4-Azapyridine		-6.66	-10.29	5-Protonated 2,3,5-Triazapyridine		-3.19	-10.17
1-protonated 2,3-Diazapyridine		-5.39	-10.35	Protonated 2,4,5-Triazapyridine		-3.82	-10.84
2-protonated 2,3-Diazapyridine		-6.24	-11.00	1-Protonated 2,3,4,5-Tetraazapyridine		-2.64	-10.22
1-Protonated 2,4-Diazapyridine		-5.84	-10.46	2-Protonated 2,3,4,5-Tetraazapyridine		-2.99	-11.17
2-Protonated 2,4-Diazapyridine		-4.94	-9.87	3-Protonated 2,3,4,5-Tetraazapyridine		-1.55	-10.30
4-Protonated 2,4-Diazapyridine		-4.73	-10.35	Protonated Pentaazapyridine		-0.63	-10.73
Protonated 3,5-Diazapyridine		-4.51	-8.96				
1-Protonated 2,3,4-Triazapyridine		-4.11	-10.53				

<sup>a</sup> All structures are fully optimized local minima (RB3LYP/6-311+G\*\*).

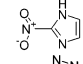
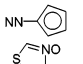
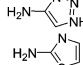
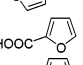
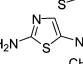
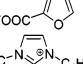
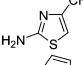
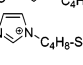
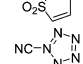
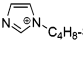
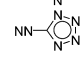

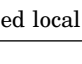

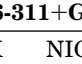


**Table 37. NICS(total) RB3LYP/6-311+G\*\* Values for Selected Substituted Hetero Six-Membered Rings<sup>a</sup>**

		NICS(0)	NICS(1)			NICS(0)	NICS(1)
(3-Fluorophenyl)lithium		-8.82	-10.10	2-Aminonicotinic acid		-4.95	-7.41
(4-Fluorophenyl)lithium		-9.13	-10.23	2-Hydroxybenzene dimer		-6.54	-8.44
1,2-Difluoro-4,5-dilithiobenzene		-9.82	-10.14	pyridin-2(1H)-one dimer		-3.68	-5.40
4-tert-Butylphenol		-9.18	-9.81	2-Amino-4-picoline		-6.15	-8.44
2-Aminophenol		-8.95	-9.57	2,2'-Bipyridine		-6.37	-9.67
3-Aminophenol		-8.05	-8.52	2,6-Bis(hydroxymethyl)pyridine		-6.49	-9.82
4-Aminophenol		-9.23	-9.05	2,6-Bis(hydroxymethyl)pyridinium		-7.29	-9.61
2,4,6-Trinitrophenol		-11.04	-9.30	2,6-Bis(aminomethyl)pyridine		-6.62	-9.82
2,4,6-Trinitrophenolate		-5.34	-5.20	2,6-Bis(aminomethyl)pyridinium		-6.88	-9.51
4-(2-Aminopropyl)benzene-1,2-diol		-10.24	-9.71	2,6-diformylpyridine		-6.83	-10.37
(2Z)-3-(3,4-Dihydroxyphenyl)acrylic acid		-9.75	-13.1	2,6-diformylpyridinium		-7.58	-10.08
3,4,5-Trihydroxybenzoic acid		-11.50	-10.02	2,6-diacetylpyridine		-6.99	-10.38
3,4,5-Trimethoxyphenethylamine		-11.18	-9.78	2,6-diacetylpyridinium		-7.89	-10.18
2-Aminobenzoic acid		-6.75	-8.11	2,6-diacetoacetylpyridine		-7.07	-10.28
2-Aminobenzoic acid (zwitter ionic)		-7.87	-8.98	3-Aminophenylamine		-7.39	-7.85
3-Aminobenzoic acid		-7.87	-8.98	3-Aminobenzenaminium		-8.22	-8.28
3-Aminobenzoic acid (zwitter ionic)		-9.71	-10.55	4-Aminophenylamine		-8.34	-8.56
4-Aminobenzoic acid		-7.34	-8.80	4-Aminobenzenaminium		-8.16	-8.28
4-Aminobenzoic acid (zwitter ionic)		-9.31	-10.33	4-Nitroaniline		-7.91	-8.61
4-(Dimethylamino)benzonitrile		-7.94	-9.02	2-Methyl-1,3,5-trinitrobenzene (TNT)		-11.55	-10.32
2-Aminophenylamine		-8.98	-9.56	2,6-Dimethylpyridine		-6.47	-9.63
2-Aminobenzenaminium		-9.25	-10.20	2,6-bis[(2Z)-3-hydroxybut-2-enyl]pyridine		-6.48	-10.04

<sup>a</sup> All structures are fully optimized local minima (RB3LYP/6-311+G\*\*).

**Table 38. NICS(total) RB3LYP/6-311+G\*\* Values for Selected Substituted Hetero Five-Membered Rings<sup>a</sup>**

		NICS(0)	NICS(1)			NICS(0)	NICS(1)
2-Nitro-1H-imidazol		-12.59	-10.17	5-Diazocyclopenta-1,3-diene		-9.63	-6.52
1H-1,2,3-triazol-4-amine		-13.03	-11.20	1,3-thiazole 3-oxide		-12.26	-8.08
2-Amionthiazol		-10.32	-8.98	2-furoic acid		-11.13	-9.21
2-Amino-5-nitrothiazol		-8.89	-6.89	2-furoate		-11.04	-9.08
2-Amino-4-methylthiazol		-9.45	-7.45	3-butyl-1-methyl-1H-imidazol-3-ium		-13.37	-9.61
Thiophendioxide		-1.18	-0.89	1-ethyl-3-(4-sulfobutyl)-1H-imidazol-3-ium		-13.42	-9.63
1H-Pentazole-1-carbonitrile		-16.78	-15.02	4-(1-ethyl-1H-imidazol-3-ium-3-yl)butane-1-sulfonate		-13.40	-9.61
5-Diazo-5H-tetrazole		-12.68	-13.36				

<sup>a</sup> All structures are fully optimized local minima (RB3LYP/6-311+G\*\*).**Table 39. NICS(total) RB3LYP/6-311+G\*\* Values for Ortho-Substituted Pyridine, X–Pyridine<sup>a</sup>**

X	NICS(0)	NICS(1)	X	NICS(0)	NICS(1)	X	NICS(0)	NICS(1)	X	NICS(0)	NICS(1)
H	-6.82	-10.17	NH <sub>2</sub>	-5.82	-8.34	MgH	—	—	Cl	-7.57	-9.84
Li	—	—	OH	-7.21	-9.24	AlH <sub>2</sub>	-5.98	-10.11	GeH <sub>3</sub>	-6.19	-10.16
HBe	—	—	F	-8.55	-10.14	SiH <sub>3</sub>	-6.16	-9.98	Br	-7.47	-9.76
BH <sub>2</sub>	-6.11	-10.15	Na	—	—	PH <sub>2</sub>	-6.15	-9.51	CO—CH <sub>3</sub>	-6.87	-10.32
CH <sub>3</sub>	-6.61	-9.89				SH	-6.22	-9.02			

<sup>a</sup> All structures are fully optimized (RB3LYP/6-311+G\*\*) and local minima (if not otherwise noted).**Table 40. NICS(total) RB3LYP/6-311+G\*\* Values for Protonated Ortho-Substituted Pyridine, X–Pyridinium<sup>a</sup>**

X	NICS(0)	NICS(1)	X	NICS(0)	NICS(1)	X	NICS(0)	NICS(1)	X	NICS(0)	NICS(1)
H	-7.75	-9.89	NH <sub>2</sub>	-5.74	-7.08	MgH	-6.78	-9.71	SH	-6.16	-8.05
Li	-6.43	-9.53	OH	-7.47	-8.53	AlH <sub>2</sub>	-7.10	-9.93	Cl	-7.49	-9.14
HBe	-7.22	-9.95	F	-8.37	-9.52	SiH <sub>3</sub>	-7.16	-9.76	Br	-7.14	-8.99
BH <sub>2</sub>	-7.25	-9.92	Na	-6.26	-9.42	PH <sub>2</sub>	-6.51	-8.85	CH=CH <sub>2</sub>	-6.39	-8.67
CH <sub>3</sub>	-7.36	-9.47									

<sup>a</sup> All structures are fully optimized (RB3LYP/6-311+G\*\*) and local minima (if not otherwise noted).**Table 41. NICS(total) RB3LYP/6-311+G\*\* Values for Meta-Substituted Pyridine, X–Pyridine<sup>a</sup>**

X	NICS(0)	NICS(1)	X	NICS(0)	NICS(1)	X	NICS(0)	NICS(1)	X	NICS(0)	NICS(1)
H	-6.82	-10.17	F	-8.92	-10.51	SH	-6.71	-9.51	SeH	-10.21	-10.11
Li	-5.46	-9.71	Na	-5.57	-9.61	Cl	-7.63	-10.05	Br	-7.55	-9.29
HBe	-6.18	-10.07	MgH	-5.83	-9.87	K	-5.53	-9.66	CN	-7.29	-10.17
BH <sub>2</sub>	-5.64	-9.71	AlH <sub>2</sub>	-5.97	-9.97	CaH	-6.30	-10.16	NO <sub>2</sub>	-8.08	-10.39
CH <sub>3</sub>	-6.93	-10.12	SiH <sub>3</sub>	-6.19	-9.96	GaH <sub>2</sub>	-10.08	-10.04	CH=CH <sub>2</sub>	-6.15	-9.59
NH <sub>2</sub>	-6.91	-9.28	PH <sub>2</sub>	-6.66	-9.93	GeH <sub>3</sub>	-6.24	-10.06	CO—NH <sub>2</sub>	-7.04	-10.52
OH	-8.12	-10.02				AsH <sub>2</sub>	-6.56	-10.62			

<sup>a</sup> All structures are fully optimized (RB3LYP/6-311+G\*\*) and local minima (if not otherwise noted).**Table 42. NICS(total) RB3LYP/6-311+G\*\* Values for Protonated Meta-Substituted Pyridine, X–Pyridinium<sup>a</sup>**

X	NICS(0)	NICS(1)	X	NICS(0)	NICS(1)	X	NICS(0)	NICS(1)	X	NICS(0)	NICS(1)
H	-7.75	-9.89	NH <sub>2</sub>	-5.50	-7.08	AlH <sub>2</sub>	-6.90	-9.76	Br	-7.55	-9.29
Li	-6.40	-9.60	OH	-8.62	-9.48	SiH <sub>3</sub>	-7.09	-9.71	CN	-8.03	-9.76
HBe	-7.12	-9.84	F	-9.59	-10.13	PH <sub>2</sub>	-6.91	-9.17	NO <sub>2</sub>	-9.24	-10.31
BH <sub>2</sub>	-6.81	-9.55	Na	-6.27	-9.52	SH	-6.67	-8.52	CH=CH <sub>2</sub>	-6.64	-8.88
CH <sub>3</sub>	-7.73	-9.80	MgH	6.72	-9.70	Cl	-8.02	-9.51			

<sup>a</sup> All structures are fully optimized (RB3LYP/6-311+G\*\*) and local minima (if not otherwise noted).**Table 43. NICS(total) RB3LYP/6-311+G\*\* Values for Para-Substituted Pyridine, X–Pyridine<sup>a</sup>**

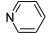
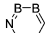
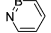
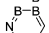
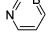
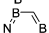
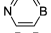
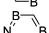
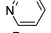
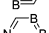

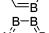
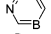
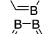
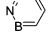
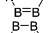
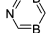
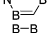

X	NICS(0)	NICS(1)	X	NICS(0)	NICS(1)	X	NICS(0)	NICS(1)	X	NICS(0)	NICS(1)
H	-6.82	-10.17	NH <sub>2</sub>	-6.60	-8.66	AlH <sub>2</sub>	-6.06	-10.18	Br	-7.32	-9.86
Li	-5.13	-9.63	OH	-8.00	-9.69	SiH <sub>3</sub>	-6.16	-10.00	CH=O	-6.89	-10.30
HBe	-5.99	-10.14	F	-8.98	-10.35	PH <sub>2</sub>	-6.66	-10.09	CH <sub>2</sub> CH <sub>3</sub>	-7.04	-10.09
BH <sub>2</sub>	-6.14	-10.17	Na	-5.27	-9.56	SH	-6.54	-9.29	CH=CH <sub>2</sub>	-6.13	-9.51
CH <sub>3</sub>	-6.87	-10.07	MgH	-5.55	-9.84	Cl	-7.64	-10.02			

<sup>a</sup> All structures are fully optimized (RB3LYP/6-311+G\*\*) and local minima (if not otherwise noted).

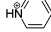
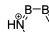
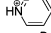
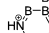
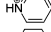
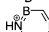
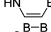
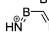
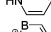
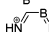
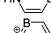
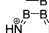
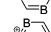
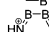
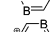
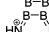
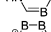
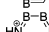
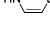
**Table 44. NICS(total) RB3LYP/6-311+G\*\* Values for Para-Substituted Protonated Pyridine, X–Pyridinium<sup>a</sup>**

X	NICS(0)	NICS(1)	X	NICS(0)	NICS(1)	X	NICS(0)	NICS(1)	X	NICS(0)	NICS(1)
H	-7.75	-9.89	NH <sub>2</sub>	-6.93	-8.17	MgH	-6.65	-9.79	Cl	-7.26	-8.92
Li	-6.24	-9.66	OH	-7.43	-8.45	AlH <sub>2</sub>	-7.02	-9.98	Br	-6.98	-9.08
HBe	-7.15	-9.97	F	-8.83	-9.47	SiH <sub>3</sub>	-6.99	-9.73	CH <sub>2</sub> CH <sub>3</sub>	-7.32	-9.46
BH <sub>2</sub>	-7.31	-9.92	Na	-6.10	-9.62	PH <sub>2</sub>	-5.99	-8.61	CH=CH <sub>2</sub>	-6.03	-8.28
CH <sub>3</sub>	-7.26	-9.45				SH	-5.68	-9.27			

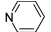
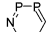

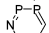

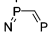

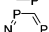
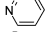
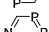
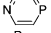
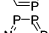
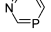
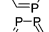
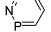
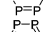
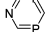
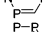

<sup>a</sup> All structures are fully optimized (RB3LYP/6-311+G\*\*) and local minima (if not otherwise noted).**Table 45. NICS(total) RB3LYP/6-311+G\*\* Values for Borapyridines<sup>a</sup>**

	NICS(0)	NICS(1)		NICS(0)	NICS(1)
Pyridine		-6.82 -10.17	2,3,5-Triborapyridine		-27.25 -11.72
2-Borapyridine		-11.26 -9.28	2,3,6-Triborapyridine		-26.67 -14.48
3-Borapyridine		-11.47 -10.06	2,4,5-Triborapyridine		-29.77 -9.83
4-Borapyridine		-12.48 -10.26	2,4,6-Triborapyridine		-17.95 -5.37
2,3-Diborapyridine		-20.53 -11.61	3,4,5-Triborapyridine		-26.22 -6.43
2,4-Diborapyridine		-12.59 -6.82	2,3,4,5-Tetraborapyridine		-4.82 +0.01
2,5-Diborapyridine		-15.84 -9.28	2,3,5,6-Tetraborapyridine		-3.21 -18.43
2,6-Diborapyridine		-14.00 -8.01	2,3,4,6-Tetraborapyridine		-15.39 -0.23
3,5-Diborapyridine		-24.35 -14.05	Pentaborapyridine		-14.98 -2.53
2,3,4-Triborapyridine		-42.46 -16.88			

<sup>a</sup> All structures are fully optimized local minima (RB3LYP/6-311+G\*\*).**Table 46. NICS(total) RB3LYP/6-311+G\*\* Values for Monoprotonated Borapyridines<sup>a</sup>**

	NICS(0)	NICS(1)		NICS(0)	NICS(1)
Protonated Pyridine		-7.75 -9.89	Protonated 2,3,5-Triborapyridine		-66.77 -102.70
Protonated 2-Borapyridine		-10.38 -8.40	Protonated 2,3,6-Triborapyridine		-29.72 -39.05
Protonated 3-Borapyridine		-13.44 -10.63	Protonated 2,4,5-Triborapyridine		--- ---
Protonated 4-Borapyridine		-11.65 -8.87	Protonated 2,4,6-Triborapyridine		-16.27 -6.79
Protonated 2,3-Diborapyridine		-23.43 -14.13	Protonated 3,4,5-Triborapyridine		-5.06 -2.08
Protonated 2,4-Diborapyridine		-14.79 -8.01	Protonated 2,3,4,5-Tetraborapyridine		-8.41 -3.85
Protonated 2,5-Diborapyridine		-15.45 -9.81	Protonated 2,3,5,6-Tetraborapyridine		-18.49 -9.89
Protonated 2,6-Diborapyridine		-17.03 -9.75	Protonated 2,3,4,6-Tetraborapyridine		-14.95 -13.13
Protonated 3,5-Diborapyridine		-17.18 -11.69	Protonated Pentaborapyridine		-28.13 -8.20
Protonated 2,3,4-Triborapyridine		-4.43 -0.86			

<sup>a</sup> All structures are fully optimized local minima (RB3LYP/6-311+G\*\*).**Table 47. NICS(total) RB3LYP/6-311+G\*\* Values for Phosphapyridines<sup>a</sup>**

	NICS(0)	NICS(1)		NICS(0)	NICS(1)
Pyridine		-6.82 -10.17	2,3,5-Triphosphapyridine		-3.46 -7.77
2-Phosphapyridine		-5.43 -9.14	2,3,6-Triphosphapyridine		-2.61 -7.17
3-Phosphapyridine		-5.69 -9.58	2,4,5-Triphosphapyridine		-3.46 -7.78
4-Phosphapyridine		-5.54 -9.61	2,4,6-Triphosphapyridine		-2.71 -7.23
2,3-Diphosphapyridine		-4.61 -8.45	3,4,5-Triphosphapyridine		-4.33 -8.41
2,4-Diphosphapyridine		-4.30 -8.51	2,3,4,5-Tetrphosphapyridine		-3.74 -7.64
2,5-Diphosphapyridine		-4.15 -8.40	2,3,5,6-Tetrphosphapyridine		-1.60 -6.45
2,6-Diphosphapyridine		-3.60 -7.94	2,3,4,6-Tetrphosphapyridine		-2.34 -6.71
3,5-Diphosphapyridine		-4.69 -8.97	Pentaphosphapyridine		-2.95 -6.91
2,3,4-Triphosphapyridine		-4.00 -7.96			

<sup>a</sup> All structures are fully optimized local minima (RB3LYP/6-311+G\*\*).



**Table 48. NICS(total) RB3LYP/6-311+G\*\* Values for Monoprotonated Phosphapyridines<sup>a</sup>**

		NICS(0)	NICS(1)			NICS(0)	NICS(1)
Protonated Pyridine		-7.75	-9.89	Protonated 2,3,5-Triphosphapyridine		-4.97	-8.22
Protonated 2-Phosphapyridine		-6.20	-8.94	Protonated 2,3,6-Triphosphapyridine		-4.23	-7.69
Protonated 3-Phosphapyridine		-6.62	-9.44	Protonated 2,4,5-Triphosphapyridine		-4.70	-7.97
Protonated 4-Phosphapyridine		-6.13	-9.15	Protonated 2,4,6-Triphosphapyridine		-3.80	-7.29
Protonated 2,3-Diphosphapyridine		-5.56	-8.46	Protonated 3,4,5-Triphosphapyridine		-5.49	-8.53
Protonated 2,4-Diphosphapyridine		-4.93	-8.20	Protonated 2,3,4,5-Tetraphosphapyridine		-5.79	-8.44
Protonated 2,5-Diphosphapyridine		-5.29	-8.53	Protonated 2,3,5,6-Tetraphosphapyridine		-4.06	-7.61
Protonated 2,6-Diphosphapyridine		-4.59	-7.97	Protonated 2,3,4,6-Tetraphosphapyridine		-4.53	-7.53
Protonated 3,5-Diphosphapyridine		-5.75	-9.01	Protonated Pentaphosphapyridine		-6.60	-8.90
Protonated 2,3,4-Triphosphapyridine		-5.36	-8.13				

<sup>a</sup> All structures are fully optimized local minima (RB3LYP/6-311+G\*\*).**Table 49. NICS(total) RB3LYP/6-311+G\*\* Values for Capped Five- and Six-Membered Rings<sup>a</sup>**

	NICS(0)	NICS(1)	NICS(0)	NICS(1)		NICS(0)	NICS(1)	NICS(0)	NICS(1)
	5 membered ring	5 membered ring	6 membered ring	6 membered ring		5 membered ring	5 membered ring	6 membered ring	6 membered ring
	-13.65	-10.34				-6.00	-9.79		
	-12.59	-10.01				-24.08	-10.77		
	-15.18	-18.85				-22.27	-11.62		
	-10.20	-9.80				-17.75	-12.77	-7.40	-9.17
	-21.75	-10.33				-14.82	-14.24	-8.32	-8.73
	-14.46	-9.27						-8.44	-10.42
								-6.80	-9.89

<sup>a</sup> All structures are fully optimized local minima (RB3LYP/6-311+G\*\*).

## 8. References

- See reviews: (a) Minkin, V. I.; Glukhovtsev, M. N.; Simkin, B. Y. *Aromaticity and Antiaromaticity*; John Wiley & Sons: New York, 1994. (b) Schleyer, P. v. R.; Jiao, H. *Pure Appl. Chem.* **1996**, *68*, 209. (c) Lloyd, D. J. *Chem. Inf. Comput. Sci.* **1996**, *36*, 442. (d) Krygowski, T. M.; Cyrański, M. K.; Czarnocki, Z.; Hafelinger, G.; Katritzky, A. R. *Tetrahedron* **2000**, *56*, 1783. (e) Schleyer, P. v. R., Guest Ed. Special issue on aromaticity. *Chem. Rev.* **2001**, *101* (5).
- Faraday, M. *Philos. Trans. R. London* **1825**, 440.
- Evans, M. G.; Warhurst, E. *Trans. Faraday Soc.* **1938**, *34*, 614.
- Calvin, M.; Wilson, K. W. *J. Am. Chem. Soc.* **1945**, *67*, 2003. See review: Masui, H. *Coord. Chem. Rev.* **2001**, *219–221*, 957.
- Winstein, S. *J. Am. Chem. Soc.* **1959**, *81*, 6524. See review: Williams, R. V. *Chem. Rev.* **2001**, *101*, 1185.
- Heilbronner, E. *Tetrahedron Lett.* **1964**, 1923.
- (a) Breslow, R. *Chem. Eng. News* **1965**, 90 (June 28) and earlier lectures. (b) Dewar, M. J. S. *Adv. Chem. Phys.* **1965**, *8*, 121. (c) Breslow, R.; Brown, J.; Gajewski, J. J. *J. Am. Chem. Soc.* **1967**, *89*, 4383. (d) Breslow, R. *Acc. Chem. Res.* **1973**, *6*, 393.
- (a) Osawa, E. *Superaromaticity. Kagaku (Chemistry)* **1970**, *25*, 854 (in Japanese). For its English translation, see: Osawa, E. *Philos. Trans. R. Soc. London A* **1993**, *343*, 1. (b) Curl, R. E.; Smalley, R. E.; Kroto, H. W.; O'Brien, S.; Heath, J. R. *J. Mol. Graph. Mod.* **2001**, *19*, 185. (c) The term "superaromaticity" was used as early as 1932 (if not earlier): Gilman, H.; Towne, E. B. *Recl. Trav. Chim. Pays-Bas Belg.* **1932**, *51*, 1054. At that time, superaromatic properties were ascribed to a compound when it undergoes a typical aromatic reaction more easily than the parent unsubstituted compound.
- (a) Baird, N. C. *J. Am. Chem. Soc.* **1972**, *94*, 4941. (b) Elaborated by: Gogonea, V.; Schleyer, P. v. R.; Schreiner, P. R. *Angew. Chem., Int. Ed.* **1998**, *37*, 1945.
- Aihara, J. *J. Am. Chem. Soc.* **1978**, *100*, 3339.
- (a) Dewar, M. J. S. *Bul. Soc. Chim. Belg.* **1979**, *88*, 957. (b) Dewar, M. J. S.; McKee, M. L. *Pure Appl. Chem.* **1980**, *52*, 1431. (c) Dewar, M. J. S. *J. Am. Chem. Soc.* **1984**, *106*, 669.
- Chandrasekhar, J.; Jemmis, E. D.; Schleyer, P. v. R. *Tetrahedron Lett.* **1979**, 3707–3710.
- Jemmis, E. D.; Schleyer, P. v. R. *J. Am. Chem. Soc.* **1982**, *104*, 4781.
- (a) Shaik, S. S.; Hiberty, P. C. *J. Am. Chem. Soc.* **1985**, *107*, 3089. (b) Hiberty, P. C.; Shaik, S. S.; Lefour, J. M.; Ohanessian, G. *J. Org. Chem.* **1985**, *50*, 4657. (c) Shaik, S. S.; Hiberty, P. C.; Lefour, J. M.; Ohanessian, G. *J. Am. Chem. Soc.* **1987**, *109*, 363.
- Kroto, H. W.; Heath, J. R.; O'Brien, S. C.; Curl, R. F.; Smalley, R. E. *Nature* **1985**, *318*, 162–163.
- Iijima, S. *Nature* **1991**, 354, 56.
- (a) Fokin, A.; Jiao, H.; Schleyer, P. v. R. *J. Am. Chem. Soc.* **1998**, *120*, 9364. Experimentally [18]transannulenes were realized as units in fullerene derivatives, see: (b) Wei, X. W.; Darwish, A. D.; Boltalina, O. V.; Hitchcock, P. B.; Taylor, R.; *Angew. Chem., Int. Ed.* **2001**, *40*, 2989. (c) Troshin, P.; Lyubovskaya, R. N.; Ioffe, I. N.; Shustova, N. B.; Kemnitz, E.; Troyanov, S. I. *Angew. Chem., Int. Ed.* **2005**, *44*, 234. (d) Canteenwala, T.; Padmawar, P. A.; Chiang, L. Y. *J. Am. Chem. Soc.* **2005**, *127*, 26. For a review see: (e) Burley, G. A. *Angew. Chem., Int. Ed.* **2005**, *44*, 3176.
- (a) Wannere, C. S.; Corminboeuf, C.; Wang, Z. X.; Wodrich, M. D.; King, R. B.; Schleyer, P. v. R. *J. Am. Chem. Soc.* **2005**, *127*, 5701. (b) Tsipis, A. C.; Tsipis, C. A. *J. Am. Chem. Soc.* **2003**, *125*, 1136. (c) Tsipis, C. A.; Karagiannis, E. E.; Kladou, P. F.; Tsipis, A. C. *J. Am. Chem. Soc.* **2004**, *126*, 12916.
- Katritzky, A. R.; Karelson, M.; Sild, S.; Krygowski, T. M.; Jug, K. *J. Org. Chem.* **1998**, *63*, 5228.
- Cyranowski, M. K.; Schleyer, P. v. R.; Krygowski, T. M.; Jiao, H.; Hohlneicher, G. *Tetrahedron* **2003**, *59*, 1657.
- Schleyer, P. v. R.; Puhlhofer, F. *Org. Lett.* **2002**, *4*, 2873.
- Bühl, M.; Hirsch, A. *Chem. Rev.* **2001**, *101*, 1153.
- (a) Hirsch, A. *The Chemistry of the Fullerenes*; Thieme: Stuttgart, Germany, 1994. (b) Hirsch, A. *Top. Curr. Chem.* **1998**, *199*, 1.
- Oth, J. F. M.; Woo, E. P.; Sondheimer, F. *J. Am. Chem. Soc.* **1973**, *95*, 7337.
- Wannere, C. S.; Corminboeuf, C.; Allen, W. D.; Schaefer, H. F.; Schleyer, P. v. R. *Org. Lett.* **2005**, *7*, 1457.
- Schleyer, P. v. R.; Maerker, C.; Dransfeld, A.; Jiao, H.; Hommes, N. J. R. v. E. *J. Am. Chem. Soc.* **1996**, *118*, 6317.
- Loschmidt, J. "Chemische Studien 1" Private Printing, Vienna 1861. This rare booklet was reprinted by Ostwalds Klassiker Exakten Wiss. 190 1913 [R. Anschütz].
- (a) Kekulé, A. *Bull. Soc. Chim. Paris* **1865**, *3*, 98. (b) Kekulé, A. *Ann.* **1866**, *137*, 129. (c) Kekulé, A. *Bull. Acad. R. Belg.* **1865**, *19*, 551. (d) Kekulé, A. *Lehrbuch der Organischen Chemie*; Enk.: Erlangen, 1866; Vol 2. (e) Kekulé, A. *Ann.* **1872**, *162*, 77.
- Erlenmeyer, E. *Ann.* **1866**, *137*, 327/344.

- (30) (a) Pascal, P. *Ann. Chim. Phys.* **1910**, 19, 5. (b) Pascal, P. *Ann. Chim. Phys.* **1912**, 25, 289. (c) Pascal, P. *Ann. Chim. Phys.* **1913**, 28, 218–243.
- (31) (a) Crocker, E. C. *J. Am. Chem. Soc.* **1922**, 44, 1618. For a review on the background of the aromatic sextet concept, see: (b) Balaban, A. T.; Schleyer, P. v. R. *Chem. Rev.* **2005**, 105, 3436.
- (32) Armit, J. W.; Robinson, R. *J. Chem. Soc.* **1925**, 127, 1604.
- (33) (a) Hückel, E. *Z. Phys.* **1931**, 70, 204. (b) Hückel, E. *Z. Phys.* **1931**, 72, 310. (c) Hückel, E. *Z. Phys.* **1932**, 76, 628.
- (34) (a) Pauling, L.; Sherman, J. *J. Chem. Phys.* **1933**, 1, 606. (b) Pauling, L. *The Nature of the Chemical Bond*, 3rd ed.; Cornell University Press: Ithaca, New York, 1960. (c) Wheland, G. W. *Resonance in Organic Chemistry*; Wiley: New York, 1955.
- (35) Kistiakowski, B.; Ruhoff, J. R.; Smith, H. A.; Vaughan, W. E. *J. Am. Chem. Soc.* **1936**, 58, 146.
- (36) (a) Ehrenfest, P. *Physica* **1925**, 5, 388; *Z. Phys.* **1929**, 58, 719. (b) Raman, C. V. *Nature* **1929**, 123, 945; **1929**, 124, 412. (c) Pauling, L. *J. Chem. Phys.* **1936**, 4, 673. (d) Lonsdale, K. *Proc. R. Soc. London A* **1937**, 159, 149. (e) See review: Lazzarretti, P. *Prog. Nucl. Magn. Reson. Spectrosc.* **2000**, 36, 1.
- (37) London, F. *J. Phys. Radium* **1937**, 8, 397.
- (38) The GIAO method has been further developed by various scientists; examples are: (a) Hameka, H. F. *Mol. Phys.* **1958**, 1, 203–215. (b) McWeeny, R. *Phys. Rev.* **1962**, 126, 1028. (c) Edwards, T. G.; McWeeny, R. *Chem. Phys. Lett.* **1971**, 10, 283. (d) Ditchfield, R. *J. Chem. Phys.* **1972**, 56, 5688. (e) Epstein, S. T. *J. Chem. Phys.* **1973**, 58, 1592. (f) Mallion, R. B. *Mol. Phys.* **1973**, 25, 1415. (g) Ditchfield, R. *Mol. Phys.* **1974**, 27, 789. (h) Dodds, J. L.; McWeeny, R.; Sadlej, A. J. *Mol. Phys.* **1980**, 41, 1419. (i) Chesnut, D. B.; Foley, C. K. *Chem. Phys. Lett.* **1985**, 118, 316. (j) Chesnut, D. B.; Moore, K. D. *J. Comput. Chem.* **1985**, 10, 648. (k) Wolinski, K.; Hinton, J. F.; Pulay, P. *J. Am. Chem. Soc.* **1990**, 112, 8251.
- (39) Meyer, L. H.; Saika, A.; Gutowski, H. S. *J. Am. Chem. Soc.* **1953**, 75, 4567.
- (40) (a) Bernstein, H. J.; Schneider, W. G.; Pople, J. A. *Proc. R. Soc. London, Ser. A* **1956**, 236, 515–528. (b) Pople, J. A. *J. Chem. Phys.* **1956**, 24, 1111. (c) Pople, J. A. *Mol. Phys.* **1958**, 1, 175.
- (41) (a) Dewar, M. J. S.; Gleicher, G. J. *J. Am. Chem. Soc.* **1965**, 87, 685. (b) Dewar, M. J. S.; Gleicher, G. J. *J. Am. Chem. Soc.* **1965**, 87, 692. (c) Dewar, M. J. S.; Gleicher, G. J. *J. Chem. Phys.* **1966**, 44, 759. (d) Dewar, M. J. S.; de Llano, C. *J. Am. Chem. Soc.* **1969**, 91, 789. (e) For a review, see: Schaad, L. J.; Hess, B. A., Jr. *Chem. Rev.* **2001**, 101, 1465.
- (42) (a) Sondheimer, F.; Calder, I. C.; Elix, J. A.; Gaoni, Y.; Garratt, P. J.; Grohmann, K.; di Maio, G.; Mayer, J.; Sargent, M. V.; Wolovsky, R. *Chem. Soc. Spec. Publ.* **1967**, 21, 75. (b) Sondheimer, F. *Acc. Chem. Res.* **1972**, 5, 81.
- (43) Jug, K. A.; François, P. *Theor. Chim. Acta* **1967**, 7, 249.
- (44) (a) Dauben, H. J., Jr.; Wilson, J. D.; Laity, J. L. *J. Am. Chem. Soc.* **1968**, 90, 811; **1969**, 91, 1991. (b) Dauben, H. J., Jr.; Wilson, J. D.; Laity, J. L. *Diamagnetic Susceptibility Exaltation as Criterion of Aromaticity*. In *Nonbenzenoid Aromatics*; Snyder, J. P., Ed.; Academic Press: New York, 1971; Vol. 2.
- (45) (a) Benson, R. C.; Flygare, W. H. *J. Am. Chem. Soc.* **1970**, 92, 7523. (b) Benson, R. C.; Norris, C. L.; Flygare, W. H.; Beak, P. *J. Am. Chem. Soc.* **1971**, 93, 5591–5593. (c) Schmalz, T. G.; Norris, C. L.; Flygare, W. H. *J. Am. Chem. Soc.* **1973**, 95, 7961. (d) Schmalz, T. G.; Gierke, T. D.; Beak, P.; Flygare, W. H. *Tetrahedron Lett.* **1974**, 33, 2885. (e) Flygare, W. H. *Chem. Rev.* **1974**, 74, 653. (f) Palmer, M. H.; Findlay, R. H. *Tetrahedron Lett.* **1974**, 33, 253. (g) Hutter, D. H.; Flygare, W. H. *Top. Curr. Chem.* **1976**, 63, 89.
- (46) (a) Hess, B. A., Jr.; Schaad, L. J. *J. Am. Chem. Soc.* **1971**, 93, 305. (b) Hess, B. A., Jr.; Schaad, L. J. *J. Am. Chem. Soc.* **1971**, 93, 2413. (c) Hess, B. A., Jr.; Schaad, L. J. *J. Org. Chem.* **1971**, 36, 3418. (d) Hess, B. A., Jr.; Schaad, L. J. *J. Am. Chem. Soc.* **1972**, 94, 3068. (e) Hess, B. A., Jr.; Schaad, L. J.; Holyoke, C. W. *Tetrahedron* **1972**, 28, 3657. (f) Hess, B. A., Jr.; Schaad, L. J. *J. Am. Chem. Soc.* **1973**, 95, 3907.
- (47) (a) Clar, E. *The Aromatic Sextet*; Wiley: London, 1972. (b) Cremer, D.; Günther, H. *Liebigs Ann. Chem.* **1972**, 763, 87.
- (48) (a) Kruszewski, J.; Krygowski, T. M. *Tetrahedron Lett.* **1972**, 3839. (b) Krygowski, T. M. *J. Chem. Inf. Comput. Sci.* **1993**, 33, 70. (c) Krygowski, T. M.; Cyrański, M. K. *Tetrahedron* **1996**, 52, 1713. (d) See review: Krygowski, T. M.; Cyrański, M. K. *Chem. Rev.* **2001**, 101, 1385.
- (49) Fringuelli, F.; Marino, G.; Taticchi, A. Grandolini, G. *J. Chem. Soc., Perkin. Trans. 2* **1974**, 2, 332.
- (50) (a) Gutman, I.; Milun, M.; Trinajstić, N. *Match* **1975**, 1, 171. (b) Gutman, I.; Milun, M.; Trinajstić, N. *J. Am. Chem. Soc.* **1977**, 99, 1692. (c) Aihara, J. *J. Am. Chem. Soc.* **1976**, 98, 2750.
- (51) (a) Kutzelnigg, W. *Isr. J. Chem.* **1980**, 19, 193. (b) Schindler, M.; Kutzelnigg, W. *J. Chem. Phys.* **1982**, 76, 1919. (c) Schindler, M.; Kutzelnigg, W. *J. Am. Chem. Soc.* **1983**, 105, 1360. (d) Kutzelnigg, W.; Fleischer, U.; Schindler, M. *NMR, Basic Principles and Progress*; Springer-Verlag: Berlin, 1990; Vol. 23, p 165.
- (52) (a) Lazzarretti, P.; Zanasi, R. *J. Chem. Phys.* **1981**, 75, 5019. (b) Lazzarretti, P.; Zanasi, R. *Chem. Phys. Lett.* **1981**, 80, 533. Ab initio current density plots have been widely applied by several groups; see reviews: (c) Gomes, J. A. N.; Mallion, R. B. *Chem. Rev.* **2001**, 101, 1349. (d) Fowler, P. W. manuscript in preparation. (e) Herges, R. *Chem. Rev.* **2005**, 105, 3758.
- (53) Jug, K. *J. Org. Chem.* **1983**, 48, 1344.
- (54) Pozharskii, A. F. *Khim. Geterotsikl. Soedin. (in Russian)* **1985**, 867.
- (55) (a) Bird, C. W. *Tetrahedron* **1985**, 41, 1409. (b) Bird, C. W. *Tetrahedron* **1986**, 42, 89. (c) Bird, C. W. *Tetrahedron* **1987**, 43, 4725. (d) Bird, C. W. *Tetrahedron* **1990**, 46, 5697. (e) Bird, C. W. *Tetrahedron* **1992**, 48, 335. (f) Bird, C. W. *Tetrahedron* **1992**, 48, 1675.
- (56) Mizoguchi, N. *Chem. Phys. Lett.* **1987**, 134, 371.
- (57) (a) Zhou, Z.; Parr, R. G.; Garst, J. F. *Tetrahedron Lett.* **1988**, 29, 4843. (b) Zhou, Z.; Parr, R. G. *J. Am. Chem. Soc.* **1989**, 111, 7371. (c) Zhou, Z.; Navangul, H. V. *J. Phys. Org. Chem.* **1990**, 3, 784. (d) Zhou, Z. *J. Phys. Org. Chem.* **1995**, 8, 103. (e) Bird, C. W. *Tetrahedron* **1997**, 53, 3319. (f) De Proft, F.; Geerling, P. *Phys. Chem. Chem. Phys.* **2004**, 6, 242. (g) See review: De Proft, F.; Geerling, P. *Chem. Rev.* **2001**, 101, 1451.
- (58) (a) Paquette, L. A.; Bauer, W.; Sivik, M. R.; Bühl, M.; Feigel, M.; Schleyer, P. v. R. *J. Am. Chem. Soc.* **1990**, 112, 8776. (b) Jiao, H.; Schleyer, P. v. R. *Angew. Chem., Int. Ed. Engl.* **1993**, 32, 1760. (c) Bühl, M.; Thiel, W.; Jiao, H.; Schleyer, P. v. R. Saunders, M.; Anet, F. A. L. *J. Am. Chem. Soc.* **1994**, 116, 6005. (d) Jiao, H.; Schleyer, P. v. R. *J. Am. Chem. Soc.* **1995**, 117, 11529.
- (59) (a) Schleyer, P. v. R.; Jiao, H.; Glukhovtsev, M. N.; Chandrasekhar, J.; Kraka, E. *J. Am. Chem. Soc.* **1994**, 116, 10129. (b) Schleyer, P. v. R.; Freeman, P. K.; Jiao, H.; Goldfuss, B. *Angew. Chem., Int. Ed. Engl.* **1995**, 34, 337. (c) Sulzbach, H. M.; Schleyer, P. v. R.; Jiao, H.; Xie, Y.; Schaefer, H. F. *J. Am. Chem. Soc.* **1995**, 117, 1369. (d) Jiao, H.; Schleyer, P. v. R. *Angew. Chem., Int. Ed. Engl.* **1996**, 35, 2383. (e) Schleyer, P. v. R.; Jiao, H.; Sulzbach, H. M.; Schaefer, H. F. *J. Am. Chem. Soc.* **1996**, 118, 2093. (f) Goldfuss, B.; Schleyer, P. v. R.; Hampel, F. *Organometallics* **1996**, 15, 1755.
- (60) (a) Jiao, H.; Schleyer, P. v. R. *Angew. Chem., Int. Ed. Engl.* **1993**, 32, 1763. (b) Jiao, H.; Schleyer, P. v. R. *J. Chem. Soc., Perkin Trans. 2* **1994**, 407. (c) Jiao, H.; Schleyer, P. v. R. *J. Chem. Soc., Faraday Trans.* **1994**, 90, 1559. (d) Herges, R.; Jiao, H.; Schleyer, P. v. R. *Angew. Chem., Int. Ed. Engl.* **1994**, 33, 1376. (e) Jiao, H.; Schleyer, P. v. R. *Angew. Chem., Int. Ed. Engl.* **1995**, 34, 334.
- (61) (a) Saunders, M.; Jiménez-Vázquez, H. A.; Cross, R. J.; Mroczkowski, S.; Freedberg, D. L.; Anet, F. A. L. *Nature* **1994**, 367, 256. (b) Saunders, M.; Cross, R. J.; Jiménez-Vázquez, H. A.; Shimshi, R.; Khong, A. *Science* **1996**, 271, 1693. (c) Saunders, M.; Jiménez-Vázquez, H. A.; Cross, R. J.; Billups, W. E.; Gesenberg, C.; Gonzalez, A.; Luo, W.; Haddon, R. C. Diederich, F.; Herrmann, A. *J. Am. Chem. Soc.* **1995**, 117, 9305.
- (62) Bühl, M. *Chem.—Eur. J.* **1998**, 4, 734.
- (63) Krygowski, T. M.; Ciesielski, A.; Cyrański, M. *Chem. Pap.* **1995**, 49, 128.
- (64) Steiner, E.; Fowler, P. W. *Int. J. Quantum Chem.* **1996**, 60, 609.
- (65) (a) Schleyer, P. v. R.; Jiao, H.; Hommes, N. J. R. v. E.; Malkin, V. G.; Malkina, O. *J. Am. Chem. Soc.* **1997**, 119, 12669. (b) Schleyer, P. v. R.; Manoharan, M.; Wang, Z. X.; Kiran, B.; Jiao, H.; Puchta, R.; Hommes, N. J. R. v. E. *Org. Lett.* **2001**, 3, 2465.
- (66) (a) Schleyer, P. v. R.; Jiao, H.; Hommes, N. J. R. v. E.; Malkin, V. G.; Malkina, O. *J. Am. Chem. Soc.* **1997**, 119, 12669. (b) Schleyer, P. v. R.; Manoharan, M.; Wang, Z. X.; Kiran, B.; Jiao, H.; Puchta, R.; Hommes, N. J. R. v. E. *Org. Lett.* **2001**, 3, 2465.
- (67) Bohmann, J. A.; Weinhold, F.; Farrar, T. C. *J. Chem. Phys.* **1997**, 107, 1173. The CMO–NICS has been available in NBO 3.0 since 1997! This is now in Gaussian 03. NBO 5.x gives both CMO– and LMO–NICS but can run only on Gaussian 98 as yet.
- (68) (a) Bean, G. P. *J. Org. Chem.* **1998**, 63, 2497. (b) Sadlej-Sosnowska, N. *J. Org. Chem.* **2001**, 66, 8737.
- (69) Balawender, R.; Komorowski, L.; De Proft, F.; Geerlings, P. *J. Phys. Chem. A* **1998**, 102, 9912.
- (70) Chesnut, D. B. *Chem. Phys.* **1998**, 231, 1.
- (71) (a) Mo, Y.; Peyerimhoff, S. D. *J. Chem. Phys.* **1998**, 109, 1687. (b) Mo, Y.; Zhang, Y.; Gao, J. *J. Am. Chem. Soc.* **1999**, 121, 5737. (c) Mo, Y.; Song, L.; Wu, W.; Cao, Z.; Zhang, Q. *J. Theor. Comput. Chem.* **2002**, 1, 137.
- (72) (a) Jusélius, J.; Sundholm, D. *Phys. Chem. Chem. Phys.* **1999**, 1, 3429. (b) Jusélius, J.; Sundholm, D. *Phys. Chem. Chem. Phys.* **2000**, 2, 2145. (c) Jusélius, J.; Sundholm, D. *J. Org. Chem.* **2000**, 65, 5233. (d) Jusélius, J.; Sundholm, D. *Phys. Chem. Chem. Phys.* **2001**, 3, 2433. (e) Jusélius, J.; Straka, M.; Sundholm, D. *J. Phys. Chem. A* **2001**, 105, 9939. (f) Berger, R. J. F.; Schmidt, M. A.; Jusélius, J.; Sundholm, D.; Sirsch, P.; Schmidbaur, H. *Z. Naturforsch. B* **2001**, 56, 979. (g) Jusélius, J.; Patzschke, M.; Sundholm, D. *THEOCHEM* **2003**, 633, 123. (h) Jusélius, J. M.Sc. Thesis, Department of Chemistry, University of Helsinki, 2000.



- (73) Giambiagi, M.; de Giambiagi, M. S.; dos Silva, C. D.; de Figueiredo, A. P. *Phys. Chem. Chem. Phys.* **2000**, *2*, 3381.
- (74) (a) Chesnut, D. B.; Bartolotti, L. *Chem. Phys.* **2000**, *253*, 1. (b) Fuster, F.; Sevin, A.; Silvi, B. *J. Phys. Chem. A* **2000**, *104*, 852. (c) Silvi, B. *Phys. Chem. Chem. Phys.* **2004**, *6*, 256.
- (75) Patchkovskii, S.; Thiel, W. *J. Mol. Model.* **2000**, *6*, 67.
- (76) Herges, R.; Geuenich, D. *J. Phys. Chem. A* **2001**, *105*, 3214–3220.
- (77) (a) Steiner, E.; Fowler, P. W. *J. Phys. Chem. A* **2001**, *105*, 9553. (b) Steiner, E.; Fowler, P. W. *Chem. Commun.* **2001**, 2220.
- (78) (a) Sakai, S. *J. Phys. Chem. A* **2002**, *106*, 10370. (b) Sakai, S. *J. Phys. Chem. A* **2003**, *107*, 9422.
- (79) (a) Poater, J.; Fradera, X.; Duran, M.; Solá, M. *Chem.—Eur. J.* **2003**, *9*, 400. (b) Poater, J.; Fradera, X.; Duran, M.; Solá, M. *Chem.—Eur. J.* **2003**, *9*, 1113.
- (80) Matta, C. F.; Hernández-Trujillo, J. J. *J. Phys. Chem. A* **2003**, *107*, 7496.
- (81) (a) Corminboeuf, C.; Heine, T.; Weber, J. *Phys. Chem. Chem. Phys.* **2003**, *5*, 246. (b) Heine, T.; Schleyer, P. v. R.; Corminboeuf, C.; Seifert, G.; Reviakine, R.; Weber, J. *J. Phys. Chem. A* **2003**, *107*, 6470. (c) Corminboeuf, C.; Heine, T.; Seifert, G.; Schleyer, P. v. R.; Weber, J. *Phys. Chem. Chem. Phys.* **2004**, *6*, 273 and references therein.
- (82) Merino, G.; Heine, T.; Seifert, G. *Chem.—Eur. J.* **2004**, *10*, 4367.
- (83) (a) Santos, J. C.; Tiznado, W.; Contreras, Fuentealba, P. *J. Chem. Phys.* **2004**, *120*, 1670. (b) Santos, J. C.; Andres, J.; Aizman, A.; Fuentealba, P. *J. Chem. Theory Comput.* **2005**, *1*, 83.
- (84) Matito, E.; Duran, M.; Solá, M. *J. Chem. Phys.* **2005**, *122*, No. 014109.
- (85) (a) Jusélius, J.; Sundholm, D.; Gauss, J. *J. Chem. Phys.* **2004**, *121*, 3952. (b) Johansson, M. P.; Jusélius, J.; Sundholm, D. *Angew. Chem., Int. Ed.* **2005**, *44*, 1843. (c) Johansson, M. P.; Jusélius, J. *Lett. Org. Chem.* **2005**, in press. (d) Lin, Y. C.; Jusélius, J.; Sundholm, D.; Gauss, J. *J. Chem. Phys.* **2005**, in press.
- (86) (a) Cremer, D.; Reichel, F.; Kraka, E. *J. Am. Chem. Soc.* **1991**, *113*, 9459. (b) Cremer, D.; Svensson, P.; Kraka, E.; Ahlberg, P. *J. Am. Chem. Soc.* **1993**, *115*, 7445. (c) Cremer, D.; Svensson, P.; Kraka, E.; Konkoli, Z.; Ahlberg, P. *J. Am. Chem. Soc.* **1993**, *115*, 7457.
- (87) (a) Bühl, M.; Kaupp, M.; Malkina, O. L.; Malkin, V. G. *J. Comput. Chem.* **1999**, *20*, 91. (b) Schreckenbach, Z.; Ziegler, T. *Theor. Chem. Acc.* **1998**, *99*, 71. (c) Wang, B.; Fleischer, U.; Hinton, P. J. F.; Pulay, P. *J. Comput. Chem.* **2001**, *22*, 1887.
- (88) Günther, H. *NMR Spectroscopy: Basic Principles, Concepts, and Applications in Chemistry*, 2nd ed.; Wiley and Sons: Chichester, U.K., 1995.
- (89) See review: Mitchell, B. H. *Chem. Rev.* **2001**, *101*, 1301.
- (90) (a) Cox, R. H.; Terry, H. W., Jr. *J. Magn. Reson.* **1974**, *14*, 317. (b) Cox, R. H.; Terry, H. W., Jr.; Harrison, L. W. *J. Am. Chem. Soc.* **1971**, *93*, 3297.
- (91) Sekiguchi, A.; Matsuo, T.; Watanabe, H. *J. Am. Chem. Soc.* **2000**, *122*, 5652.
- (92) Sekiguchi, S.; Ebata, K.; Kabuto, C.; Sakurai, H. *J. Am. Chem. Soc.* **1991**, *113*, 7081.
- (93) Balci, M.; McKee, M. L.; Schleyer, P. v. R. *J. Phys. Chem. A* **2000**, *104*, 1246.
- (94) Elser, V.; Haddon, R. C. *Nature* **1987**, *325*, 162.
- (95) Haddon, R. C.; Pasquarello, A. *Phys. Rev. B* **1994**, *50*, 16459.
- (96) Cioslowski, J. *J. Am. Chem. Soc.* **1994**, *116*, 3619.
- (97) Bühl, M.; Thiel, W. *Chem. Phys. Lett.* **1995**, *233*, 585.
- (98) (a) Nyulaszi, L.; Schleyer, P. v. R. *J. Am. Chem. Soc.* **1999**, *121*, 6872. (b) Alkorta, I.; Elguero, J. *New. J. Chem.* **1999**, *23*, 951. (c) Krygowski, T. M.; Cyrański, M. K. *Chem. Rev.* **2001**, *101*, 1385. (d) Cyrański, M. K.; Krygowski, T. M.; Katritzky, A. R.; Schleyer, P. v. R. *J. Org. Chem.* **2002**, *67*, 1333.
- (99) (a) Klod, S.; Kleinpeter, E. *J. Chem. Soc., Perkin Trans. 2* **2001**, 1893. (b) Klod, S.; Koch, A.; Kleinpeter, E. *J. Chem. Soc., Perkin Trans. 2* **2002**, 1506. (c) Kleinpeter, E.; Klod, S. *J. Mol. Struct.* **2004**, *704*, 79–82.
- (100) Lazzeretti, P. *Phys. Chem. Chem. Phys.* **2004**, *6*, 217.
- (101) Chen, Z.; King, R. B. *Chem. Rev.* **2005**, *105*, 3613.
- (102) Günther, H. *NMR Spectroscopy-Basis Principles, Concepts, and applications in Chemistry*, 2nd ed.; John Wiley & Sons: Chichester, U.K., 1995.
- (103) Williams, R. V.; Armantrout, J. R.; Twamley, B.; Mitchell, R. H.; Ward, T. R.; Bandyopadhyay, S. *J. Am. Chem. Soc.* **2002**, *124*, 13495.
- (104) Martin, N. H.; Brown, J. D.; Nance, K. H.; Schaefer, H. F., III; Schleyer, P. v. R.; Wang, Z. X.; Woodcock, H. L. *Org. Lett.* **2001**, *3*, 3823.
- (105) Fleischer, U.; Kutzelnigg, W.; Lazzeretti, P.; Mühlenkamp, V. *J. Am. Chem. Soc.* **1994**, *116*, 5298 and references therein.
- (106) Heine, T.; Corminboeuf, C.; Seifert, G. *Chem. Rev.* **2005**, *105*, 3889.
- (107) (a) Eschrig, H.; Seifert, G.; Ziesche, P. *Solid State Commun.* **1985**, *56*, 777. (b) Friedrich, K.; Seifert, G.; Grossmann, G. *Phys. D: At., Mol. Clusters* **1990**, *17*, 45. (c) Bieger, W.; Seifert, G.; Eschrig, H.; Grossmann, G. **1985**, *115*, 275.
- (108) Helgaker, T.; Jaszunski, M.; Ruud, K. *Chem. Rev.* **1999**, *99*, 293.
- (109) Malkin, V. G.; Malkina, O. L.; Casida, M. E.; Salahub, D. R. *J. Am. Chem. Soc.* **1994**, *116*, 5898.
- (110) (a) Cheeseman, J. R.; Trucks, G. W.; Keith, T. A.; Frisch, M. J. *J. Chem. Phys.* **1996**, *104*, 5497. (b) Schreckenbach, G.; Ziegler, T. *J. Phys. Chem.* **1995**, *99*, 606. (c) Schreckenbach, G.; Ziegler, T. *Theor. Chem. Acc.* **1998**, *99*, 71.
- (111) Pipek, J.; Mezey, P. G. *J. Chem. Phys.* **1989**, *90*, 4916.
- (112) (a) Foster, J. M.; Boys, S. F. *Rev. Mod. Phys.* **1960**, *32*, 300. (b) Foster, J. M.; Boys, S. F. *Rev. Mod. Phys.* **1960**, *32*, 303. (c) Foster, J. M.; Boys, S. F. *Rev. Mod. Phys.* **1960**, *32*, 305. (d) Boys, S. F. *Rev. Mod. Phys.* **1960**, *32*, 296.
- (113) (a) Kiran, B.; Phukan, A. K.; Jemmis, E. D. *Inorg. Chem.* **2001**, *40*, 3615. (b) Chiavarino, B.; Crestoni, M. E.; Fornarini, S. *J. Am. Chem. Soc.* **1999**, *121*, 2619. (c) Chiavarino, B.; Crestoni, M. E.; Marzio, A. D.; Fornarini, S.; Rosi, M. *J. Am. Chem. Soc.* **1999**, *121*, 11204. (d) Jemmis, E. D.; Kiran, B. *Inorg. Chem.* **1998**, *37*, 2110. (e) Madura, I.; Krygowski, T. M.; Cyrański, M. K. *Tetrahedron* **1998**, *54*, 14913.
- (114) (a) Fink, W. H.; Richards, J. C. *J. Am. Chem. Soc.* **1991**, *113*, 3393. (b) Matsunaga, N.; Cundari, T. R.; Schmidt, M. W.; Gordon, M. S. *Theor. Chim. Acta* **1992**, *83*, 57. (c) Matsunaga, N.; Gordon, M. S. *J. Am. Chem. Soc.* **1994**, *116*, 11407. (d) Cyrański, M. K.; Krygowski, T. M.; Bird, C. W. *Tetrahedron* **1998**, *54*, 9711.
- (115) Glendening, E. D.; Badenhoop, J. K.; Reed, A. E.; Carpenter, J. E.; Weinhold, F. *NBO-5.0*; Theoretical Chemistry Institute, University of Wisconsin-Madison: Madison, WI, 1994.
- (116) Corminboeuf, C.; Heine, T.; Weber, J. *Org. Lett.* **2003**, *5*, 1127.
- (117) (a) Chen, Z.; Corminboeuf, C.; Heine, T.; Bohmann, J.; Schleyer, P. v. R. *J. Am. Chem. Soc.* **2003**, *125*, 13930. (b) King, R. B.; Heine, T.; Corminboeuf, C.; Schleyer, P. v. R. *J. Am. Chem. Soc.* **2004**, *126*, 430.
- (118) Merino, G.; Méndez-Rojas, M. A.; Beltrán, H. I.; Corminboeuf, C.; Heine, T.; Vela, A. *J. Am. Chem. Soc.* **2004**, *126*, 16160.
- (119) Kuznetsov, A. E.; Birch, K. A.; Boldyrev, A. I.; Li, X.; Zhai, A. I.; Wang, L. S. *Science* **2003**, *300*, 622.
- (120) Boldyrev, A. I.; Wang, L. S. *Chem. Rev.* **2005**, *105*, 3716.
- (121) Ritter, S. *Chem. Eng. News* **2003**, *81* (50), 23.
- (122) Schiemenz, B.; Huttner, G. **1993**, *105*, 295.
- (123) Corminboeuf, C.; King, R. B.; Schleyer, P. v. R. manuscript in preparation.
- (124) Davies, D. W. *The theory of the electric and magnetic properties of molecules*; Wiley: London, 1967.
- (125) Ruiz-Morales, Y. *J. Phys. Chem. A* **2004**, *108*, 10873.
- (126) Chen, Z.; Heine, T.; Schleyer, P. v. R.; Sundholm, D. Aromaticity indices from magnetic shieldings. In *Calculation of NMR and EPR Parameters. Theory and Applications*; Kaupp, M., Buehl, M., Malkin, V. G., Eds.; Wiley-VCH: Weinheim, Germany, 2004; pp 395–407.
- (127) (a) Balaban, A. T.; Banciu, M.; Ciorba, V. *Annulenes, Benzo-Hetero-, Homo- Derivatives, and Their Valence Isomers*; CRC Press: Boca Raton, FL, 1986. (b) Minkin, V. I.; Glukhovtsev, M. N.; Simkin, B. Y. *Aromaticity and Antiaromaticity. Electronic and Structural Aspects*; John Wiley & Sons: New York, 1994. (c) Kennedy, R. D.; Lloyd, D.; McNab, H. *J. Chem. Soc., Perkin Trans. 2* **2002**, *1*, 1601. (d) Garrat, P. *J. Aromaticity*; John Wiley & Sons: New York, 1986. (e) Lolyd, D. *Nonbenzenoid Conjugated Carbocyclic Compounds*; Elsevier: Amsterdam, 1984. (f) Lolyd, D. *The Chemistry of Conjugated Cyclic Compounds*; John Wiley & Sons: New York, 1989. (g) Kennedy, R. D.; Lloyd, D.; McNab, H. *J. Chem. Soc., Perkin Trans 1* **2002**, 1601.
- (128) (a) Matzger, A. J.; Vollhardt, K. P. C. *Tetrahedron Lett.* **1998**, *39*, 6791. (b) Nendel, M.; Houk, K. N.; Tolbert, L. M.; Vogel, E.; Jiao, H.; Schleyer, P. v. R. *J. Phys. Chem. A* **1998**, *102*, 7191. (c) Krygowski, T. M.; Cyrański, M. K. *Tetrahedron* **1999**, *55*, 11143. (d) Lepetit, C.; Godard, C.; Chauvin, R. *New. J. Chem.* **2001**, *25*, 572. (e) Alkorta, I.; Rozas, I.; Elguero, J. *Tetrahedron* **2001**, *57*, 6043. (f) Krygowski, T. M.; Pindelska, E.; Cyrański, M. K.; Hafelinger, G. *Chem. Phys. Lett.* **2002**, *359*, 158. (g) Jiao, H. J.; Hommes, N. J. R. V.; Schleyer, P. v. R. *Org. Lett.* **2002**, *4*, 2393. (h) Boydston, A. J.; Haley, M. M.; Williams, R. V.; Armantrout, J. R. *J. Org. Chem.* **2002**, *67*, 8812. (i) Schleyer, P. v. R.; Nyulaszi, L.; Karpati, T. *Eur. J. Org. Chem.* **2003**, 1923. (j) Hisaki, I.; Eda, T.; Sonoda, M.; Tobe, Y. *Chem. Lett.* **2004**, *33*, 620.
- (129) Longuet-Higgins, H. C.; Salem, L. *Proc. R. Soc.* **1959**, *251*, 172.
- (130) Coulson, C. A.; Dixon, W. T. *Tetrahedron* **1962**, *17*, 215.
- (131) Ermer, O. *Angew. Chem., Int. Ed. Engl.* **1987**, *26*, 782.
- (132) (a) Hiberty, P. C.; Danovich, D.; Shurki, A.; Shaik, S. *J. Am. Chem. Soc.* **1995**, *117*, 7760. (b) Haas, Y.; Zilberg, S. *J. Am. Chem. Soc.* **1995**, *117*, 5387. (c) Shaik, S.; Shurki, A.; Danovich, D.; Hiberty, P. C. *J. Am. Chem. Soc.* **1996**, *118*, 666. (d) Shaik, S.; Shurki, A.; Danovich, D.; Hiberty, P. C. *Chem. Rev.* **2001**, *101*, 1501. (e) Jug, K.; Hiberty, P. C.; Shaik, S. *Chem. Rev.* **2001**, *101*, 1477.

- (133) Dewar, M. J. S.; Dougherty, R. C. *The PMO Theory of Organic Chemistry*; Plenum: New York, 1975.
- (134) Chiang, C. C.; Paul, I. C. *J. Am. Chem. Soc.* **1972**, *94*, 4741.
- (135) (a) Bregman, J.; Hirshfeld, F. L.; Rabinovich, D.; Schmidt, G. M. *J. Acta Crystallogr.* **1965**, *19*, 227. (b) Hirshfeld, F. L.; Rabinovich, D. *Acta Crystallogr.* **1965**, *19*, 235. (c) Gorter, S.; Keulemans, E. R.; Krevier, M.; Romers, C.; Cruickshank, D. W. *J. Acta Crystallogr.* **1995**, *B51*, 1036.
- (136) Yoshizawa, K.; Kato, T.; Yamabe, T. *J. Phys. Chem.* **1996**, *100*, 5697.
- (137) (a) Choi, C. H.; Kertesz, M.; Karpfen, A. *J. Am. Chem. Soc.* **1997**, *119*, 11994. (b) Choi, C. H.; Kertesz, M. *J. Chem. Phys.* **1998**, *108*, 6681.
- (138) Wannere, C. S.; Sattelmeyer, K. W.; Schaefer, H. F., III; Schleyer, P. v. R. *Angew. Chem., Int. Ed.* **2004**, *43*, 4200.
- (139) For example: (a) Aihara, J.; Kanno, H. *J. Phys. Chem. A* **2005**, *109*, 3717. (b) Aihara, J. *Bull. Chem. Soc. Jpn.* **2004**, *77*, 101. (c) Aihara, J.; Oe, S. *Int. Electron. J. Mol. Des.* **2002**, *1*, 443.
- (140) Wannere, C. S.; Schleyer, P. v. R. *Org. Lett.* **2003**, *5*, 865.
- (141) King, R. A.; Crawford, T. D.; Stanton, J. F.; Schaefer, H. F., III *J. Am. Chem. Soc.* **1999**, *121*, 10788.
- (142) Kang, J. K.; Musgrave, C. B. *J. Chem. Phys.* **2001**, *115*, 11040.
- (143) Baldrige, K. K.; Uzan, O.; Martin, J. M. L. *Organometallics* **2000**, *19*, 1477.
- (144) Maoche, B.; Gayoso, J.; Ouamerali, O. *Rev. Roum. Chem.* **1984**, *29*, 613.
- (145) (a) Keith, T. A.; Bader, R. F. W. *Chem. Phys. Lett.* **1993**, *210*, 223. (b) Cheeseman, J. R.; Frisch, M. J.; Trucks, G. W.; Keith, T. A. *J. Chem. Phys.* **1995**, *104*, 5497.
- (146) Increment scheme was based on magnetic susceptibilities of ethylene and butadiene. The CH<sub>2</sub>= and =CH— increments are −7.3 and −5.1 cgs-ppm, respectively.
- (147) (a) Sondheimer, F.; Wolovsky, R.; Amiel, Y. *J. Am. Chem. Soc.* **1962**, *84*, 274. (b) Oth, J. F. M. *Pure Appl. Chem.* **1971**, *25*, 573. (c) Mcquilki, R. M.; Metcalf, B. W.; Sondheimer, F. *J. Chem. Soc., Chem. Commun.* **1971**, 338. (d) Stevenson, C. D.; Kurth, T. L. *J. Am. Chem. Soc.* **2000**, *122*, 722.
- (148) Streitwieser, A., Jr. *Molecular Orbital Theory for Organic Chemists*; John Wiley: New York, 1961.
- (149) Wiberg, K. B. *Chem. Rev.* **2001**, *101*, 1317.
- (150) Wannere, C. S.; Moran, D.; Allinger, N. L.; Hess, B. A.; Schaad, L. J.; Schleyer, P. v. R. *Org. Lett.* **2003**, *5*, 2983.
- (151) (a) Klärner, F.-G. *Angew. Chem., Int. Ed.* **2001**, *40*, 3977. (b) Anet, F. A. L. *J. Am. Chem. Soc.* **1962**, *84*, 671. (c) Anet, F. A. L.; Bourn, A. J. R.; Lin, Y. S. *J. Am. Chem. Soc.* **1964**, *86*, 3576. (d) Luz, Z.; Meiboom, S. *J. Chem. Phys.* **1973**, *59*, 1077. (e) Naor, R.; Luz, Z. *J. Chem. Phys.* **1982**, *76*, 5662.
- (152) (a) Allinger, N. L.; Sprague, J. T.; Finder, C. J. *Tetrahedron* **1973**, *29*, 2519. (b) Roth, W. R.; Lennartz, H.-W.; Vogel, E.; Leien-decker, M.; Oda, M. *Chem. Ber.* **1986**, *119*, 837. (c) Nevins, N.; Lii, J. H.; Allinger, N. L. *J. Comput. Chem.* **1996**, *17*, 695.
- (153) Deniz, A. A.; Peters, K. S.; Snyder, G. J. *Science* **1999**, *286*, 1119.
- (154) (a) Bally, T.; Masamune, S. *Tetrahedron* **1980**, *36*, 343. (b) Cram, D. J.; Tanner, M. E.; Thomas, R. *Angew. Chem., Int. Ed. Engl.* **1991**, *30*, 1024. (c) Wannere, C. S.; Schleyer, P. v. R. *Org. Lett.* **2003**, *5*, 605.
- (155) (a) Kreyenschmidt, M.; Uckert, F.; Müllen, K. *Macromolecules* **1995**, *28*, 4577. (b) Tyutyulkov, N.; Karabunarliev, S.; Müllen, K.; Baumgarten, M. *Synth. Met.* **1993**, *53*, 205.
- (156) (a) Gama, V.; Henriques, R. T.; Bonfait, G.; Almeida, M.; Meetsma, A.; van Smaalen, S.; de Boer, J. L. *J. Am. Chem. Soc.* **1992**, *114*, 1986. (b) Dias, C. B.; Santos, I. C.; Gama, V.; Henriques, R. I.; Almeida, M. *Synth. Met.* **1993**, *56*, 1688.
- (157) (a) Hiramoto, M.; Kishigami, Y.; Yokoyama, M. *Chem. Lett.* **1990**, 119. (b) Seybold, G.; Wagenblast, G. *Dyes Pigm.* **1989**, *11*, 303.
- (158) (a) Law, K.-Y. *Chem. Rev.* **1993**, *93*, 449. (b) Schlichting, P.; Rohr, U.; Müllen, K. *Liebigs Ann.* **1997**, 395.
- (159) Zander, M. *Angew. Chem.* **1960**, *72*, 513.
- (160) Moran, D.; Stahl, F.; Bettinger, H. F.; Schaefer, H. F., III; Schleyer, P. v. R. *J. Am. Chem. Soc.* **2003**, *125*, 6746.
- (161) Schleyer, P. v. R.; Manoharan, M.; Jiao, H.; Stahl, F. *Org. Lett.* **2001**, *3* (23), 3643.
- (162) Cyranowski, M. K.; Stępień, B. T.; Krygowski, T. M. *Tetrahedron* **2000**, *56*, 9663.
- (163) Nakamura, E.; Tahara, K.; Matsuo, Y.; Sawamura, M. *J. Am. Chem. Soc.* **2003**, *125*, 2834.
- (164) The Clar VB model employs both conventional two-electron  $\pi$ -bonds, represented by lines, and aromatic sextets, represented by circles.
- (165) Matsuo, Y.; Tahara, K.; Nakamura, E. *Org. Lett.* **2003**, *5*, 3181. Erratum, see: Matsuo, Y.; Tahara, K.; Nakamura, E. *Org. Lett.* **2003**, *5*, 5103.
- (166) Ormsby, J. L.; King, B. J. *J. Org. Chem.* **2004**, *69*, 4287.
- (167) Rao, C. N. R.; Satishkumar, B. C.; Govindaraj, A.; Nath, M. *Chem. Phys. Phys. Chem.* **2001**, *2*, 78.
- (168) (a) Zimmerman, H. E. *J. Am. Chem. Soc.* **1966**, *88*, 1564. (b) Zimmerman, H. E. *Acc. Chem. Res.* **1972**, *4*, 272.
- (169) Havenith, R. W. A.; Van Lenthe, J. H.; Jenneskens, L. W. *Int. J. Quantum Chem.* **2001**, *85*, 52.
- (170) Rzepa, H. S. *Chem. Rev.* **2005**, *105*, 3697.
- (171) Barborak, T.; Su, T. M.; Schleyer, P. v. R.; Boche, G.; Schneider, J. *J. Am. Chem. Soc.* **1971**, *93*, 279.
- (172) (a) Anastassiou, A. G.; Yakali, E. *J. Am. Chem. Soc.* **1971**, *93*, 3803. (b) Anastassiou, A. G.; Yakali, E. *J. Chem. Soc., Chem. Commun.* **1972**, 92. (c) Yakali, E. Dissertation, Syracuse University, Syracuse, NY, 1973.
- (173) Mauksch, M.; Gogonea, V.; Jiao, H.; Schleyer, P. v. R. *Angew. Chem., Int. Ed.* **1998**, *37*, 2395.
- (174) Martin-Santamaria, S.; Lavan, B.; Rzepa, H. S. *Chem. Commun.* **2000**, 1089.
- (175) Martin-Santamaria, S.; Rzepa, H. S. *J. Chem. Soc., Perkin Trans 2* **2000**, 2372.
- (176) Karney, W. L.; Kastrup, C. J.; Oldfield, S. P.; Rzepa, H. S. *J. Chem. Soc., Perkin Trans 2* **2002**, 388.
- (177) Kastrup, C. J.; Oldfield, S. P.; Rzepa, H. S. *Chem. Commun.* **2002**, 642.
- (178) (a) Rzepa, H. S.; Taylor, K. R. *J. Chem. Soc., Perkin Trans 2* **2002**, 1499. (b) Hall, D.; Rzepa, H. S. *Org. Biomol. Chem.* **2003**, *1*, 182.
- (179) Castro, C.; Isborn, C. M.; Karney, W. L.; Mauksch, M.; Schleyer, P. v. R. *Org. Lett.* **2002**, *4*, 3431.
- (180) Ajami, D.; Oeckler, O.; Simon, A.; Herges, R. *Nature* **2003**, *426*, 819.
- (181) Castro, C.; Chen, Z.; Wannere, C. S.; Jiao, H.; Karney, W. L.; Mauksch, M.; Puchta, R.; Hommes, N. J. R. v. E.; Schleyer, P. v. R. *J. Am. Chem. Soc.* **2005**, *127*, 2425.
- (182) (a) Woodward, R. B.; Hoffmann, R. *J. Am. Chem. Soc.* **1965**, *87*, 395. (b) Hoffmann, R.; Woodward, R. B. *J. Am. Chem. Soc.* **1965**, *87*, 2046. (c) Woodward, R. B.; Hoffmann, R. *J. Am. Chem. Soc.* **1965**, *87*, 2511. (d) Hoffmann, R.; Woodward, R. B. *J. Am. Chem. Soc.* **1965**, *87*, 4389. (e) Hoffmann, R.; Woodward, R. B. *Acc. Chem. Res.* **1968**, *1*, 17. (f) Woodward, R. B.; Hoffmann, R. *Angew. Chem., Int. Ed. Engl.* **1969**, *81*, 781. (g) Hoffmann, R.; Woodward, R. B. *Science* **1970**, *167*, 825. (h) Woodward, R. B.; Hoffmann, R. *The Conservation of Orbital Symmetry*; Verlag Chemie: Weinheim, Germany, 1970.
- (183) Houk, K. N. In *Pericyclic Reactions*; Marchand, A. P., Lehr, R. E., Eds.; Academic Press: New York, 1977; Vol. 2.
- (184) Reetz, M. T. *Tetrahedron* **1973**, *29*, 2189.
- (185) (a) Herges, R. *Angew. Chem., Int. Ed. Engl.* **1994**, *33*, 255. (b) Herges, R. *J. Chem. Inf. Comput. Sci.* **1994**, *34*, 91. (c) Berger, C.; Bresler, C.; Dilger, U.; Geuenich, R.; Herges, R.; Röttele, H.; Schröder, G. *Angew. Chem., Int. Ed.* **1998**, *37*, 1850. (d) Berger, C.; Dieterich, S.; Dilger, U.; Geuenich, R.; Helios, H.; Herges, R.; Kirchmer, P.; Röttele, H.; Schröder, G. *Angew. Chem., Int. Ed.* **1998**, *37*, 1854.
- (186) (a) Sauer, J.; Sustmann, R. *Angew. Chem., Int. Ed. Engl.* **1980**, *19*, 779. (b) Carruthers, W. *Cycloaddition Reactions in Organic Synthesis*; Pergamon: Oxford, U.K., 1990. (c) Oppolzer, W. In *Comprehensive Organic Synthesis*; Trost, B. M., Fleming, I., Paquette, L. A., Eds.; Pergamon: Oxford, U.K., 1991; Vol. 5, p 315.
- (187) Diels, O.; Alder, K. *Ann.* **1928**, *460*, 98.
- (188) (a) Houk, K. N.; Li, Y.; Evansek, J. D. *Angew. Chem., Int. Ed. Engl.* **1992**, *31*, 682. (b) Houk, K. N.; González, J.; Li, Y. *Acc. Chem. Res.* **1995**, *28*, 81. (c) Wiest, O.; Houk, K. N. *Top. Curr. Chem.* **1996**, *183*, 1.
- (189) (a) Cossio, F. P.; Morao, I.; Jiao, H.; Schleyer, P. v. R. *J. Am. Chem. Soc.* **1999**, *121*, 6737. (b) Sawika, D.; Houk, K. N. *J. Mol. Model.* **2000**, *6*, 158. (c) Morao, I.; Cossio, F. P. *J. Org. Chem.* **2000**, *65*, 7971. (d) Manoharan, M.; De Proft, F.; Geerlings, P. *J. Org. Chem.* **2000**, *65*, 6132. (e) Manoharan, M.; De Proft, F.; Geerlings, P. *J. Chem. Soc., Perkin 2* **2000**, 1767. (f) Martin-Santamaria, S.; Lavan, B.; Rzepa, H. S. *J. Chem. Soc., Perkin 2* **2000**, 1415. (g) Alajarin, M.; Sanchez-Andrada, P.; Cossio, F. P.; Arrieta, A.; Lecea, B. *J. Org. Chem.* **2001**, *66*, 8470. (h) Nguyen, L. T.; De Proft, F.; Chandra, A. K.; Uchimaru, T.; Nguyen, M. T.; Geerlings, P. *J. Org. Chem.* **2001**, *66*, 6096. (i) Nguyen, L. T.; De Proft, F.; Nguyen, M. T.; Geerlings, P. *J. Org. Chem.* **2001**, *66*, 4316. (j) Tantillo, D. J.; Hoffmann, R. *Helv. Chim. Acta* **2001**, *84*, 1396. (k) Wannere, C. S.; Bansal, R. K.; Schleyer, P. v. R. *J. Org. Chem.* **2002**, *67*, 9162. (l) De Lera, A. R.; Cossio, F. P. *Angew. Chem., Int. Ed.* **2002**, *41*, 1150. (m) Alabugin, I. V.; Manoharan, M.; Breiner, B.; Lewis, F. D. *J. Am. Chem. Soc.* **2003**, *125*, 9329. (n) Alabugin, I. V.; Manoharan, M. *J. Phys. Chem. A* **2003**, *107*, 3363. (o) Rodriguez-Otero, J.; Cabaleiro-Lago, E. M. *Chem.—Eur. J.* **2003**, *9*, 1837.
- (190) (a) Subramanian, G.; Schleyer, P. v. R.; Jiao, H. *Angew. Chem., Int. Ed. Engl.* **1996**, *35*, 2638. (b) Subramanian, G.; Schleyer, P. v. R.; Jiao, H. *Organometallics* **1997**, *16*, 2362. (c) Jiao, H.; Schleyer, P. v. R.; Mo, Y.; McAllister, M. A.; Tidwell, T. T. *J. Am. Chem. Soc.* **1997**, *119*, 6561. (d) Schleyer, P. v. R.; Manoharan, M.; Jiao, H.; Stahl, F. *Org. Lett.* **2001**, *3*, 3643.
- (191) (a) Bouma, W. J.; Vincent, M. A.; Radom, L. *Int. J. Quantum Chem.* **1978**, *14*, 767. (b) Saettel, N. J.; Wiest, O. *J. Org. Chem.* **2000**, *65*, 2331. (c) Carpenter, J. E.; Sosa, C. P. *THEOCHEM* **1994**, *117*, 325. (d) Bachrach, S. M. *J. Org. Chem.* **1993**, *58*, 5414. (d)



- Chantranupong, L.; Wildman, T. A. *J. Am. Chem. Soc.* **1990**, *112*, 4151. (e) Loncharich, R. J.; Houk, K. N. *J. Am. Chem. Soc.* **1988**, *110*, 2089. (f) Hess, B. A., Jr.; Schaad, L. J.; Pancir, J. *J. Am. Chem. Soc.* **1985**, *107*, 149. (g) Rondan, N. G.; Houk, K. N. *Tetrahedron Lett.* **1984**, *25*, 2519. (h) Hess, B. A., Jr.; Schaad, L. J. *J. Am. Chem. Soc.* **1983**, *105*, 7185.
- (192) (a) Jensen, F.; Houk, K. N. *J. Am. Chem. Soc.* **1987**, *109*, 3139 and references therein. (b) Jiao, H.; Schleyer, P. v. R. *J. Phys. Org. Chem.* **1998**, *11*, 655.
- (193) (a) Delbecq, F.; Nguyen Trong, A. *Nouv. J. Chim.* **1983**, *7*, 505. (b) Osamura, Y.; Kato, S.; Morokuma, K.; Feller, D.; Davidson, E. R.; Borden, W. T. *J. Am. Chem. Soc.* **1984**, *106*, 3362. (c) Dewar, M. J. S.; Healy, E. F. *Chem. Phys. Lett.* **1987**, *141*, 521. (d) Maluendes, S. A.; Dupuis, M. *J. Chem. Phys.* **1990**, *93*, 5902. (e) Houk, K. N.; Gustafson, S. M.; Black, K. A. *J. Am. Chem. Soc.* **1992**, *114*, 8565. (f) Hrovat, D. A.; Morokuma, K.; Borden, W. T. *J. Am. Chem. Soc.* **1994**, *116*, 1072. (g) Borden, W. T.; Davidson, E. R. *Acc. Chem. Res.* **1996**, *29*, 67. (h) Baumann, H.; Voellinger-Borel, A. *Helv. Chim. Acta* **1997**, *80*, 2112. (i) Roth, W. R.; Gleiter, R.; Paschmann, V.; Hackler, U. E.; Fritzsche, G.; Lange, H. *Eur. J. Org. Chem.* **1998**, *961*, 1. (j) Sakai, S. *Int. J. Quantum Chem.* **2000**, *80*, 1099. (k) Staroverov, V. N.; Davidson, E. R. *THEOCHEM* **2001**, *573*, 81. (l) Borden, W. T. *Mol. Phys.* **2002**, *100*, 337. (m) Sakai, S. *THEOCHEM* **2002**, *583*, 181. (n) Guner, V.; Khuong, K. S.; Leach, A. G.; Lee, P. S.; Bartberger, M. D.; Houk, K. N. *J. Phys. Chem. A* **2003**, *107*, 11445. (o) Bethke, S.; Hrovat, D. A.; Borden, W. T.; Gleiter, R. *J. Org. Chem.* **2004**, *69*, 3294. (p) Blavins, J. J.; Cooper, D. L.; Karadakov, P. B. *J. Phys. Chem. A* **2004**, *108*, 194. (q) Hayase, S.; Hrovat, D. A.; Borden, W. T. *J. Am. Chem. Soc.* **2004**, *126*, 10028. (r) Su, J. T.; Sarpong, R.; Stoltz, B. M.; Goddard, W. A. *J. Am. Chem. Soc.* **2004**, *126*, 24.
- (194) (a) Dupis, M.; Murray, C.; Davidson, E. R. *J. Am. Chem. Soc.* **1991**, *113*, 9756. (b) Kozłowski, P. M.; Dupuis, M.; Davidson, E. R. *J. Am. Chem. Soc.* **1995**, *117*, 774. (c) Wiest, O.; Black, K. A.; Houk, K. N. *J. Am. Chem. Soc.* **1994**, *116*, 10336. (d) Wiest, O.; Montiel, D. C.; Houk, K. N. *J. Phys. Chem. A* **1997**, *101*, 8378. (e) Yoo, H. Y.; Houk, K. N. *J. Am. Chem. Soc.* **1994**, *116*, 12047. (f) Navarro-Vazquez, A.; Prall, M.; Schreiner, P. R. *Org. Lett.* **2004**, *6*, 2981.
- (195) Roth, W. R.; Lenartz, H.-W.; Doering, W. v. E.; Birladeanu, L.; Guyton, C.; Kitagawa, T. *J. Am. Chem. Soc.* **1990**, *112*, 1722.
- (196) (a) Vance, R. L.; Rondan, N. G.; Houk, K. N.; Jensen, F.; Borden, W. T.; Komornicki, A.; Wimmer, E. *J. Am. Chem. Soc.* **1988**, *110*, 2314. (b) Severance, D. L.; Jorgensen, W. L. *J. Am. Chem. Soc.* **1992**, *114*, 10966. (c) Davidson, M. M.; Hillier, I. H.; Hall, R. J.; Burton, N. A. *J. Am. Chem. Soc.* **1994**, *116*, 9294. (d) Davidson, M. M.; Hillier, I. H. *Chem. Phys. Lett.* **1994**, *225*, 293. (e) Yamabe, S.; Okumoto, S.; Hayashi, T. *J. Org. Chem.* **1997**, *62*, 6121. (f) Yoo, H. Y.; Houk, K. N. *J. Am. Chem. Soc.* **1997**, *119*, 2877. (g) Hu, H.; Kobrak, M. N.; Xu, C.; Hammes-Schiffer, S. *J. Phys. Chem. A* **2000**, *104*, 8058.
- (197) (a) Lewis, K. E.; Steiner, H. *J. Chem. Soc.* **1964**, 3080. (b) Marvell, E. N. *Tetrahedron* **1973**, *29*, 3791. (c) Orchard, S. W.; Thrush, B. A. *J. Chem. Soc., Chem. Commun.* **1973**, *14*. (d) Spangler, C. W.; Jondahl, T. P.; Spangler, B. *J. Org. Chem.* **1973**, *38*, 2478. (e) Komornicki, A.; McIver, J. W., Jr. *J. Am. Chem. Soc.* **1974**, *96*, 5798. (f) Nohira, H. *Tetrahedron Lett.* **1974**, 2573. (g) Halevi, E. A. *Helv. Chim. Acta* **1975**, *58*, 2136. (h) Baldwin, J. E.; Reddy, V. P.; Hess, B. A., Jr.; Schaad, L. J. *J. Am. Chem. Soc.* **1988**, *110*, 8554. (i) Pichko, V. A.; Simkin, B. Y.; Minkin, V. I. *THEOCHEM* **1989**, *57*, 129. (j) Jefford, C. W.; Bernardinelli, G.; Wang, Y.; Spellmeyer, D. C.; Buda, A.; Houk, K. N. *J. Am. Chem. Soc.* **1992**, *114*, 1157. (k) Pichko, V. A.; Simkin, B. Y.; Minkin, V. I. *J. Org. Chem.* **1992**, *57*, 7087. (l) Wiest, O.; Houk, K. N.; Black, K. A.; Thomas, B., IV. *J. Am. Chem. Soc.* **1995**, *117*, 8594. (m) Garavelli, M.; Celani, P.; Fato, M.; Bearpark, M. J.; Smith, B. R.; Olivucci, M.; Robb, M. A. *J. Phys. Chem. A* **1997**, *101*, 2023. (n) Wiest, O.; Montiel, D. C.; Houk, K. N. *J. Phys. Chem. A* **1997**, *101*, 8378. (o) Rodriguez-Otero, J. *J. Org. Chem.* **1999**, *64*, 6842. (p) Sakai, S.; Takane, S.-y. *J. Phys. Chem. A* **1999**, *103*, 2878.
- (198) (a) Doering, W. v. E.; Toscano, V. G.; Beasley, G. H. *Tetrahedron* **1971**, *27*, 5299. (b) Doering, W. v. E.; Beasley, G. H. *Tetrahedron* **1973**, *29*, 2231.
- (199) (a) Jones, R. R.; Bergman, R. G. *J. Am. Chem. Soc.* **1972**, *94*, 660. (b) Bergman, R. G. *Acc. Chem. Res.* **1973**, *6*, 25.
- (200) Galbraith, G. M.; Schreiner, P. R.; Harris, N.; Wie, W.; Wittkopp, A.; Shaik, S. *Chem.—Eur. J.* **2000**, *6*, 1446.
- (201) (a) Snyder, J. P. *J. Am. Chem. Soc.* **1989**, *111*, 7630. (b) Snyder, J. P. *J. Am. Chem. Soc.* **1990**, *112*, 5367. (c) Snyder, J. P.; Tipsword, G. E. *J. Am. Chem. Soc.* **1990**, *112*, 4040. (d) Koga, N.; Morokuma, K. *J. Am. Chem. Soc.* **1991**, *113*, 1907. (e) Wierschke, S. G.; Nash, J. J.; Squires, R. R. *J. Am. Chem. Soc.* **1993**, *115*, 11958. (f) Kraka, E.; Cremer, D. *J. Am. Chem. Soc.* **1994**, *116*, 4929. (g) Lindh, R.; Persson, B. J. *J. Am. Chem. Soc.* **1994**, *116*, 4963. (h) Roth, W. R.; Hopf, H.; Horn, C. *Chem. Ber.* **1994**, *127*, 1765. (i) Lindh, R.; Lee, T. J.; Bernhardsson, A.; Persson, B. J.; Karlstroem, G. *J. Am. Chem. Soc.* **1995**, *117*, 7186. (j) Schmittel, M.; Kiau, S. *Chem. Lett.* **1995**, 953. (k) Lindh, R.; Schuetz, M. *Chem. Phys. Lett.* **1996**, *258*, 409. (l) Cramer, C. J.; Nash, J. J.; Squires, R. R. *Chem. Phys. Lett.* **1997**, *277*, 311. (m) Chen, W.-C.; Chang, N.-y.; Yu, C.-h. *J. Phys. Chem. A* **1998**, *102*, 2584. (n) Cramer, C. J. *J. Am. Chem. Soc.* **1998**, *120*, 6261. (o) Schreiner, P. R. *J. Am. Chem. Soc.* **1998**, *120*, 4184. (p) Schreiner, P. R. *Chem. Commun.* **1998**, 483. (q) Schreiner, P. R.; Prall, M. *J. Am. Chem. Soc.* **1999**, *121*, 8615. (r) Graefenstein, J.; Hjerpe, A. M.; Kraka, E.; Cremer, D. *J. Phys. Chem. A* **2000**, *104*, 1748. (s) Stahl, F.; Moran, D.; Schleyer, P. v. R.; Prall, M.; Schreiner, P. R. *J. Org. Chem.* **2002**, *67*, 1453.
- (202) Feller, D. F.; Schmidt, M. W.; Ruedenberg, K. *J. Am. Chem. Soc.* **1982**, *104*, 960.
- (203) McKee, M. L.; Stanbury, D. M. *J. Am. Chem. Soc.* **1992**, *114*, 3214.
- (204) (a) Alder K.; Pascher, F.; Schmitz A. *Ber. Dtsch. Chem. Ges.* **1943**, *76*, 27. (b) Loncharich, R.; Houk, K. N. *J. Am. Chem. Soc.* **1988**, *110*, 2089. (c) Paderes, G. D.; Jorgensen, W. L. *J. Org. Chem.* **1992**, *57*, 1904.
- (205) (a) Loncharich, R.; Houk, K. N. *J. Am. Chem. Soc.* **1987**, *109*, 6947. (b) Uchimaru, T.; Tsuzuki, S.; Tanabe, K.; Hayashi, Y. *J. Chem. Soc., Chem. Commun.* **1989**, 1861. (c) Uchimaru, T.; Tsuzuki, S.; Tanabe, K.; Hayashi, Y. *Bull. Chem. Soc. Jpn.* **1990**, *63*, 2246. (d) Yliniemelä, A.; Konschinn, H.; Neagu, C.; Pajunene, A.; Hase, T.; Brunow, G.; Telemann, O. *J. Am. Chem. Soc.* **1995**, *117*, 5120. (e) Yliniemelä, A.; Konschinn, H.; Pietilä, L. O.; Telemann, O. *J. Mol. Struct. (THEOCHEM)* **1995**, *334*, 173. (f) Pranata, J. *Int. J. Quantum Chem.* **1997**, *62*, 509.
- (206) (a) Houk, K. N.; Beno, B. R.; Nendel, M.; Black, K.; Yoo, H. Y.; Wilsey, S.; Lee, J. K. *J. Mol. Struct. (THEOCHEM)* **1997**, *398*–*399*, 169. (b) Li Y.; Houk, K. N. *J. Am. Chem. Soc.* **1993**, *115*, 7478. (c) Goldstein, E.; Beno, B. R.; Houk, K. N. *J. Am. Chem. Soc.* **1996**, *118*, 6036. (d) Singleton, D. A.; Thomas, A. A. *J. Am. Chem. Soc.* **1995**, *117*, 9357. (e) Beno, B. R.; Houk, K. N.; Singleton, D. A. *J. Am. Chem. Soc.* **1996**, *118*, 9904.
- (207) (a) Dormans, G. J. M.; Buck, H. M. *J. Mol. Struct. (THEOCHEM)* **1986**, *136*, 121. (b) Dormans, G. J. M.; Buck, H. M. *J. Am. Chem. Soc.* **1986**, *108*, 3253.
- (208) (a) Zimmerman, H. *Acc. Chem. Res.* **1971**, *4*, 272. (b) Dewar, M. J. S. *Angew. Chem., Int. Ed. Engl.* **1971**, *10*, 761.
- (209) Schlattman, J. L. M. A.; Pot, J.; Havinga, E. *Recl. Trav. Chim. Pays-Bas* **1964**, *83*, 1173.
- (210) (a) Longuet-Higgins, H. C.; Abrahamson, E. W. *J. Am. Chem. Soc.* **1965**, *87*, 2045. (b) Branton, G. R.; Frey, H. M.; Skinner, R. F. *Trans. Faraday Soc.* **1966**, *62*, 1546.
- (211) (a) Hsu, K.; Bunker, R. J.; Peyerimhoff, S. D. *J. Am. Chem. Soc.* **1972**, *94*, 5639. (b) Dewar, M. J. S.; Kirschner, S. J. *Am. Chem. Soc.* **1974**, *96*, 6809. (c) Thiel, W. *J. Am. Chem. Soc.* **1981**, *103*, 1420. (d) Breulet, J.; Schaefer, H. F., III. *J. Am. Chem. Soc.* **1984**, *106*, 1221. (e) Kirmse, W.; Rondan, N. G.; Houk, K. N. *J. Am. Chem. Soc.* **1984**, *106*, 7989. (f) Rondan, N. G.; Houk, K. N. *J. Am. Chem. Soc.* **1985**, *107*, 2099. (g) Clark, K. B.; Leigh, W. J. *J. Am. Chem. Soc.* **1987**, *109*, 6086. (h) Spellmeyer, D. C.; Houk, K. N. *J. Am. Chem. Soc.* **1988**, *110*, 3412. (i) Spellmeyer, D. C.; Houk, K. N.; Rondan, N. G.; Miller, R. D.; Franz, L.; Fickes, G. N. *J. Am. Chem. Soc.* **1989**, *111*, 5356. (j) Bernardi, F.; De, S.; Olivucci, M.; Robb, M. A. *J. Am. Chem. Soc.* **1990**, *112*, 1737. (k) Olivucci, M.; Ragazos, I. N.; Bernardi, F.; Robb, M. A. *J. Am. Chem. Soc.* **1993**, *115*, 3710. (l) Deng, L.; Ziegler, T. *J. Phys. Chem.* **1995**, *99*, 612. (m) Jursic, B. S.; Zdravkovski, Z. *Int. J. Quantum Chem.* **1995**, *56*, 115. (n) Dolbier, W. R., Jr.; Koroniak, H.; Houk, K. N.; Sheu, C. *Acc. Chem. Res.* **1996**, *29*, 471. (o) Niwayama, S.; Kallel, E. A.; Spellmeyer, D. C.; Sheu, C.; Houk, K. N. *J. Org. Chem.* **1996**, *61*, 2813. (p) Sakai, S. *THEOCHEM* **1999**, *461*–*462*, 283. (q) Lee, P. S.; Sakai, S.; Hoerstermann, P.; Roth, W. R.; Kallel, E. A.; Houk, K. N. *J. Am. Chem. Soc.* **2003**, *125*, 5839.
- (212) Huisgen, R.; Dahmen, A.; Huber, H. *J. Am. Chem. Soc.* **1967**, *89*, 7130.
- (213) (a) Breslow, R. J.; Groves, J. T.; Ryan, G. I. *J. Am. Chem. Soc.* **1957**, *79*, 5318. (b) Ciabattini, J.; Nathan, E. C., III. *J. Am. Chem. Soc.* **1969**, *91*, 4766. (c) Sunderlingham, M.; Jensen, L. H. *J. Am. Chem. Soc.* **1966**, *88*, 198.
- (214) Radom, L.; Hariharan, P. C.; Pople, J. A.; Schleyer, P. v. R. *J. Am. Chem. Soc.* **1976**, *98*, 10.
- (215) (a) Cremer, D.; Kraka, E. *J. Am. Chem. Soc.* **1985**, *107*, 3800. (b) Cremer, D.; Kraka, E. *J. Am. Chem. Soc.* **1989**, *107*, 3811.
- (216) (a) Sauers, P. R. *Tetrahedron* **1998**, *54*, 337. (b) Exner, K.; Schleyer, P. v. R. *J. Phys. Chem. A* **2001**, *105*, 3407.
- (217) (a) Wilberg, K. N.; Nist, B. J. *J. Am. Chem. Soc.* **1961**, *94*, 3143. (b) Patel, D. J.; Howden, M. E. H.; Roberts, J. D. *J. Am. Chem. Soc.* **1963**, *85*, 3218. (c) Burke, J. J.; Lauterbur, P. C. *J. Am. Chem. Soc.* **1964**, *86*, 1870. (d) Poulter, C. D.; Boikess, R. S.; Brauman, J. I.; Winstein, S. *J. Am. Chem. Soc.* **1972**, *94*, 2291. (e) Hahn, R. C.; Howard, Ph. H. *J. Am. Chem. Soc.* **1972**, *94*, 3143. (f) Jason, M. E.; Kurzweil, P. R. *J. Org. Chem.* **1991**, *56*, 3664.
- (218) Moran, D.; Manoharam, M.; Heine, T.; Schleyer, P. v. R. *Org. Lett.* **2003**, *5*, 23.

- (219) Balci, M.; McKee, M. L.; Schleyer, P. v. R. *J. Phys. Chem. A* **2000**, *104*, 1246.
- (220) Havenith, R. W. A.; Fowler, P. W.; Steiner, E. *Chem. Phys. Lett.* **2003**, *371*, 276.
- (221) (a) Jiao, H.; Schleyer, P. v. R.; Glukhovstev, M. N. *J. Phys. Chem.* **1996**, *100*, 12299. (b) Jursic, B. S. *Int. J. Quantum Chem.* **1999**, *73*, 451. (c) Jursic, B. S. *J. Mol. Struct. (THEOCHEM)* **1999**, *490*, 81. (d) Jursic, B. S. *Int. J. Quantum Chem.* **1998**, *69*, 679. (e) Jursic, B. S. *J. Mol. Struct. (THEOCHEM)* **2000**, *498*, 159.
- (222) Alexandrova, A. N.; Boldyrev, A. I. *J. Phys. Chem. A* **2003**, *107*, 554.
- (223) Li, Z. H.; Moran, D.; Fan, K. N.; Schleyer, P. v. R. *J. Phys. Chem. A* **2005**, *109*, 3711.
- (224) Havenith, R. W. A.; De Proft, F.; Fowler, P. W.; Geerlings, P. *Chem. Phys. Lett.* **2005**, *407*, 391.
- (225) Chen, Z.; Jiao, H.; Schleyer, P. v. R. Unpublished results.
- (226) (a) Li, X.; Kuznetsov, A. E.; Zhang, H. F.; Boldyrev, A. I.; Wang, L. S. *Science* **2001**, *291*, 859. (b) Li, X.; Zhang, H. F.; Wang, L. S.; Boldyrev, A. I. *Angew. Chem., Int. Ed.* **2001**, *40*, 1867. (c) Kuznetsov, A. E.; Boldyrev, A. I.; Li, X.; Wang, L. S. *J. Am. Chem. Soc.* **2001**, *123*, 8825. (d) Boldyrev, A. I.; Kuznetsov, A. E. *Inorg. Chem.* **2002**, *41*, 532. (e) Kuznetov, A. E.; Boldyrev, A. I. *Struct. Chem.* **2002**, *13*, 141. (f) Kuznetsov, A. E.; Boldyrev, A. I.; Zhai, H.-J.; Wang, L. S. *J. Am. Chem. Soc.* **2002**, *124*, 11791. (g) Juselius, J.; Straka, M.; Sundholm, D. *J. Phys. Chem. A* **2001**, *105*, 6886.
- (227) Li, X. W.; Pennington, W. T.; Robinson, G. H. *J. Am. Chem. Soc.* **1995**, *117*, 7578.
- (228) Xie, Y. M.; Schreiner, P. R.; Schaefer, H. F.; Li, X. W.; Robinson, G. H. *J. Am. Chem. Soc.* **1996**, *118*, 10635.
- (229) Kuznetsov, A. E.; Corbett, J. D.; Wang, L. S.; Boldyrev, A. I. *Angew. Chem., Int. Ed.* **2001**, *40*, 3369.
- (230) Hirsch, A.; Chen, Z.; Jiao, H. *Angew. Chem., Int. Ed.* **2001**, *40*, 2834.
- (231) Twamley, B.; Power, P. P. *Angew. Chem., Int. Ed.* **2000**, *39*, 3500.
- (232) Li, X.; Kuznetsov, A. E.; Zhang, H. J.; Boldyrev, A. I.; Wang, L. S. *Science* **2001**, *291*, 859.
- (233) (a) Fowler, P. W.; Havenith, R. W. A.; Steiner, E. *Chem. Phys. Lett.* **2001**, *342*, 85. (b) Fowler, P. W.; Havenith, R. W. A.; Steiner, E. *Chem. Phys. Lett.* **2002**, *359*, 530. (c) Juselius, J.; Straka, M.; Sundholm, D. *J. Phys. Chem. A* **2001**, *105*, 9939. (d) Zhan, C. G.; Zheng, F.; Dixon, D. A. *J. Am. Chem. Soc.* **2002**, *124*, 14795. (e) Havenith, Remco W. A.; van Lenthe, Joop H. *Chem. Phys. Lett.* **2004**, *385*, 198. (f) Havenith, R. W. A.; Fowler, P. W.; Steiner, E.; Shetty, S.; Kanhere, D.; Pal, S. *Phys. Chem. Chem. Phys.* **2004**, *6*, 285.
- (234) Mercero, J. M.; Ugalde, J. M. *J. Am. Chem. Soc.* **2004**, *126*, 3380.
- (235) Datta, A.; Pati, S. K. *J. Am. Chem. Soc.* **2005**, *127*, 3496.
- (236) Xu, Q.; Jiang, L.; Tsumori, N. *Angew. Chem., Int. Ed.* **2005**, *44*, 4338.
- (237) Tanaka, H.; Neukermans, S.; Janssens, E.; Silverans, R. E.; Lievens, P. *J. Am. Chem. Soc.* **2003**, *125*, 2862.
- (238) (a) Hess, B. A.; Schaad, L. J.; Nakagawa, M. *J. Org. Chem.* **1977**, *42*, 1669. (b) Haddon, R. C. *J. Am. Chem. Soc.* **1979**, *101*, 1722.
- (239) (a) Katritzky, A. R.; Barczynski, P.; Musumarra, G.; Pisano, D.; Szafran, M. *J. Am. Chem. Soc.* **1989**, *111*, 7. (b) Katritzky, A. R.; Karelson, M.; Malhotra, N. *Heterocycles* **1991**, *32*, 127.
- (240) (a) Krygowski, T. M.; Ciesielski, A.; Bird, C. W.; Kotschy, A. *J. Chem. Inf. Comput. Sci.* **1995**, *35*, 203. (b) Cyrański, M.; Krygowski, T. M. *Pol. J. Chem.* **1995**, *69*, 1088. (c) Krygowski, T. M.; Cyrański, M. *Tetrahedron* **1996**, *52*, 1713. (d) Krygowski, T. M.; Cyrański, M. *Tetrahedron* **1996**, *52*, 10255. (e) Krygowski, T. M. *J. Chem. Inf. Comput. Sci.* **1993**, *33*, 70. (f) Krygowski, T. M.; Cyrański, M.; Ciesielski, A.; Swirska, B.; Leszczynski, P. *J. Chem. Inf. Comput. Sci.* **1996**, *36*, 1135. (g) Krygowski, T. M.; Wisiorowski, M.; Nakata, K.; Fujio, M.; Tsuno, Y. *Bull. Chem. Soc. Jpn.* **1996**, *69*, 2275.
- (241) Jug, K.; Koster, A. M. *J. Phys. Org. Chem.* **1991**, *4*, 163.
- (242) Chesnut, D. B. *Chem. Phys. Lett.* **1998**, *231*, 1.
- (243) Bird, C. W. *Tetrahedron* **1996**, *52*, 9945.
- (244) Cyrański, M. K.; Krygowski, T. M. *Tetrahedron* **1999**, *55*, 6205.
- (245) Quiñonero, D.; Garau, C.; Frontera, A.; Ballester, P.; Costa, A.; Deyà, P. M. *Chem.—Eur. J.* **2002**, *8*, 433.
- (246) Poater, J.; García-Gruz I.; Illas, F.; Solá, M. *Phys Chem Chem Phys.* **2004**, *6*, 314.
- (247) Sadlej-Sosnowska, N. *J. Phys. Org. Chem.* **2004**, *17*, 303.

CR030088+